Electronic Theses and Dissertations

2014

The Role of LIM Kinase 1 and its Substrates in Cell Cycle Progression

Lisa Ritchey
University of Central Florida

STARS Citation

University of Central Florida

STARS
Showcase of Text, Archives, Research & Scholarship

THE ROLE OF LIM KINASE 1 AND ITS SUBSTRATES IN CELL CYCLE PROGRESSION

by

LISA RITCHEY
B.S. Florida State University 2007
M.S. University of Central Florida 2010

A dissertation submitted in partial fulfillment of the requirements
for the degree of Doctor of Philosophy
in the Burnett School of Biomedical Sciences
in the College of Graduate Studies
at the University of Central Florida
Orlando, Florida

Summer Term
2014

Major Professor: Ratna Chakrabarti

ABSTRACT

LIM Kinase 1 (LIMK1), a modulator of actin and microtubule dynamics, has been shown to be involved in cell cycle progression. In this study we examine the role of LIMK1 in G1 phase and mitosis. We found ectopic expression of LIMK1 resulted in altered expression of p27Kip1, the G1 phase Cyclin D1/Cdk4 inhibitor. Overexpression of LIMK1 resulted in lower levels of p27Kip1 and p27Kip1-pY88 (inactive p27Kip1). Knockdown of LIMK1 resulted in elevated levels of p27Kip1 and p27Kip1-pY88. Together, these results suggest LIMK1 regulates progression of G1 phase through modulation of p27Kip1 expression.

LIMK1 is involved in the mitotic process through inactivating phosphorylation of Cofilin. Aurora kinase A (Aur-A), a mitotic kinase, regulates initiation of mitosis through centrosome separation and proper assembly of bipolar spindles. Phosphorylated LIMK1 is recruited to the centrosomes during early prophase, where it colocalizes with γ-tubulin. Here, we report a novel functional cooperativity between Aur-A and LIMK1 through mutual phosphorylation. LIMK1 is recruited to the centrosomes during early prophase and then to the spindle poles, where it colocalizes with Aur-A. Aur-A physically associates with LIMK1 and activates it through phosphorylation, which is important for its centrosomal and spindle pole localization. Aur-A also acts as a substrate of LIMK1, and the function of LIMK1 is important for its specific localization and regulation of spindle morphology. Taken together, the novel

molecular interaction between these two kinases and their regulatory roles on one other's function may provide new insight on the role of Aur-A in manipulation of actin and microtubular structures during spindle formation.

The substrates of LIMK1, Aur-A and Cofilin, are also involved in the mitotic process. Aur-A kinase regulates early mitotic events through phosphorylation and activation of a variety of proteins. Specifically, Aur-A is involved in centrosomal separation and formation of mitotic spindles in early prophase. The effect of Aur-A on mitotic spindles is mediated by modulation of microtubule dynamics and association with microtubule binding proteins. In this study we show that Aur-A exerts its effects on spindle organization through regulation of the actin cytoskeleton. Aur-A phosphorylates Cofilin at multiple sites including S^3 resulting in inactivation of its actin depolymerizing function. Aur-A interacts with Cofilin in early mitotic phases and regulates its phosphorylation status. Cofilin phosphorylation follows a dynamic pattern during progression of prophase to metaphase. Inhibition of Aur-A activity altered subcellular localization of Cofilin and induced a delay in the progression of prophase to metaphase. Aur-A inhibitor also disturbed the pattern of Cofilin phosphorylation, which correlated with the mitotic delay. Our results establish a novel function of Aur-A in the early mitotic stage through regulation of actin cytoskeleton reorganization.

ACKNOWLEDGMENTS

TABLE OF CONTENTS

LIST OF FIGURES

LIST OF TABLES

CHAPTER ONE: INTRODUCTION

The cell cycle is a highly complex process that is regulated by two main proteins: Cyclins and their counter parts Cyclin-Dependent Kinases (Cdks). Together Cyclin/Cdk complexes regulate the transition from one cell cycle phase to another. Cell cycle progression follows four distinct phases: G1, S, G2, and M or mitosis. Each phase-to-phase transition has a specific set of Cyclin/Cdks that are required for that particular phase transition. Expression and degradation of each Cyclin and Cdk is highly regulated as to prevent premature entry into the next phase of the cell cycle.

Dysregulation of cell cycle regulatory proteins has been implicated in the pathophysiology of a variety of diseases. In normal cells, the harmful effects of aberrantly expressed cell cycle regulatory proteins are contained through apoptosis. When too little cell death occurs the cells will grow uncontrollably and develop a malignant phenotype leading to tumor formation and cancer. Too much cell death may cause neurodegenerative diseases, autoimmune diseases, metabolic disorders, and ischemic injury [1]-[4].

1.1 Regulation of Progression Through G1 Phase

Progression of G1 phase is regulated by Cyclin D and Cyclin E and their respective Cdks, Cdk4/6 and Cdk2. Cyclin D/Cdk4 regulates progression of cells from early to late G1, while Cyclin E/Cdk2 promotes progression from late G1 into S phase [5]. The main target of G1 Cdks is the retinoblastoma protein (pRb) which, when hypophosphorylated, binds to and inhibits the activity of the E2F

family of transcription factors [6]-[10]. Activated Cdk4 upon binding to Cyclin D, phosphorylates pRb leading to its dissociation from the inhibitory complex with E2F. Released E2F triggers transcription of genes that promote progression to late G1 phase, such as Cyclin E and Cdk2 [11], [12]. Active Cdk2 also phosphorylates pRb, which results in increased E2F activity and transcription of genes that promote progression into S phase, including Cyclin A [13]. Phosphorylation of pRb is maintained throughout the S, G2, and M phases. During the transition of cells from M to G1 phase, pRb is dephosphorylated by protein phosphatase 1, which allows pRb to form an inhibitory complex with E2F and inhibit cell cycle progression [14].

Growth factors in serum are required for progression of cells from G0 or quiescent stage to G1 phase.   After cells progress through the Restriction point in late G1, removal of serum does not have any effect on cell cycle progression. If serum is removed before the Restriction point, cells become arrested in G1 and are not able to progress further [15]. One of the main proteins responsible for cell cycle arrest is the Cdk inhibitor, p27^{Kip1} [16]-[18]. p27^{Kip1} is able to inhibit both Cyclin D1/Cdk4 and Cyclin E/Cdk2 complexes [19]-[22].

Upon addition of serum, G0 cells progress to G1. At early G1, p27^{Kip1} is phosphorylated at S^{10}, which leads to its translocation from the nucleus to the cytoplasm [23], [24]. Phosphorylation of p27^{Kip1} at S^{10} has also been implicated in increasing the stability of the protein [23], [25]-[27]. Hyperphosphorylation of p27^{Kip1} at S^{10} and T^{187} has been shown to prevent the inhibitory activity of p27^{Kip1} against Cdk2 [28]-[32]. As cells progress into late G1, Cyclin D/Cdk4 complexes

2

can sequester p27^{Kip1} and allow some of the Cyclin E/Cdk2 complexes to remain unbound to p27^{Kip1}. Early in S phase, active Cyclin E/Cdk2 complexes can phosphorylate p27^{Kip1} at T^{187}, which leads to its degradation through polyubiquitination by SCF-Skp2 [33]-[36].

Phosphorylation of p27^{Kip1} at Y^{88} by Src, Lyn, and BCR-ABL prevents the inhibitory activity of p27^{Kip1} while still bound to its respective Cdk [37], [38]. Phosphorylation at this residue ejects the inhibitory 3$_{10}$ helix from the active site of Cdk4/Cdk2. Cdk2 is then able to phosphorylate p27^{Kip1} at T^{187} leading to degradation of the protein [39], [40] (Fig. 1). Binding of p27^{Kip1} may actually act as a promoter of Cyclin D/Cdk4 complex formation [38].
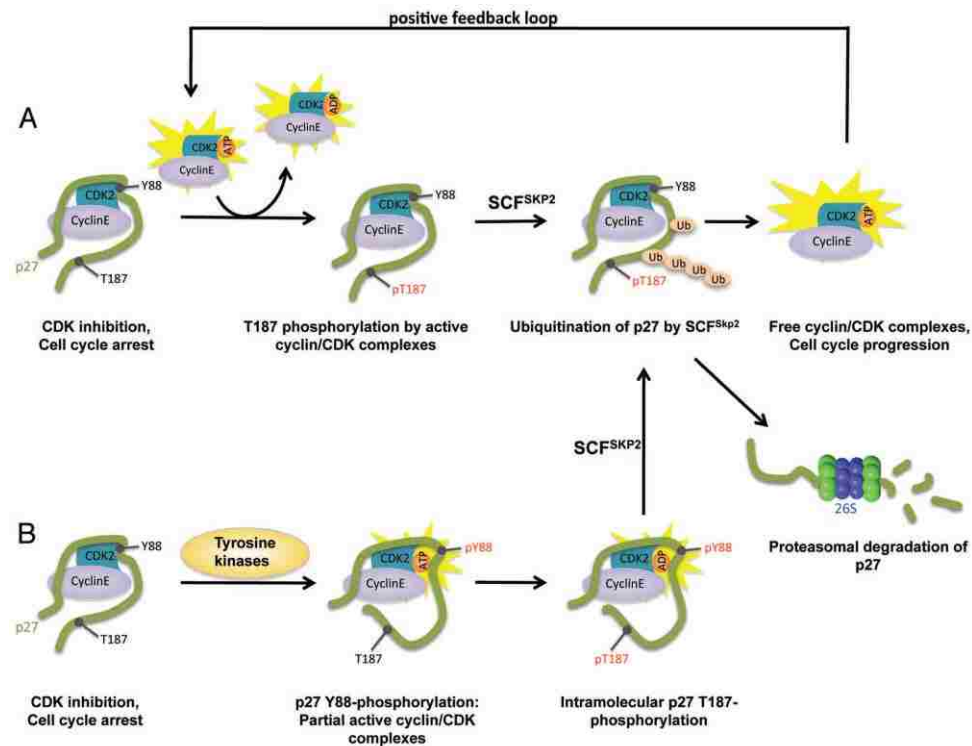
Figure 1: Model of p27^{Kip1} degradation at the G1/S transition.

(A) A self-amplifying feedback mechanism governs p27^{Kip1} stability at the G1/S transition. p27^{Kip1} stability and protein level decrease dramatically when cells progress from G1-phase to S-phase. Free Cyclin E/Cdk2 can phosphorylate Cdk-bound p27^{Kip1} on T^{187}. The resulting phosphodegron is recognized by the SCF-Skp2 ubiquitin ligase. SCF-Skp2 polyubiquitinates p27^{Kip1}, which is subsequently degraded by the 26S proteasome. The released Cyclin/Cdk complexes become active and can phosphorylate additional Cdk-bound p27^{Kip1} on T^{187}. (B) Phosphorylation of Y^{88} of p27^{Kip1} evokes the ejection of an inhibitory 3$_{10}$ helix of p27^{Kip1} from the catalytic cleft of Cdk2, allowing access of ATP to the ATP-binding pocket of the kinase. The resulting partial active cyclin-Cdk2 complex is now able to phosphorylate bound p27^{Kip1} on T^{187}, resulting in ubiquitination by SCF-Skp2 and proteasomal degradation [see (A)].

Cyclin E/Cdk2 complexes are also negatively regulated by phosphorylation. Cdk2 can be inhibited by phosphorylation at T^{14} and Y^{15} by the kinases Wee1 and Myt1 [41], [42]. The phosphatase Cdc25A promotes cell cycle progression by removing this inhibitory phosphorylation [43]. Overexpression of Cdc25A leads to early activation of Cyclin E/Cdk2 and premature progression from G1 to S phase [44].

1.1.1 LIM Kinase 1

The LIM Kinases (LIMK1/2) are a family of LIM domain containing serine/threonine and tyrosine kinases whose established function is to modulate the actin cytoskeleton. The LIM kinases contain two N-terminal zinc finger LIM domains which are involved in protein-protein interaction and may also have a role in protein-DNA interaction [45], [46]. The LIM domains are followed by a PDZ domain, which facilitates protein-protein interactions in signaling proteins [47]. The C-terminal of the protein contains a proline/serine rich region of unknown function, and a C-terminal kinase domain. LIMK1 contains a nuclear localization sequence between the PDZ and kinase domains and a nuclear export sequence within the PDZ domain [48]-[51] (Fig. 2). LIMK1 and LIMK2 share an overall identity of 50% while the kinase domain is highly conserved between the two with an identity of 70% [19], [21], [52].

Figure 2: The Structure of LIMK1.

LIMK1 contains two N-terminal LIM domains and a C-terminal PDZ and kinase domain separated by a proline/serine (P/S) rich region. The PDZ domain contains a nuclear exit signal (NES) and a nuclear localization signal (NLS) lies between the PDZ and kinase domain.

The main known substrate of LIMK1 is the actin depolymerizing protein, Cofilin [53]. Active Cofilin depolymerizes filamentous actin to produce pools of actin monomers [54]. LIMK1 phosphorylates Cofilin at S^3, which inhibits its ability to bind to actin, thereby preventing actin depolymerization [55], [56]. Overexpression of LIMK1 has been shown to cause the accumulation of filamentous actin through excessive Cofilin phosphorylation [53], [57].

The LIM domains of LIMK1 can bind to the kinase domain and prevent catalytic activity. Phosphorylation at T^{508} can activate LIMK1 by interrupting the interaction between the LIM and kinase domains, allowing full catalytic activity (Fig. 3) [23], [58], [59]. Activation of LIMK1 is mediated by Rho-GTPases, specifically by Pak1 activated by Rac, Pak4 activated by Cdc42, and ROCK activated by RhoA [23], [25], [27], [54]. This activation results in the formation of membrane ruffles and lamellipodia (Rac), filopodia (Cdc42), and stress fibers and focal adhesion (ROCK) [28], [30]-[32], [60]. LIMK1 activity is also regulated by dephosphorylation at T^{508} by Slingshot-1 phosphatase (SSH-1) [33].
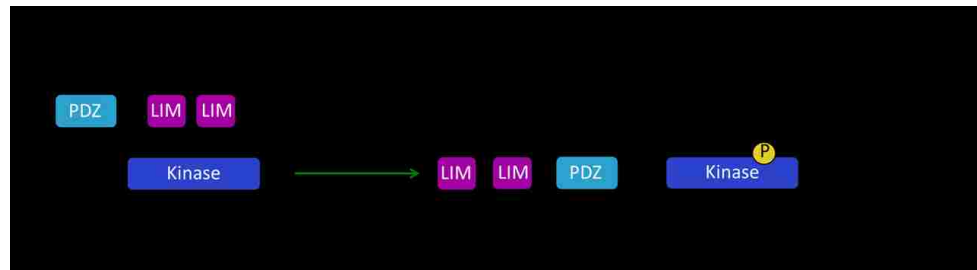
Figure 3: Regulation of LIMK1 Activity by Phosphorylation at T^{508}.

Binding of the LIM domains to the kinase domain autoinhibits LIMK1. Phosphorylation by Pak1, Pak4, or ROCK at T^{508} removes the LIM and kinase domain binding, resulting in full activity of LIMK1. Active LIMK1 can result in formation of lamellipodia, filopodia, and stress fibers.

It has also been suggested that LIMK1 can be activated by phosphorylation at S^{323} by MAPKAPK-2 in VEGF-A treated cells. Treatment also induced phosphorylation at S^{310} by p38 MAPK but did not cause activation of the protein [37]. PKA was also able to activate LIMK1 by phosphorylation at S^{323} [61]. Additionally, Hsp90 may promote dimerization of LIMK1 which then may cause transphosphorylation of LIMK1 dimers, thereby increasing protein stability [39], [62]-[64].

LIMK1 was first implicated in cell cycle regulation when LIMK1 overexpression was noted to retard growth of fibroblast cells [65]. Additionally, we found overexpression of LIMK1 delayed the G1-S and G2-M transitions [45]. It is unknown how LIMK1 contributes to G1-S phase progression.

One study has suggested that p57^{Kip2} regulates actin dynamics through interaction with LIMK1. Interaction with p57^{Kip2} increases LIMK1 catalytic activity and results in its nuclear translocation [48], [66]. A separate study suggested that interaction with p57^{Kip2} increased LIMK1 activity but concluded that this

protein-protein interaction occurred only in the cytoplasm [52], [67]. Additionally, silencing of p57[Kip2] expression led to increased migration and invasion of nasopharyngeal carcinoma cells via modulating LIMK1 phosphorylation/activity [59], [68]-[70]. Although these studies do show an interaction between LIMK1 and p57[Kip2], this interaction has not been studied during cell cycle progression.

Overexpression of LIMK1 has been noted in a variety of cancers including breast, prostate, and melanoma [71]-[74]. Overexpression of LIMK1 was associated with increased cell motility, while inhibition of LIMK1 expression decreased the invasiveness of prostate cancer cells [72], [73]. In addition to cancer, LIMK1 has been reported to be involved in Williams syndrome, primary pulmonary hypertension, and the formation of intracranial aneurysms [75]-[77].

1.1.2 Cofilin

Through regulation of the actin cytoskeleton, Cofilin is vital for various cellular functions including cell cycle progression, cell motility, and cell migration. Cofilin modulates the actin cytoskeleton through the depolymerization of actin filaments (F-actin) into monomers (G-actin) [54], [67], [78]. Cofilin increases the treadmilling of actin filaments in a pH dependent manner [79].

Cofilin activity is regulated via phosphorylation at S^3 by LIMK1/2 and TESK1/2 [55], [80], [81]. Phosphorylation at S^3 inactivates Cofilin by blocking its ability to bind to actin [56]. Cofilin activity is also regulated by the dephosphorylation of S^3 by Slingshot-1 phosphatase (SSH1), Chronophin phosphatase, and protein phosphatase 1 and 2A [82], [83]. V-Src

phosphorylation of Cofilin at Y^{68} increases ubiquitination and proteasomal degradation [84].

The actin cytoskeleton is involved in cellular response to growth factors and G1 phase progression. The extracellular matrix and the actin cytoskeleton have both been shown to play a role in the induction of G1 phase regulatory proteins, including Cyclin D [85]-[89]. Interestingly, overexpression of Cofilin blocked G1 phase progression through destabilization of the actin cytoskeleton and induction of p27^{Kip1} expression [90]. Together, these studies suggest Cofilin may play a role in G1 progression through modulation of the actin cytoskeleton.

Cofilin has been implicated in tumor invasion and metastasis through modulation of the actin cytoskeleton. Cofilin severs actin filaments to produce shorter filaments with free barbed ends. These free barbed ends can be used to produce F-actin rich structures such as lamellopodia and invadopodia. Lamellopodia are present at the leading edge of the cell and are involved in cell migration [91]-[93]. Cancer cells produce invadopodia to degrade the surrounding extracellular matrix and invade surrounding tissue during dissemination [94], [95].

1.2 Regulation of Progression Through Mitosis

A common factor in many cancer types is the overexpression of mitotic kinases. Overexpression of mitotic kinases is associated with centrosome instability and aneuploidy [96]-[100]. Therefore, regulation of mitotic kinases is essential for proper mitotic progression and cell division.

9

1.2.1 Aurora A Kinase

The Aurora kinases are a family of serine/threonine kinases involved in regulation of the mitotic process. The family consists of three members, Aurora A, Aurora B, and Aurora C [60], [68], [69], [101], [102]. Aurora A localizes to the centrosome and mitotic spindle and is involved in centrosome maturation and mitotic spindle assembly [5], [103]. Aurora B localizes to the centromere, central spindle, and later the contractile ring and is involved the chromosome separation and cytokinesis [24], [104], [105]. Little is known about the function of Aurora C but it has been shown to localize to the centrosome from anaphase to telophase and is involved in the formation of cilia and flagella [62]-[64], [66]. Aurora A and B share 71% sequence identity within their C-terminal catalytic domain, while they vary greatly in their N-terminal domain [67], [69], [103], [106]. While the active site of Aurora B and C are identical, there are three amino acid variants in Aurora A [107].

Aurora A is expressed throughout all phases of the cell cycle but only becomes highly expressed during G2 phase. Aurora A localizes to the centrosome after centrosome duplication in S phase and the protein remains localized to the centrosome throughout mitosis. Although Aurora A is expressed in all mitotic phases, it has only been well studied during the early mitotic phases such as, prophase and metaphase.

Depletion of Aurora A in Xenopus oocytes resulted in delayed mitotic entry through delayed activation of Cdk1 [108]. In contrast, down regulation of Aurora

A expression by RNAi in HeLa cells did not effect mitotic entry but rather resulted in a mitotic arrest with cells containing monopolar spindles [102], [109], [110]. These conflicting reports can be explained by a regulatory feedback loop between Aurora A, Polo-like kinase 1 (Plk1), Bora, and Cdk1 [111]. Individual inhibition of Aurora A or Plk1 did not effect Cdk1 activation while dual inhibition of both kinases delayed activation of Cdk1 resulting in delayed mitotic entry [112]. Plk1 is activated by phosphorylation at T^{210} within its activation loop [113]-[116]. When unphosphorylated the Polo-box domain (PDB) binds to the kinase domain, preventing its catalytic activity [116], [117]. During G2 phase, Bora binds to Plk1 and removes the autoinhibition of the PDB [118]. It has been suggested that interaction with Plk1 first requires a priming phosphorylation by Cdk1 [119]. Aurora A then phosphorylates Plk1 at T^{210} leading to full activation of the protein [118], [120]. Once active, Plk1 regulates Cdk1 activation by phosphorylating/activating Cdc25 and downregulating Wee1 [113], [121], [122].

During G2 phase, Aurora A is activated by autophosphorylation after interaction with protein cofactors. One such partner is the LIM-domain containing protein Ajuba, which is involved in the early activation of Aurora A at the centrosomes [123]. Bora has also been shown to interact with Aurora A, resulting in Aurora A autophosphorylation [124]. To date, nine Aurora A protein cofactors have been identified [125].

During prophase, Aurora A is involved in centrosome separation and maturation. Introduction of dominant negative Aurora A induces monopolar spindle formation through a defect in centrosome separation [66], [126]. It has

11

been suggested that Aurora A is not necessary for initial centrosome separation, but is necessary to maintain centrosome separation prior to the mitotic spindle formation [67], [127].

Aurora A has been implicated in centrosome maturation as RNAi silencing of Aurora A results in defects in centrosome maturation including reduced microtubule length and organization [67], [69], [128]-[130]. Additionally, absence of Aurora A results in ~60% reduction in the mass of spindle microtubules and aberrant spindle morphology [67], [78], [131]. Centrosome maturation occurs through recruitment of proteins involved in microtubule nucleation. The microtubule organization center (MTOC) at the centrosome is the site of microtubule nucleation to form the mitotic spindle. Within the MTOC, the γ-tubulin ring complex (γTuRC) forms a cap at the minus end of the microtubule and allows for nucleation at the plus end of the microtubule to produce the mitotic spindle. Aurora A contributes to centrosome maturation by recruiting proteins involved in microtubule nucleation to the centrosome. These proteins include: members of the γTuRC such as γ-tubulin, centrosomin, XMAP215, SPD-2, Lats2, NDEL1, and TACC [68]-[70], [131]-[134].

Aurora A and centrosomin (CNN) interact in the cytoplasm and are dependent on one another for their localization to the centrosome [67], [68]. In Drosopohila CNN plays a role in microtubule nucleation at the centrosome by its recruitment of γ-tubulin. Through phosphorylation, Aurora A is able to regulate Lats2 localization to the centrosome [133]. Lats2 has also been shown to recruit

12

γ-tubulin to the centrosome [135]. Aurora A interaction with CNN and Lats2, regulates centrosome maturation via recruitment of γ-tubulin to the centrosome.

Aurora A phosphorylates NDEL1 which recruits TACC3 to the centrosome [134]. In Drosophila, Aurora A directly interacts with D-TACC which functions to nucleate and stabilize microtubules [136]. In C. elegans, Aurora A interacts with SPD-2 which is involved in recruiting γ-tubulin and Zyg-9 to the centrosome [70].

In addition to centrosome maturation, it has been suggested that Aurora A may regulate bipolar spindle assembly through interaction with motor proteins. During interphase the motor binding protein TPX2 is maintained in the nucleus by importin α/β. During mitosis, a gradient of Ran GTP interacts with importin α/β, allowing TPX2 to then interact with centrosomal Aurora (Fig. 4). This interaction leads to activation of Aurora A through autophosphorylation and its translocation to the spindle microtubules [68], [69], [101], [102], [123]. At the mitotic spindle, Aurora A interacts with a Ran-dependent protein complex, consisting of TPX2, XMAP215, Eg5, and HURP, to form the bipolar mitotic spindle [137]. Aurora A kinase activity is necessary for the formation of this complex.
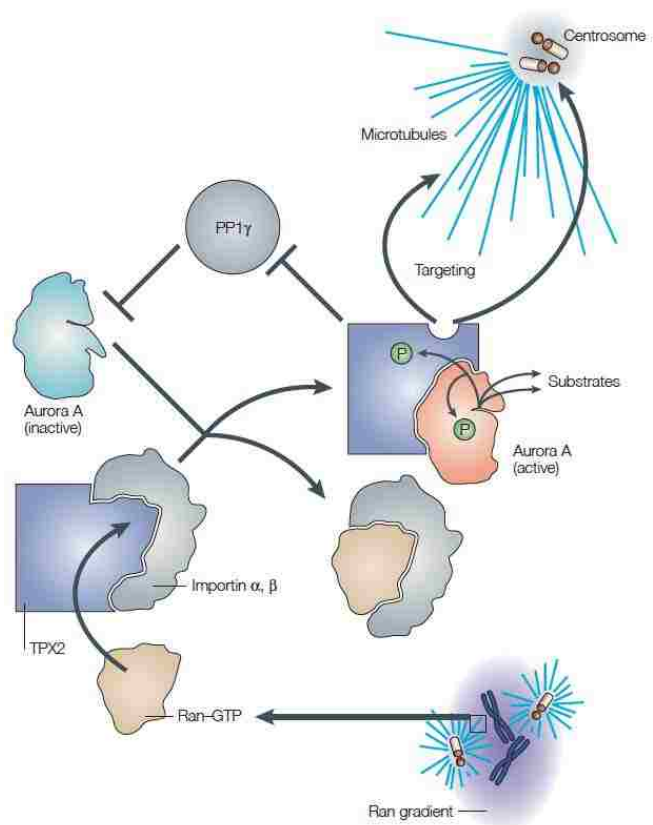
Figure 4: Regulation of Aurora-A activity by Ran–GTP and TPX2.

As cells enter mitosis, targeting protein for XKLP2 (TPX2) is in a complex with importins α or β. A gradient of Ran–GTP surrounding chromosomes (lower right) promotes the release of TPX2 from the importin. TPX2 then binds to Aurora A, which has been kept in an inactive state by protein phosphatase 1 γ (PP1γ). TPX2 interferes with PP1 action, enabling the kinase to autophosphorylate and activate itself and other substrates, including TPX2. TPX2 then also targets the kinase to microtubules proximal to the centrosome. Note that the kinase might not require continued association with TPX2 to phosphorylate other substrates.

Source: M. Carmena and W. C. Earnshaw, "The cellular geography of aurora kinases," Nature reviews. Molecular cell biology, vol. 4, no. 11, pp. 842–854, Nov. 2003.

Aurora A phosphorylates the kinesin, Eg5, which may activate the protein [66], [139]. Aurora A also regulates the spindle associated protein, HURP, via phosphorylation [140]. When hypophosphorylated, the C-terminal region of HURP binds to its N-terminal microtubule binding domain, inhibiting its interaction with microtubules. Phosphorylation in the C-terminal region prevents its interaction with the microtubule binding domain. Aurora A phosphorylates the kinesin MCAK at two sites, S^{196} and S^{719}, to promote proper pole focusing and bipolar spindle formation [141].

Aurora A is activated by phosphorylation at T^{288}, which lies within the activation loop of the protein [126], [127], [130]. Although PKA has been shown to phosphorylate Aurora A at T^{288} *in vivo* it is widely accepted that Aurora A activation occurs through autophosphorylation after interaction with a variety of protein cofactors [127], [142]. The most studied protein cofactor of Aurora A is TPX2. Binding of TPX2 induces autophosphorylation of Aurora A, enhancing Aurora A activity [131], [132], [143]. Additionally, binding of TPX2 induces a conformational change which orients the phosphate residue at T^{288} inward thereby preventing dephosphorylation by protein phosphatase 1 and allowing Aurora A to retain full activity [97], [103], [131], [144]-[149].

In addition to interaction with protein cofactors, a negative regulator of Aurora A has been recently identified, the Aurora A kinase interacting protein (AIP). AIP is a nuclear protein and specifically interacts with Aurora A *in vivo*. Co-expression of AIP and Aurora A results in the downregulation of Aurora A expression through proteasome-dependent degradation [139], [150].

15

Aurora A concentration is maintained throughout all stages of mitosis but is reduced upon mitotic exit through proteasomal degradation. Aurora A contains a N-terminal A-box and a C-terminal D-box and is degraded through the APC/C-ubiquitin-proteasome pathway [128]-[130], [151], [152]. Phosphorylation of S^{51} within the A-box prevents degradation of the protein by Cdh1 activated APC/C [127], [130], [153]. Protein phosphatase 2A dephosphorylates S^{51} at the end of mitosis and induces degradation of the protein [142], [154]. Constitutive phosphorylation at this site has been attributed to overexpression of Aurora A in cancer cells [143].

The gene encoding *Aurora A* is located on the 20q13 chromosome and is frequently overexpressed in many cancer types including breast, colorectal, bladder, lung, pancreatic, prostate, hepatocellular, and esophageal squamous cell carcinoma with poor prognosis [97], [103], [144]-[149], [155]-[158]. Though not considered a strong inducer of cell transformation, Aurora A overexpression was able to transform rat fibroblast cells [103], [159]. Aurora A is considered an oncogene, but the exact mechanism of Aurora A contribution to a malignant phenotype is not fully understood. Overexpression of Aurora A induces aneuploidy and genetic instability, which are the leading causes of tumor development [160]. Aurora A overexpression overrides G2 arrest induced by DNA damage and interferes with the spindle assembly checkpoint [160], [161].

1.2.2. LIM Kinase 1

LIMK1 has been shown to play an important role in the mitotic process. One major contribution of LIMK1 to the mitotic process is through its regulation of the actin cytoskeleton via Cofilin phosphorylation. Although not widely studied, LIMK1 may also contribute to the mitotic process through the regulation of microtubule polymerization.

During mitosis the subcellular localization of LIMK1 is regulated by phosphorylation of T^{508}. Phospho-LIMK1 (pT^{508}) colocalizes with γ-tubulin from prophase throughout telophase where it additionally localizes to the cleavage furrow/contractile ring during cytokinesis [151], [152]. Additionally, LIMK1 colocalized with F-actin at the cleavage furrow, suggesting it plays a role in cytokinesis via actin cytoskeleton remodeling [151]. LIMK1 is involved in mitotic progression, as LIMK1 knockdown arrested cells at G2-M phase [72].

Upon entry into mitosis, LIMK1 becomes hyperphosphorylated at a site other than T^{508} [150]. The specific site of phosphorylation was not identified but was found to lie outside of the kinase domain. Additionally, both ROCK and PAK, interphase activators of LIMK1, were not responsible for the mitotic phosphorylation of LIMK1. Treatment with the Cdk inhibitor roscovitine did reduce phospho-LIMK1 levels, suggesting Cdk1 may have a role in the phosphorylation of LIMK1 [162]. Although the proteins responsible for the mitotic activation of LIMK1 have yet to be identified, a mitotic protein that inhibits LIMK1 activity has been identified. Lats1, a member of the family of large tumor

suppressor proteins, has been shown to interact with and inhibit LIMK1 activity [154]. Interaction with Lats1 is able to suppress the formation of multinucleated cells induced by LIMK1 overexpression.

The primary known function of LIMK1 during the early stages of mitosis is regulation of the actin cytoskeleton via Cofilin phosphorylation. LIMK1 phosphorylation of Cofilin is necessary for the mitotic spindle to maintain proper orientation within the cell [163]. siRNA knockdown of LIMK1 caused mislocalization of Cofilin to the cell cortex, suggesting that cortical actin maintains the orientation of the mitotic spindle. Knockdown of LIMK1 also leads to a mitotic delay, which may be mediated through low levels of phospho-Cofilin since overexpression of a non-phosphorylatable Cofilin (S3A) mutant induced a similar phenotype.

In addition to the regulation of actin dynamics during mitosis, LIMK1 may also participate in the regulation of microtubule dynamics. LIMK1 was shown to interact, via the PDZ domain, with tubulin in endothelial cells [164]. This interaction was shown to be necessary for thrombin induced actin polymerization and microtubule depolymerization. LIMK1 also phosphorylates p25α/tubulin polymerizing promoting protein (TPPP), preventing its ability to polymerize tubulin [153]. LIMK1 overexpression has been associated with abnormal mitotic spindle structures and multiple centrosomes [45]. LIMK1 knockdown resulted in centrosome defocusing and multipolar spindles [165]. Together these studies suggest LIMK1 may play a role in mitotic microtubule disassembly.

Overexpression of LIMK1 induces cytokinesis defects leading to the formation of multinucleated cells [150]. It is likely that these cytokinesis defects occur through enhanced F-actin accumulation as a result of excessive Cofilin phosphorylation [150]. LIMK1 catalytic activity is necessary for the formation of multinucleate cells as kinase dead LIMK1 did not alter cytokinesis. Additionally, co-expression of the LIMK1 inhibitor, Lats1, and LIMK1 prevented the multinuclear cell phenotype [154]. Overexpression of a phosphatase inactive SSH1 mutant also resulted in accumulation of F-actin and multinucleated cells [166].

1.2.3 Cofilin

Studies have shown that the function of Cofilin is necessary for mitosis. Regulation of Cofilin phosphorylation is critical for proper mitotic progression and cytokinesis. During mitosis, LIMK1 phosphorylates Cofilin during prometaphase and metaphase [150], [166]. As cells progress into anaphase and telophase, Cofilin is dephosphorylated by SSH-1 phosphatase [150], [166]. In early mitotic stages, Cofilin is localized to the cytoplasm but then localizes to the cleavage furrow in late mitosis [150].

Regulation of Cofilin phosphorylation is the key to its function during each phase of mitosis. In early mitosis, phosphorylation of Cofilin by LIMK1 is necessary for proper orientation of the mitotic spindle [163]. Additionally, Cofilin knockdown results in spindle oscillation and as shown in studies in *Xenopus laevis,* dephosphorylation of Cofilin is necessary for spindle assembly [167],

19

[168]. Cofilin may regulate mitotic spindle orientation through interaction with cortical actin. Altered actin distribution during mitosis alters the cortical rigidity leading to increased astral microtubule numbers and decreased centrosome integrity [165]. Mitotic accumulation of F-actin has been attributed to a delay in mitosis [169].

Cofilin has also been implicated in the formation and constriction of the contractile ring during cytokinesis. Actin depolymerization by Cofilin is necessary for actomyosin ring constriction [170]. Overexpression of LIMK1 blocked cytokinesis and increased the number of multinucleated cells and F-actin accumulation [150], [154]. Inhibition of LIMK1 activity does not affect cytokinesis suggesting that the phospho-regulation of Cofilin is critical for proper cell division during cytokinesis [150], [154]. Similarly, loss of Cofilin results in excessive F-actin accumulation at the contractile ring [167], [171]-[174].

CHAPTER TWO: HYPOTHESIS AND SPECIFIC AIMS

Abnormal processes during cell cycle progression can lead to incorrect mitotic spindle positioning, chromosomal instability, and formation of multinucleated cells, all of which are cancer phenotypes. Proper maintenance of interphase and mitosis by cell cycle regulatory proteins is essential for prevention of abnormal cell division and accumulation of genetic abnormalities. LIMK1 has been shown to play an important role in cell cycle regulation. LIMK1 has been found to be overexpressed in a variety of advanced cancer types including prostate, lung, advanced breast, and pancreatic cancer. Studies from our laboratory indicate that LIMK1 expression needs to be tightly regulated for proper progression of G1/S and G2/M phases. Our studies showed that increased expression of LIMK1 promoted accumulation of chromosomal abnormalities and induced transient G1/S phase arrest. However, the exact mechanism whereby LIMK1 exerts its regulatory role in G1/S and mitosis is not clear. We hypothesize that LIMK1 participates in the regulation of cell cycle progression, specifically in G1 and mitosis. In this project, we plan to define the role of LIMK1 in G1/S phase and mitotic progression by pursuing the following specific aims.

Aim #1. Examine the role of LIMK1 on G1/S Phase Progression.

In this aim we will examine how LIMK1 expression affects the subcellular localization and expression of G1 phase regulatory proteins.

Aim #2. Examine the role of LIMK1 during mitosis.

In this aim we will identify mitotic kinases that interact with LIMK1 during mitosis. We will also examine how this interaction affects mitotic progression.

Aim #3. Examine the involvement of LIMK1 substrates on the mitotic process.

In this aim we will identify kinases responsible for the phosphorylation of Cofilin during mitosis. We will also examine how Cofilin phosphorylation is regulated during mitosis.

CHAPTER THREE: METHODOLOGY

3.1 Cell Culture and Cell Cycle Enrichment

RWPE-1 cells were maintained in keratinocyte media supplemented with bovine pituitary extract and EGF (Gibco), at 37°C and 5% CO_2. At ~75% confluency the cells were trypsinized and incubated at 37°C for 8 min. Cells were transferred to a tube containing 2% FBS in PBS to inactivate the trypsin. Cells were centrifuged at 125 x g for 6 min at 4°C, then resuspended in complete media (1:3) and plated.

PC3 cells were maintained in F-12 HAM (Sigma) with 10% FBS (Atlanta Biologicals) and 1% antibiotic/antimycotic (Gibco) at 37°C and 5% CO_2. At ~75% confluency cells were trypsinized for 30 seconds at room temperature then incubated at 37°C without trypsin for 10 min. Cells were resuspended in complete media (1:3) and plated.

P69 and M12 cells were maintained in RPMI-1640 (Sigma) containing EGF (10ng/ml) (BD), dexamethasone (0.1uM) (Sigma), Gentamycin (50μg/ml) (Gibco), ITS (Insulin 5μg/ml, Transferrin 5μg/ml, Selenium 5ng/ml) (Fisher). At ~75% confluency cells were trypsinized for 5 min at room temperature then trypsin was removed and the cells were incubated at 37°C without trypsin for 15 min. Cells were resuspended in complete media (1:3 or 1:5) containing 5% FBS and plated. The next day the cells were washed once with PBS and incubated in complete media without FBS.

NIH-3T3 and MCF7 cells were maintained in DMEM (Gibco) containing 10% FBS and 1% antibiotic/antimycotic. At ~75% confluency cells were trypsinized for 30 seconds at room temperature then cells were incubated at 37°C without trypsin for 10 min. Cells were resuspended in fresh media (1:5) and plated.

3.2 Cell Cycle Enrichment

PC3 cells were synchronized to G0 by serum starvation. Cells (5×10^5) were seeded onto a 10 cm dish in complete media. 24 hrs later the media was removed and cells were washed three times with PBS and incubated with F12-HAM media without FBS for 48 hrs. Cells were released from G0 by the addition of EGF (10ng/ml) to the media and harvested at specific time points. G0 enrichment was confirmed by flow cytometry as described below.

M12, 3T3, and PC3 cells were synchronized to G2/M by treatment with nocodazole (Sigma). Cells were seeded in complete media and 24 hrs later were treated with nocodazole at a concentration of 80ng/ml (M12), 600ng/ml (3T3), or 2nM (PC3) for 24 hrs. To enrich cells at metaphase, media was changed to complete media without nocodazole and cells were incubated at 37°C for 35 min. For some experiments, nocodazole treated cells were incubated in complete media without nocodazole and harvested at 0, 30, and 60 min. For inhibitor treatments, cells were treated with MLN8237 (100nM), BMS-5 (5µM), BMS-5 (5µM) and MLN8237 (100nM), or DMSO (Vehicle) and nocodazole for 24 hr. Cells were washed to remove nocodazole and released into mitosis for

30 or 60 mins with fresh media containing either MLN8237 (100nM), BMS-5 (5µM), BMS-5 (5µM) and MLN8237 (100nM), or DMSO.

3.3 Transfection

All plasmid DNA used in transfections was extracted using the PureYield Plasmid Miniprep System (Promega). 3mL of LB broth containing the appropriate antibiotic (30mg/mL kanamycin or 10mg/mL ampicillin) was inoculated with 20µl glycerol stock of the appropriate plasmid DNA construct. Cultures were incubated at 37°C, shaking at 250 rpm, for 16-18 hrs. Bacterial cultures were centrifuged at 2000 rpm for 3 mins and pellets were resuspended in 600µl dH_2O and lysed with 100µl Cell Lysis Buffer. The lysis buffer was neutralized with 350µl of Neutralization Solution and centrifuged at 12,000 rpm for 3 min. The supernatant containing plasmid DNA was transferred to a PureYield Minicolumn and centrifuged at 12,000 rpm for 1 min. The column was washed with 200µl Endotoxin Removal Wash and spun at 12,000 rpm for 1 min. The column was washed with 400µl Column Wash Solution and centrifuged at 12,000 rpm for 1 min. The DNA was eluted with 50µl sterile dH_2O in aseptic condition and spun at 12,000 rpm for 1 min. DNA purity and yield was determined using a nanodrop spectrophotometer and confirmed by restriction enzyme digestion and DNA gel electrophoresis. All plasmid DNA samples were stored at 4°C.

For ectopic expression of LIMK1, RWPE-1 cells were seeded onto a 6-well ($3.5x10^4$) or 10 cm dish ($2.4x10^5$). The next day, p3XFlag-CMV-14 (vector

only) or LIMK1-p3XFlag-CMV-14 plasmid DNA constructs (2μg or 12μg) were incubated with Fugene HD (Promega) in OPTI-MEM serum free medium (Life Technologies) at a ratio of 1:2 for 20 min at room temperature. The mixture was added drop-wise to the dishes and the cells were harvested after 24 hrs. Expression of Flag-tagged LIMK1 was validated by immunoblotting as described below with anti-Flag antibodies.

For inhibition of LIMK1 expression in G0 synchronized PC3 cells, cells were seeded onto a 6-well (3.5×10^4) or 10cm dish (1.05×10^5). The next day, DNA contructs (2μg or 12μg) of LIMK1 shRNA or scrambled shRNA were incubated for 20 min at room temperature in OPTI-MEM with either Fugene HD at a ratio of 1:4 or X-tremeGENE HP (Roche) at a ratio of 1:1. The mixture was then added drop-wise to the cells. 24 hrs later the cells were washed three times with PBS and incubated with HAM-F12 without FBS for 48 hrs to enrich the cells to G0. Reduced expression of LIMK1 was validated by immunoblotting as described below with anti-LIMK1 antibodies.

For LIMK1 overexpression experiments in P69 cells, cells were seeded onto a 6-well dish (3.5×10^4). The next day, cells were transfected with p3XFlag-CMV-14 (vector only) or LIMK1-p3XFlag-CMV-14 plasmid DNA constructs. Plasmid DNA (2μg) was incubated with X-tremeGENE HP in OPTI-MEM at a ratio of 1:1 at room temperature for 20 min. The mixture was added drop-wise to the cells and cells were incubated for 24 hrs. Expression of Flag-tagged LIMK1 was detected by immunoblotting as described below with anti-Flag antibodies.

For Cofilin-RFP expression, M12 cells ($3x10^4$) were seeded onto poly-L-lysine coated coverslips. The next day, cells were transfected with Cofilin-RFP or Cofilin$^{S3A/S8A/T25A}$-RFP plasmid DNA. DNA constructs (200ng) were incubated with X-tremeGENE HP in OPTI-MEM at a ratio of 1:1 at room temperature for 20 min, added to the cells and cells were incubated at 30°C. After 48 hrs, cells were fixed and stained as described below. The expression/localization of Cofilin-RFP constructs was visualized by confocal microscopy.

3.4 LIMK1 Inhibition with BMS-5

PC3 cells ($5x10^5$) were seeded onto a 10cm dish and treated with BMS-5 (5μM) for 24 hrs. LIMK1 inhibition was confirmed by immunoblotting as described below with anti-pS^3-Cofilin antibodies.

3.5 Nuclear/Cytoplasmic Protein Extraction

Nuclear and cytoplasmic proteins were isolated from G1 released PC3 cells using the NE-PER kit (Pierce). After G0 enrichment and EGF release as described above, cells were trypsinized and washed three times in PBS and centrifuged at 1000 rpm for 10 min. Cell pellets were resuspended in CERI buffer at a volume 10 times greater than the volume of the cell pellet and incubated on ice for 10 min. CERII buffer was added at 1/20 of the volume of CERI buffer, samples were vortexed and incubated on ice for 1 min. Nuclei was pelleted by centrifugation at 12,000 rpm for 5 min at 4°C. The supernatant, containing cytoplasmic proteins, was transferred to a chilled microcentrifuge tube. The pelleted nuclei were resuspended in NERI buffer at a volume 2 times

greater than the original cell pellet volume. The sample was then incubated on ice for 40 min while, vortexing every 10 min. The lysed nuclei were pelleted by centrifugation at 12,000 rpm for 10 min at 4°C and the supernatant containing nuclear protein was transferred to a chilled microcentrifuge tube. Protein concentration was determined by Bradford assay. Nuclear (20µg) and cytoplasmic (50µg) proteins were diluted in sample buffer and denatured by boiling at 95°C for 5 min. All proteins were stored in aliquots -80°C or -20°C after boiling, prior to using them for immunoblotting. Protein aliquots were electrophoresed, transferred to PVDF membrane, and immunoblotted as described below.

3.6 Whole Cell Protein Extraction and Immunoblotting

Whole cell lysate was prepared from pelleted cell lines by resuspension in RIPA lysis buffer (5mM Tris, pH 7.5, 2mM EDTA, 150mM NaCl, 1% Nonidet P-40, 1mM phenylmethylsulfonylfluoride, 1mM sodium orthovanadate, 1mM sodium fluoride, 40mM β-glycerophosphate, 1µg/mL aprotinin, 1µg/mL leupeptin) and lysed by 6 freeze-thaw cycles in a dry ice/ethanol bath and incubation at 37°C. Samples were clarified by centrifugation at 12,000 rpm for 15 min at 4°C. Protein concentration was quantified by Bradford assay. 50µg whole cell extract was diluted in sample buffer (240mM Tris, pH6.8, 5% β-mercaptoethanol, 8% SDS, 40% Glycerol, 0.04% bromophenol blue) and denatured by boiling at 95°C for 5 min. Proteins were separated in a 12% SDS-PAGE gel transferred to a PVDF membrane (Pall). Separated proteins were visualized on the membrane by

staining with India ink and the membrane was blocked for 90 min with 5% milk in

TBS-T (20mM Tris base, 137mM NaCl, 0.1% Tween, pH 7.6). The membrane

was aligned to SURF blotter slots and primary antibodies (Table 1) were diluted

in milk and incubated on the membrane for either 1 hr at room temperature or

overnight at 4°C. Unbound primary antibodies were removed by washing three

times with milk for 10 min at room temperature.   Horseradish peroxidase

conjugated secondary antibodies (Table 2) were diluted in milk and incubated

with bound primary antibodies on the membrane for 45 min at room temperature.

Unbound secondary antibodies were removed by washing in TBS-T for 5 min at

room temperature, for seven times with the final wash in TBS. Proteins were

visualized using a chemiluminiscence ECl kit (Pierce) or Immun-Star WesternC

kit (Biorad).

Table 1. Immunoblotting Primary Antibodies

Antigen	Company	Catalog No.	Host	Dilution	Blotting Condition
Aur-A	Abcam	ab1324	Mouse	1:100	o/n; 4°C
Aur-A(pT^{288})	Cell Signaling	3079	Rabbit	1:100	o/n; 4°C
Cdc25A	Santa Cruz	sc-97	Rabbit	1:100	o/n; 4°C
Cdk2	Santa Cruz	sc-6248	Mouse	1:100	o/n; 4°C
Cdk4	Santa Cruz	sc-260	Rabbit	1:100	o/n; 4°C
Cofilin	Novus	NBP1-19828	Rabbit	1:1000	o/n; 4°C
Cofilin	Cytoskeleton	PA5-19727	Rabbit	1:1000	o/n; 4°C
Cofilin(pS^3)	Cell Signaling	3313	Rabbit	1:100	o/n; 4°C
Cyclin D1	Neomarker	MS-210-P1	Mouse	1:100	o/n; 4°C
Flag	Sigma	F1804	Mouse	1:1000	1hr; RT
GAPDH	Sigma	G8795	Mouse	1:1000	1hr; RT
LIMK1	BD Transduction	611748	Mouse	1:100	o/n; 4°C
LIMK1	Santa Cruz	sc-5576	Rabbit	1:1000	o/n; 4°C
LIMK1	Millipore	MAB10750	Rat	1:800	o/n; 4°C
LIMK1(pT^{508})/ LIMK2(pT^{505})	Cell Signaling	3841	Rabbit	1:100	o/n; 4°C
p27	Santa Cruz	sc-528	Rabbit	1:100	o/n; 4°C
p27(pS^{10})	Santa Cruz	sc-12939	Rabbit	1:100	o/n; 4°C
p27(pY^{88})	----	---	Rabbit	1:1000	o/n; 4°C
p57	Santa Cruz	Sc8298	Rabbit	1:100	o/n; 4°C
γ-tubulin	Sigma	T3559	Rabbit	1:500	1hr; RT
SSH-1	Cell Signaling	13578	Rabbit	1:1000	o/n; 4°C
α-tubulin	Sigma	T9206	Mouse	1:1000	1hr; RT

Table 2. Immunoblotting Secondary Antibodies

Antigen	Company	Catalog No.	Host	Dilution
Rabbit IgG	Jackson Laboratories	111-035-003	Goat	1:5000
Mouse IgG	Jackson Laboratories	115-035-003	Goat	1:5000
Rat IgG	Jackson Laboratories	112-035-003	Goat	1:5000

3.7 Production of a p27^{Kip1} phospho-Y^{88} antibody

An antibody specific for p27^{Kip1}-pY^{88} was produced by GenScript using the peptide sequence EF(pTyr)YRPPRPPKGAC. The specificity of the antibody was confirmed by a competition assay with the peptide. Antibodies at 1:10,000 dilution were incubated with 1, 2, 5, 10x molar ratio of the peptide, in milk for 1 hr at 4°C. This mixture was used for incubation with total proteins (50µg) of PC-3 cell lyates immobilized on a PVDF membrane overnight at 4°C. The immunoblot was completed as described above.

3.8 Plasmid DNA and shRNA Constructs

The coding sequence of human LIMK1 was previously cloned into the p3XFlag-CMV-14 (Sigma) and pET-50b(+) vectors (Novagen). A kinase domain only construct (nucleotides 774-1941) was generated by PCR amplification using the primers listed in Table 4 and cloned into the p3XFlag-CMV-14 and pET-30Ek/Lic (Novagen) vectors. A LIM domain only construct (nucleotides 1-411) was generated by PCR amplification using the primers listed in Table 4 and cloned into p3XFlag-CMV-14. The coding sequence of human Aur-A was previously cloned into the pET-30Ek/LIC vector. The coding sequence of human cofilin was previously cloned into the pET-30Ek/LIC vector [71]. This sequence was PCR amplified using primers listed in Table 4 and cloned into the pCMV6-AC-RFP vector. The *LIMK1^{S307A}* and *LIMK1^{T508A}* non-phosphorylatable mutants, *Aur-A^{K162M}* kinase dead mutant, and *Cofilin^{S3A}*, *Cofilin$^{S3A/S8A}$*, and *Cofilin$^{S3A/S8A/T25A}$* non-phosphorylatable mutants were all generated by site-

31

directed mutagenesis using the QuikChange II XL Site-Directed Mutagenesis Kit (Agilent Technologies). Specific primers for each construct were created following the manufacturer's guidelines: between 25-45 base length, Tm ≥78°C, and G/C content ≥40%. The PCR reactions were carried out following the manufacturers protocol. 25ng template DNA and 125ng of each primer were used (Table 4). PCR cycling parameters are shown in Table 3.

Table 3. Site-Directed Mutagenesis PCR Cycling Parameters

Segment	Cycles	Temperature	Time
1	1	95°C	1 minute
2	18	95°C	50 seconds
		60°C	50 seconds
		68°C	1 minute/kb of plasmid length
3	1	68°C	7 minutes

To reduce the expression of LIMK1, a HuSH shRNA construct against LIMK1 was cloned into the pGFP-V-RS vector (Origene Techonologies) was used. Four different shRNA constructs with LIMK1 shRNAs directed against a 29 base sequence within the kinase domain of LIMK1 were screened and the construct with the highest reduction in LIMK1 expression was used in subsequent experiments (AAGGACAAGAGGCTCAACTTCATCACTGA). A scrambled shRNA construct was also used to monitor produced to control for off target effects of transfection.

Table 4. Plasmid DNA Constructs and Primers

Sequence	Construct	Vector	Mutation
F: 5'-GGCTCAACTTCATCGGTGAGTACATCAAGGG R: 5'-CCCTTGATGTACTCACCGATGAAGTTGAGCC	LIMK1	p3XFlag-CMV-14	N/A
F: 5'-AAGCTTATGGCCCCAGGTGTGGCTGTCTCT R: 5'-AGAGAAGCCACACCTGGGGCCATAAGCTT	LIMK1^K	p3XFlag-CMV-14	Kinase domain only
F: 5'-<u>ATCGAT</u>ATGAGGTTGACGCTACTTTG R: 5'-<u>TCTAGA</u>GGTGACGGTGTGGGGCAG	LIMK1^L	p3XFlag-CMV-14	Lim domains only
F: 5'-CGGGGAGCCCAGTGCGCCAGCGCCCGGAG R: 5'-CTCCGGGCGCTGGCGCACTGGGCTCCCCG	LIMK1^{S307A}	p3XFlag-CMV-14	Non-phos. at S307
F: 5'-GCAAGAAGCGCTACGCCGTGGTGGGCAAC R: 5'-GTTGCCCACCACGGCGTAGCGCTTCTTGC	LIMK1^{T508A}	p3XFlag-CMV-14	Non-phos. at T508
F: 5'- AAGCTTATGGCCCCAGGTGTGGCTGTCTCT R: 5'- AGAGAAGCCACACCTGGGGCCATAAGCTT	LIMK1^K	pET-30	Kinase domain only
F: 5'- GGCTCAACTTCATCGGTGAGTACATCAAGGG R: 5'- CCCTTGATGTACTCACCGATGAAGTTGAGCC	LIMK1	pET50b(+)	N/A
F: 5'-CGGGGAGCCCAGTGCGCCAGCGCCCGGAG R: 5'-CTCCGGGCGCTGGCGCACTGGGCTCCCCG	LIMK1^{S307A}	pET50b(+)	Non-phos. at S307
F: 5'-GCAAGAAGCGCTACGCCGTGGTGGGCAAC R: 5'-GTTGCCCACCACGGCGTAGCGCTTCTTGC	LIMK1^{T508A}	pET50b(+)	Non-phos. at T508
F: 5'-GACGACGACAAGATGGACCGATCTAAAGAAAACTGC R: 5'-GAGGAGAAGCCCGGTCTAAGACTGTTTGCTAGCTG	Aur-A	pET-30	N/A
F: 5'-GTTTATTCTGGCTCTTATGGTGTTATTTAAAGC R: 5'-GCTTTAAATAACACCATAAGAGCCAGAATAAAC	Aur-A^{K162M}	pET-30	Kinase dead
F: 5'-GACGACGACAAGATGGCCTCCGGTGTGGCTG R:5'GAGGAGAAGCCCGGTTCACAAAGGCTTGCCC	Cofilin	pET-30	N/A
F: 5'-ACAGCCACACCGGCGGCCATGAATTCG R: 5'-CGAATTCATGGCCGCCGGTGTGGCTGT	Cofilin^{S3A}	pET-30	Non-phos. at S3
F: 5'-GGTGTGGCTGTCCCAGATGGTGTCATCAAGTG R: 5'-CACCTTGATGACACCATCTGGGACAGCCACACC	Cofilin$^{S3A/S8A}$	pET-30	Non-phos. at S3 and S8
F: 5'-GGTGCGTAAGTCTTCACCACCAGAGGAGG R: 5'-CCTCCTCTGGTGGTGAAGACTTACGCACC	Cofilin$^{S3A/S8A/T25A}$	pET-30	Non-phos. at S3, S8, and T25
5'-AAGAAGGAGATATACATATGGAGACCAAGGAGAGCAAG	Cofilin$^{90-166}$	pET-30	C-terminal truncation
F: 5'-AAGCTTATGGCCTCCGGTGTGGCTG R: 5'CTCGAGACACAAAGGCTTGCCCTCCA	Cofilin	pCMV6-AC-RFP	N/A
F: 5'-TGCGTAAGTCTTCAGCGCCAGAGGAGG R: 5'-CCTCCTCTGGCGCTGAAGACTTACGCA	Cofilin$^{S3A/S8A/T25A}$	pCMV6-AC-RFP	Non-phos. at S3, S8, and T25

3.9 Recombinant Protein Expression and Purification

LIMK1, Aur-A, and Cofilin constructs were all expressed by transforming BL21-CodonPlus (DE3) RIPL cells. Protein expression in transformed cells was induced with 1mM IPTG at 20°C, overnight. Recombinant Aur-A and Cofilin expressing bacterial cultures were then spun down at 2000 rpm for 20 min. The bacteria pellet was resuspended in PBS containing Complete ULTRA Protease Inhibitor Cocktail Tablets EDTA-free (Roche) and lysed by sonication. The sample was clarified by centrifugation at 12,000 rpm for 20 min. The recombinant proteins were bound to a Talon bead cobalt affinity column (Clontech) and washed with wash buffer (50mM Sodium Phosphate, 300mM NaCl, 10% Glycerol) to remove unbound protein. Proteins were eluted with a 700mM imidazole (Fisher) linear gradient. The proteins were concentrated and the buffer was changed to storage buffer (50mM Tris, pH7.5, 150mM NaCl, 250µM DTT, 15% Glycerol for Aur-A; 50mM HEPES, 150mM NaCl, 5mM $MgCl_2$, 5mM $MnCl_2$; 15% Glycerol for Cofilin) with Pierce Concentrators 9K MWCO columns (Pierce).

Expression of recombinant LIMK1 was induced with 1mM IPTG at 20°C, overnight. Protein was isolated using a Protein Refolding kit (Novagen). Inclusion bodies were solubilized in 1x solubilization buffer (50mM CAPS, pH 11.0, 0.3% N-lauroylscarcosine, 1mM DTT) at room temperature for 15 min. Proteins were clarified by centrifugation at 10,000x g for 10 min at room temperature and refolded in dialysis buffer (1M Tris-HCL, pH 8.5) with 0.1 mM

DTT for 3 hrs at 4°C. DTT was removed by additional dialysis using dialysis buffer without DTT for 3 hrs at 4°C. Next, the protein was dialyzed in dialysis buffer with 1mM reduced glutathione and 0.2mM oxidized glutathione, overnight at 4°C. Proteins were concentrated and buffer was changed to storage buffer (50mM HEPES, 150mM NaCl, 5mM $MgCl_2$, 5mM $MnCl_2$, 15% Glycerol) with Pierce Concentrators 9K MWCO columns (Pierce). Purity of expressed proteins was determined by SDS-PAGE followed by Coomassie staining. Catalytic activity of His-Aur-A and His-LIMK1 recombinant proteins was quantified by *in vitro* kinase assays as described below. All proteins were stored in aliquots at -80°C or -20°C.

<div align="center">3.10 Kinase assays</div>

In vitro kinase assays for Aur-A, LIMK1, and Cdk4, were done using the following assay buffers: 50mM MOPS, pH7.2, 25mM β-glycerophosphate, 10mM EGTA, 4mM EDTA, 50mM $MgCl_2$, 0.5mM DTT for Aur-A; 50mM HEPES, 150mM NaCl, 5mM $MgCl_2$, 5mM $MnCl_2$ for LIMK1; 250mM HEPES, 50mM $MgCl_2$, 5mM DTT for Cdk4.

For Aur-A *in vitro* kinase assays, 500ng or 220ng His-Aur-A, His-Aur-A^{K162M}, or 50ng GST-Aur-A (Cell Signaling) was incubated with its substrate, either myelin basic protein (MBP) (500ng) (Sigma), GST-LIMK1 (Abnova) (1µg), His-LIMK1 (1µg), His-LIMK1^K (1µg), His-LIMK1^{S307A} (1µg), His-LIMK1^{T508A} (1µg), His-Cofilin (1µg), His-Cofilin^{S3A} (1µg), His-Cofilin$^{S3A/S8A}$ (1µg), or His-

<div align="center">35</div>

Cofilin$^{S3A/S8A/T25A}$ (1μg) in kinase assay buffer containing 250μM ATP and 5nM γ-^{32}P-ATP. The reaction mix was incubated for 30 min at room temperature.

For Aur-A immunocomplex kinase assays, Aur-A was immunoprecipitated from 500μg PC-3 whole cell extract with 2μg anti-Aur-A antibodies for 4 hr at 4°C with rotation. Protein/antibody complexes were incubated with 40μl Sepharose A/G beads (Santa Cruz), overnight at 4°C with rotation. Unbound proteins were removed by washing the complex three times with Aur-A kinase assay buffer. The immunocomplexes were then resuspended in kinase assay buffer containing 250μM ATP and 5nM γ-^{32}P-ATP and incubated with 1μg His-Cofilin for 30 min at room temperature.

For LIMK1 immunocomplex kinase assays, LIMK1 was immunoprecipitated from 500μg PC-3 whole cell extract with 2μg anti-LIMK1 antibodies for 4 hr at 4°C with rotation. Protein/antibody complexes were incubated with 40μl Sepharose A/G beads, overnight at 4°C with rotation. Unbound proteins were removed by washing three times with LIMK1 kinase assay buffer. The immunocomplexes were then resuspended in kinase assay buffer containing 250μM ATP and 5nM γ-^{32}P-ATP and incubated with the appropriate substrate (1μg His-cofilin or 1μg His-Aur-A^{K162M}) for 30 min at 30°C.

For G1 synchronized immunocomplex kinase assays, LIMK1, or Cdk4 was immunoprecipitated from 100μg nuclear PC-3 extract with 200ng anti-LIMK1 or anti-Cdk4 antibodies for 4 hr at 4°C with rotation. Protein/antibody complexes were incubated with 20μl Sepharose A/G beads overnight at 4°C with rotation. Unbound proteins were removed by washing three times with the appropriate

kinase assay buffer. The immunocomplexes were then resuspended in kinase assay buffer containing 250μM ATP and 5nM γ-^{32}P-ATP and incubated with 1μg His-Cofilin (LIMK1) or 1μg purified recombinant His-Rb (amino acids 779-928) (Millipore) for 30min at 30°C.

All reactions were stopped by the addition of sample buffer and proteins were denatured by boiling at 95°C for 5 min. Proteins were run on 12% SDS gel and visualized by staining with coomassie stain (1% coomassie brilliant blue R-250, 50% methanol, 10% acetic acid) for 1 hr or overnight. The unbound dye was removed with destaining buffer (50% methanol, 10% acetic acid) for 2 hrs. Gels were placed in between two cellophane sheets and then dried. The dried gels were placed in an autoradiography cassette with Classic Blue Autoradiography Film (Midsci) at -80°C.

Aur-A non-radioactive kinase assays were performed as described above except in the absence of γ-^{32}P-ATP. In some experiments, whole cell extract (50μg lysate or 500μg IP) of PC-3 or transfected RWPE-1 cells were prepared with RIPA lysis buffer without phosphatase inhibitors and incubated with calf intestinal phosphatase (100 units for IP, 5 units for lysate) at 37°C for 30 min (NEB) to remove existing phosphorylation. Next, either lysate or immunoprecipitated LIMK1 were used for kinase assays in the presence or absence of phosphatase inhibitors (sodium orthovanadate, sodium fluoride, and β-glycerophosphate). LIMK1 phosphorylation was detected by immunoblotting as described above with anti-pT^{508}-LIMK1 antibodies.

LIMK1 non-radioactive kinase assays were performed as described above except in the absence of γ-^{32}P-ATP. LIMK1 was immunoprecipitated from 500μg PC-3 whole cell extract as described above and incubated with 1μg His-Aur-A or His-Aur-A^{K162M}. Aur-A phosphorylation at T^{288} was detected by immunoblotting as described above and with anti-pT^{288}-Aur-A antibodies.

3.11 His-pull-down assays

His-tag affinity precipitation was performed using PC-3 and RWPE-1 whole cell extracts. RWPE-1 cells were transfected with LIMK1 constructs as describe above and harvested at 24 hrs post-transfection. For the assay, 30μg of recombinant His-Aur-A or His-Aur-A^{K162M} was incubated with MagNi-His beads (Promega) for 45 min at room temperature. Beads were washed with 100mM HEPES, pH 7.5 three times and incubated with 500μg whole cell lysates at room temperature for 1 hr. Beads were washed three times with a buffer (100mM HEPES, pH 7.5) containing 20mM Imidazole and proteins were eluted in the same buffer containing 500mM imidazole. The presence of LIMK1 in the eluates was determined by immunoblotting as described above with anti-LIMK1 or anti-Flag antibodies.

3.12 Co-Immunoprecipitation assays

For Aur-A/Cofilin co-immunoprecipitation, PC-3 cells (5x10^5) were seeded onto a 10cm dish. The next day, cells were treated with 2nM nocodazole for 24 hr to enrich the cells at G2/M. Cells were released into mitosis with fresh media without nocodazole for 0, 30, or 60 min. Cells were harvested by trypsinization

and total protein extracted in RIPA lysis buffer as described above. Extracts (500µg) were incubated with 2µg anti-Aur-A antibodies for 4 hr at 4°C. Sepharose A/G beads (40µl) were added and incubated overnight at 4°C. Protein/antibody complexes were washed in RIPA lysis buffer three times. The beads were resuspended in 10µl dh_20 and diluted in sample buffer and boiled at 95°C for 5 min. The immunoprecipitate was electrophoresed, transferred to PVDF membrane, and immunoblotted as described above with anti-Cofilin antibodies.

3.13 Phosphopeptide analysis

For analysis of phosphorylation sites in LIMK1, 1µg GST-LIMK1 was incubated with 1µg His-Aur-A or His-Aur-A^{K162M} in Aur-A kinase assay buffer containing 250µM ATP at room temperature for 30 min and separated on a 4-20% SDS gradient gel. For Cofilin phosphorylation site analysis, 1µg His-Cofilin was incubated with 1µg His-Aur-A or His-Aur-A^{K162M} in Aur-A kinase assay buffer containing 250µM ATP at room temperature for 30 min and separated on a 12% SDS gel. Proteins were coomassie stained and LIMK1 or Cofilin bands were excised from the gel for LC MS/MS analysis performed at the W.M. Keck Foundation Biotechnology Resource Laboratory (Yale Cancer Center Mass Spectrometry Resources). Samples were digested with trypsin and phosphopeptides were enriched with TiO_2. Enriched fractions and flow through were analyzed on a LTQ Orbitrap mass spectrometer. The enriched fraction contained phosphopeptides and the flow through contained all the other peptides

39

that did not bind to the TiO_2 column. All MS/MS spectra were searched using the automated Mascot algorithm with a confidence level set at 95% against the NCBInr database human taxonomy.

3.14 Immunofluorescence

For immunofluorescence of mitotic cells, PC-3 or M12 (1.5x104) cells were seeded onto a coverslip in a 24-well dish. The next day, the cells were treated with nocodazole as described above for 24 hrs. Media was removed by washing with PBS three times and the cells were fixed with 4% paraformaldehyde (Sigma) for 5 min at room temperature. Next, cells were further fixed with cold methanol for 10 min at -20°C. The coverslips were blocked in PBS containing 10% goat serum (Sigma), 2% BSA (Sigma), and 0.2% tween-20 (Fisher). Cells were incubated with primary antibodies (Table 5) diluted in blocking solution for 1 hr at room temperature. Unbound primary antibodies were removed by washing with blocking solution three times. Cells were incubated next with fluorophore conjugated secondary antibodies (Table 6) in blocking solution for 30 min at room temperature in the dark. Unbound secondary antibodies were removed by washing with 100mM sodium phosphate buffer three times, 5 min each. Coverslips were mounted using DAPI Fluoromount G (Southern Biotech).

M12 cells ($4x10^4$) were seeded onto poly-L-lysine coated glass coverslips and transfected with Cofilin-RFP constructs 24 hrs later as described above. At 48 hrs post-transfection, cells were washed with PBS, fixed using 4%

paraformaldehyde and permeablized with 4% paraformaldehyde containing 0.2% tween-20 as described above. Cells were stained with phalloidin and DAPI mounted as described above.

For F-actin staining of MCF7 cells, 3×10^4 cells were seeded onto poly-L-lysine coated glass coverslips. Coverslips were washed with PBS and fixed with 4% paraformaldehyde and permeabilized with 4% paraformaldehyde containing 0.2% Tween-20 as described above. Coverslips were stained with phalloidin and DAPI mounted as described above. Cells were visualized on a Leica TCS SP5II confocal microscope.

Table 5. Immunofluorescence Primary Antibodies and Stains

Antigen	Company	Catalog No.	Host	Dilution
A-tubulin	Sigma	T9026	Mouse	1:200
Aur-A	Abcam	Ab13824	Mouse	1:200
Aur-A(pY^{88})	Cell Signaling	3079	Rabbit	1:250
Cofilin	Cytoskeleton	PA5-19727	Rabbit	1:200
Cofilin(pS^3)	Cell Signaling	3313	Rabbit	1:75
Phalloidin-488	Molecular Probes	A12379	---	1:200

Table 6. Immunofluorescence Secondary Antibodies

Antigen	Fluorophore	Company	Catalog No.	Host	Dilution
Mouse IgG	488	Molecular Probes	A11001	Goat	1:300
Mouse IgG	Cy3	Molecular Probes	A10521	Goat	1:300
Rabbit IgG	Cy3	Molecular Probes	A10520	Goat	1:300
Mouse IgG	647	Molecular Probes	A21244	Goat	1:300
Rabbit IgG	647	Molecular Probes	A21235	Goat	1:300
Sheep IgG	647	Molecular Probes	A21448	Donkey	1:300

3.15 Flow Cytometry

G0 enriched and asynchronous populations of PC3 cells were trypsinzed, washed with PBS and resuspended in PBS at a concentration of 5×10^5 cells/mL. Cells were fixed with 4% paraformaldehyde in PBS on ice for 10 min. Paraformaldehyde was removed by washing with PBS three times and cells were permeablized with PBS containing 0.25% saponin (Sigma) and 100ng RNAse A (Sigma) at room temperature for 20 min. Saponin was removed by washing

three times with PBS and cells were resuspended in PBS containing 2% BSA and 0.1% pluronic (Sigma). DNA was stained with propidium iodide (400µg/mL) (BD Pharmagen) for 30 min at room temperature in the dark. Flow cytometry was performed on a FACS-Calibur (Becton Dickinson) and data was analyzed using ModFit software (Verity Software House).

<u>3.16 Actin Depolymerization Assays</u>

Pyrene labeled actin (Cytoskeleton) was polymerized in the presence of polymerization buffer (2mM $MgCl_2$, 0.5mM ATP, 0.2M KCl, pH 7.0) for 2 hr at RT. The polymerized actin was then incubated with His-Cofilin, His-Cofilin^{S3A}, His-Cofilin$^{S3A/S8A/T25A}$ that had previously been phosphorylated by Aur-A as described above for 10 min at RT. F-actin was stained with phalloidin (1:200 dilution) as described above and the actin/protein mixture was mounted on coverslips. Actin filaments were visualized by confocal microscopy.

CHAPTER FOUR: THE ROLE OF LIMK1 IN G1/S PHASE PROGRESSION

4.1 Introduction

LIMK1 has been implicated to play a role in G1/S phase progression. Previous studies in our laboratory showed that overexpression of LIMK1 resulted in a transient G1/S phase arrest, but the mechanism behind this arrest is currently unknown [45]. In this study, we examined how expression of LIMK1 altered the expression of G1 phase regulatory proteins. Ectopic expression of LIMK1 altered the amounts of $p27^{Kip1}$, $p27^{Kip1}$-pY^{88}, and $p27^{Kip1}$-pS^{10} in G0 enriched cell populations. We noted decreased levels of $p27^{Kip1}$, $p27^{Kip1}$-pY^{88}, and $p27^{Kip1}$-pS^{10} upon overexpression of LIMK1 and increased levels $p27^{Kip1}$, $p27^{Kip1}$-pY^{88}, and $p27^{Kip1}$-pS^{10} upon knockdown of LIMK 1.

To examine the role of LIMK1 during G1 phase progression, we enriched PC-3 cells in G0 by serum starvation. Cells were released in to G1 phase by the addition of EGF and nuclear accumulation of the G1 phase regulatory proteins: such as LIMK1, Cyclin D1, $p27^{Kip1}$-pY^{88}, and Cdc25A, were quantified by immunoblotting. Immunocomplex kinase assay was used to determine the kinase activities of nuclear LIMK1 and Cdk4. Our results showed increased phosphorylation of LIMK1 and Cdk4 activities as early as 30 min after EGF release. Increased phosphorylation of $p27^{Kip1}$ at Y^{88} was also noted at 30 min after release, suggesting early progression of G1 phase.

.

4.2 Results

4.2.1 Ectopic Expression of LIMK1 Altered p27^{Kip1} Expression and Phosphorylation

To study the expression and subcellular localization of G1 phase regulatory proteins, PC-3 cells were synchronized at G0. PC-3 cells were seeded onto 10cm dish and next day the media was changed to F12-HAM without FBS. Cells were incubated for 48 hrs and were harvested. Cell cycle profile of the serum starved cells was analyzed by propidium iodide staining and quantified by flow cytometry (Fig. 5). Serum starvation enriched the G0 population of cells (~20%) compared to the asynchronous cell population.

To study p27^{Kip1} phosphorylation during G1, we produced antibodies directed against a peptide that would recognize Y^{88} phosphorylation. To confirm the specificity of the antibodies a peptide/antibody competition assay was performed. Fifty µg of the whole cell extract was separated by SDS-PAGE and transferred to a PVDF membrane. The p27^{Kip1}-pY^{88} antibodies were incubated with 0, 1, 2, 5, or 10 times the molar ratio of the phospho-peptide to antibodies for 1 hr at 4°C (Fig. 6). A PVDF membrane bound p27^{Kip1} was incubated with the phospho-peptide bound antibodies overnight at 4°C. p27^{Kip1} bound to the membrane was detected by immunoblotting using p^{27Kip1}-pY^{88} antibodies. Our results showed that p27^{Kip1}-pY^{88} antibodies specifically recognized the phospho-peptides as the intensity of p27^{Kip1} polypeptide bands was reduced significantly

when antibodies were incubated with the peptide at 2x molar ratio compared to untreated antibodies. No polypeptide bands were detected with antibodies incubated with the peptides at 5x and 10x molar ratios.

Next, we examined if alteration of LIMK1 expression affects the expression of $p27^{Kip1}$. P69 cells, which express low levels of LIMK1 were transfected with a construct containing Flag-tagged full-length LIMK1. At the same time, cells were incubated in serum free media for 48 hrs, to enrich the G0 population (Fig. 7A&B). Cells were harvested and expressions of $p27^{Kip1}$, $p27^{Kip1}$-pY^{88}, and $p27^{Kip1}$-pS^{10} were detected by immunoblotting. Cells expressing LIMK-Flag showed reduced levels of $p27^{Kip1}$, $p27^{Kip1}$-pY^{88}, and $p27^{Kip1}$-pS^{10} compared to the vector only cells. Next, we transfected PC-3 cells, which express higher levels of LIMK1, with LIMK1 shRNA or scrambled shRNA and cells were incubated in serum free media to enrich the G0 population (Fig. 8A&B). Cell transfected with LIMK1 shRNA expressed higher levels of $p27^{Kip1}$ and $p27^{Kip1}$-pY^{88} compared to cells transfected with the scrambled shRNA control. Together, this data suggests that LIMK1 regulates G1 phase progression through alteration of $p27^{Kip1}$ expression and phosphorylation.
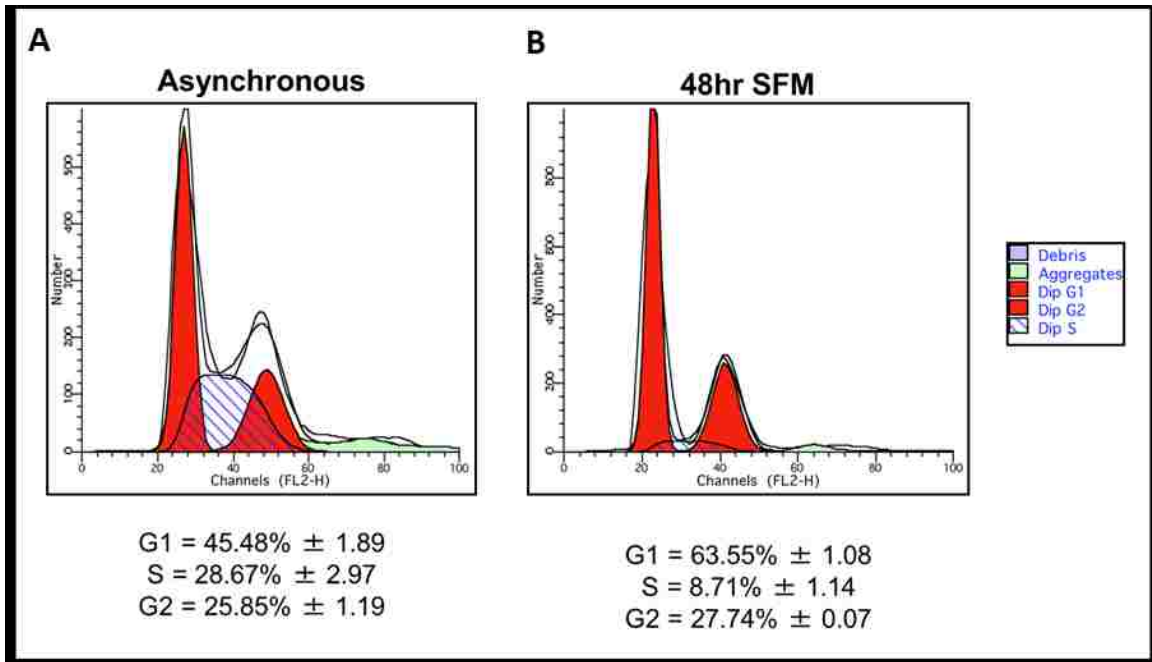
Figure 5: Enrichment of PC-3 cells at G0.

Two parameter histogram showing progression of asynchronous (A) or G0 enriched (B). The X-axis represents the DNA content and the Y-axis represents number of cells. Data shows an increased percentage of cells in G1 phase of serum starved cells compared to the asynchronous PC-3 cells.
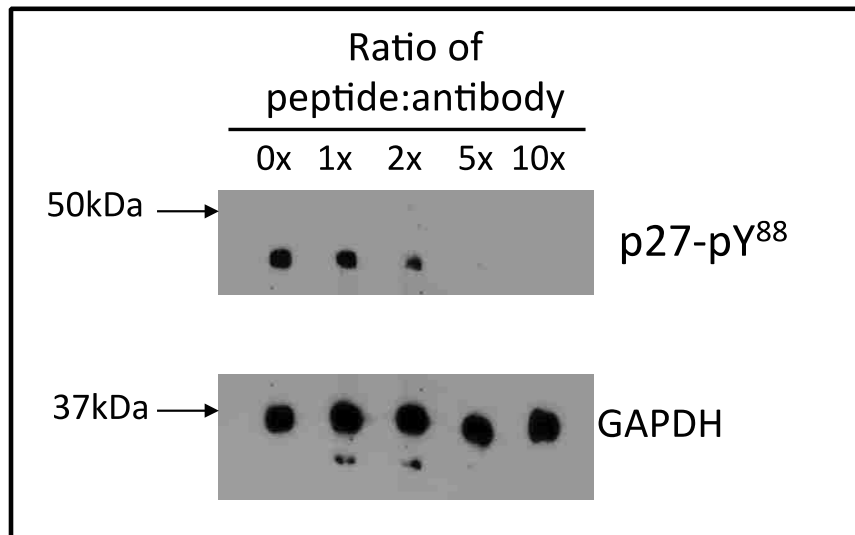
Figure 6: Confirmation of p27^{Kip1}-pY^{88} antibody specificity.

Western blot analysis of the p27^{Kip1} in the whole cell extracts using peptide-bound p27^{Kip1}-pY^{88} antibodies. Data shows a gradual decrease in the band intensity upon incubation of antibodies with increasing molar ratio of phospho-peptides . GAPDH was used as a loading control.
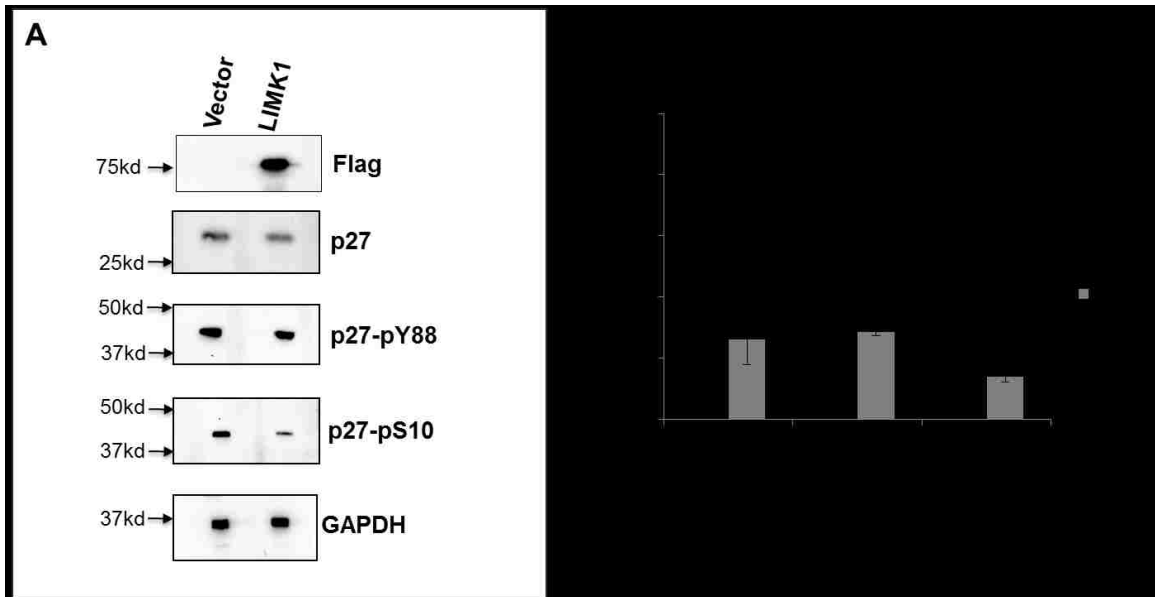
Figure 7: Overexpression of LIMK1 altered p27^{Kip1} expression.

(A) Western blot analysis of the expression of p27^{Kip1}, p27^{Kip1}-pY^{88} and p27^{Kip1}-pS^{10} in LIMK1-Flag expressing P69 cells using specific anti-p27^{Kip1}, anti-p27^{Kip1}-pY^{88} and anti-p27^{Kip1}-pS^{10} primary antibodies. Expression of LIMK1-Flag was detected using anti-Flag antibodies. GAPDH was used as the loading control. Data shows decreased levels of unphophorylated and phosphorylated p27^{Kip1} in cells expressing LIMK1 compared to the vector control. (B) Densitometric analysis of p27^{Kip1}, p27^{Kip1}-pY^{88}, and p27^{Kip1}-pS^{10} levels from A normalized to the vector only control.
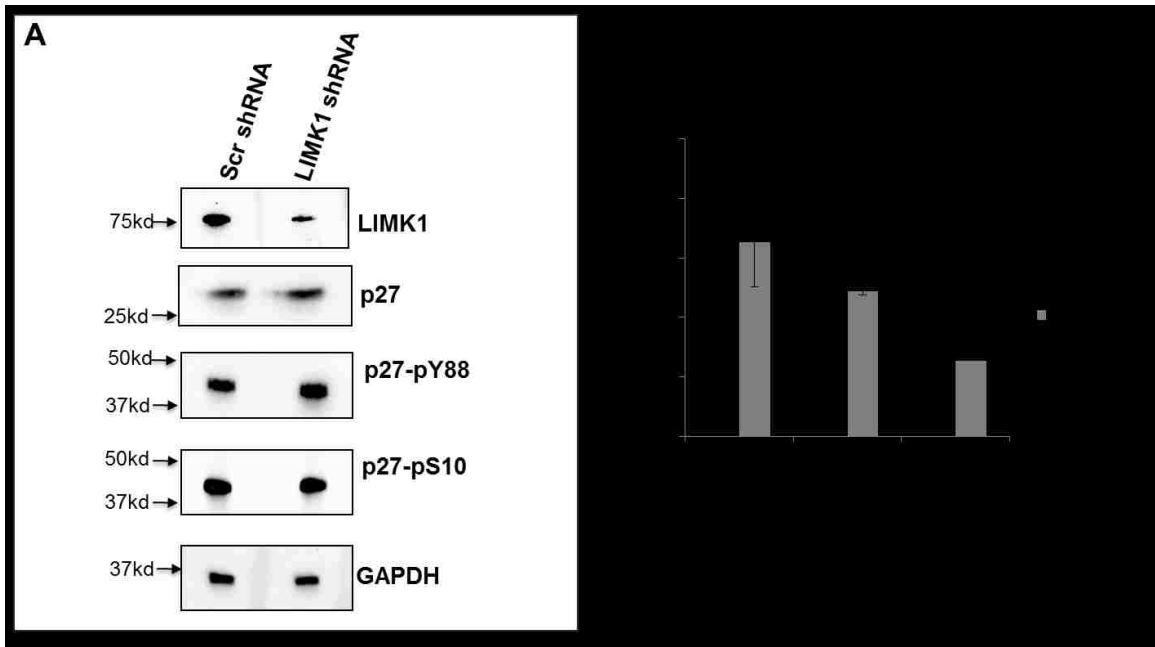
Figure 8: Knockdown of LIMK1 Altered p27^{Kip1} Expression.

(A) Western blot analysis of the expression of p27^{Kip1}, p27^{Kip1}-pY^{88} and p27^{Kip1}-pS^{10} in LIMK1-shRNA expressing PC-3 cells using specific anti-p27^{Kip1}, anti-p27^{Kip1}-pY^{88} and anti-p27^{Kip1}-pS^{10} primary antibodies. Expression of endogenous LIMK1-Flag was detected using anti-LIMK1 antibodies. GAPDH was used as the loading control. Data shows increased levels of unphosphorylated and phosphorylated p27^{Kip1} in cells expressing LIMK1-shRNA compared to the cells expressing scrambled RNA. (B) Densitometric analysis of p27^{Kip1}, p27^{Kip1}-pY^{88}, and p27^{Kip1}-pS^{10} levels from A normalized to the scrambled RNA control only control.

4.2.2 Expression and Activities of Nuclear Localized G1 Phase Regulatory Proteins

To study the role of LIMK1 on G1 phase regulatory proteins we first examined the steady state expression and activities of these proteins. PC-3 cells were synchronized to G0 by serum starvation and released into G1 by the addition of EGF for 0, 15, 30, 120, 240, or 480 mins. Cells were harvested and nuclear and cytoplasmic proteins were prepared. Immunoblot analysis revealed the highest nuclear localization of LIMK1 at 15 and 30 mins, which decreased ~2-fold at 120, 240, and 480 mins (Fig. 9A&B). Catalytic activity of nuclear LIMK1 was highest at 30 mins and remained relatively stable at all other timepoints (Fig. 10A&B). Nuclear localization of Cyclin D was stimulated early as high levels were detected at 15 and 30 mins, but then slowly declined from 120 through 480 mins (Fig. 11A&B). Nuclear expression of $p27^{Kip1}\text{-}pY^{88}$ followed the opposite pattern with low levels at 15 and 30 mins, but increased greatly from 120-480 mins (Fig. 12A&B). The kinase activity of nuclear Cdk4 followed a similar pattern, as the activity was low at 15 mins but increased at 30 and 120 mins and plateaued out at 240 and 480 mins (Fig. 13A&B). Expression of Cdc25A was not detected in the nuclear extracts upto 24 hrs but was detected in the cytoplasmic extracts in all timepoints (Fig. 14).
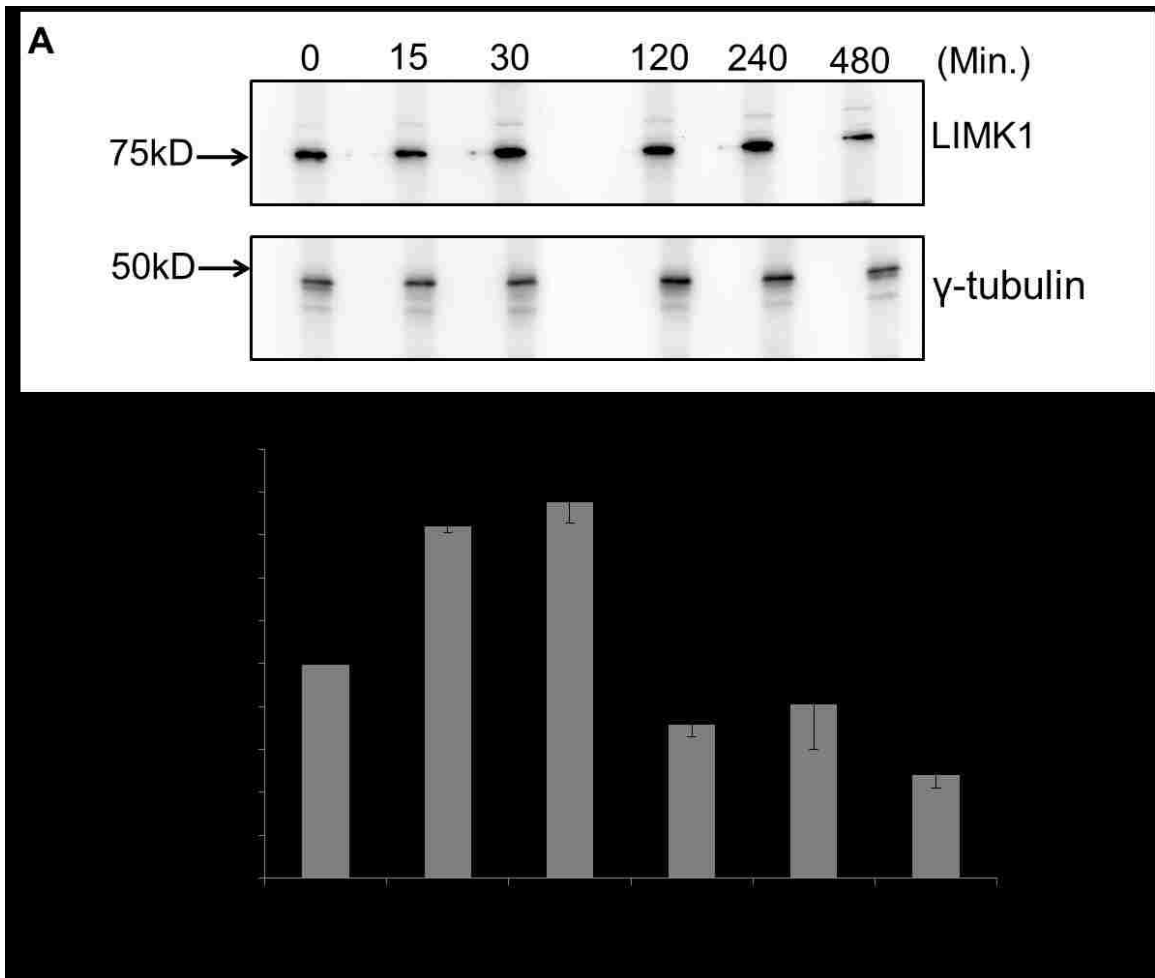
Figure 9: Nuclear localization of LIMK1 During G1 progression.

(A) Western blot analysis LIMK1 expression in G0 enriched PC-3 cells at specified time points upon treatment with EGF using anti-LIMK1 antibodies. (B) Densitometric analysis of the values from A normalized to 0hr.
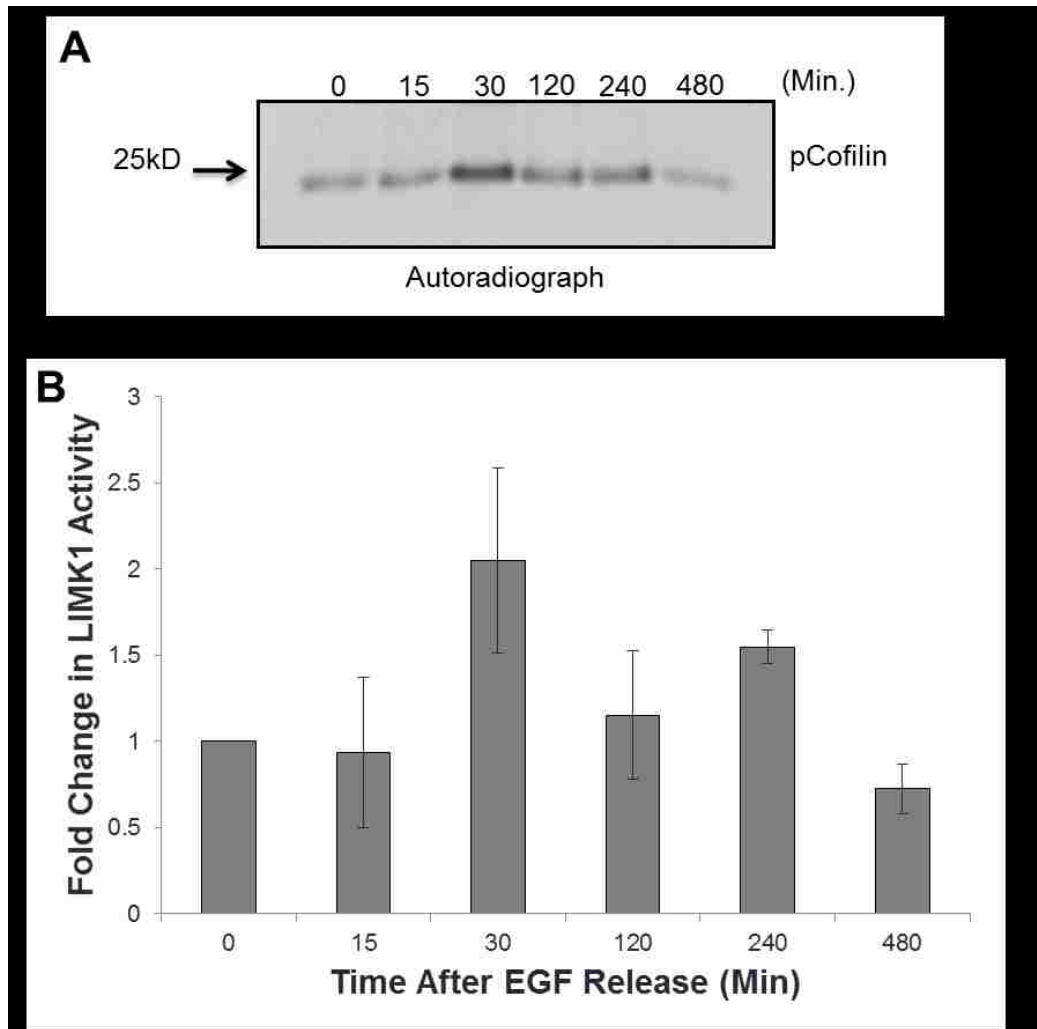
Figure 10: Kinase activity of nuclear LIMK1 during G1 progression.

(A) Autoradiograph of the immunocomplex kinase assay of nuclear LIMK1 in G0 enriched PC-3 cells at various time points after EGF treatment were enriched at G0 by serum starvation for 48 hours and stimulated with EGF. (B) Densitometric analysis of the radioactive pCofilin bands in A normalized to 0hr.
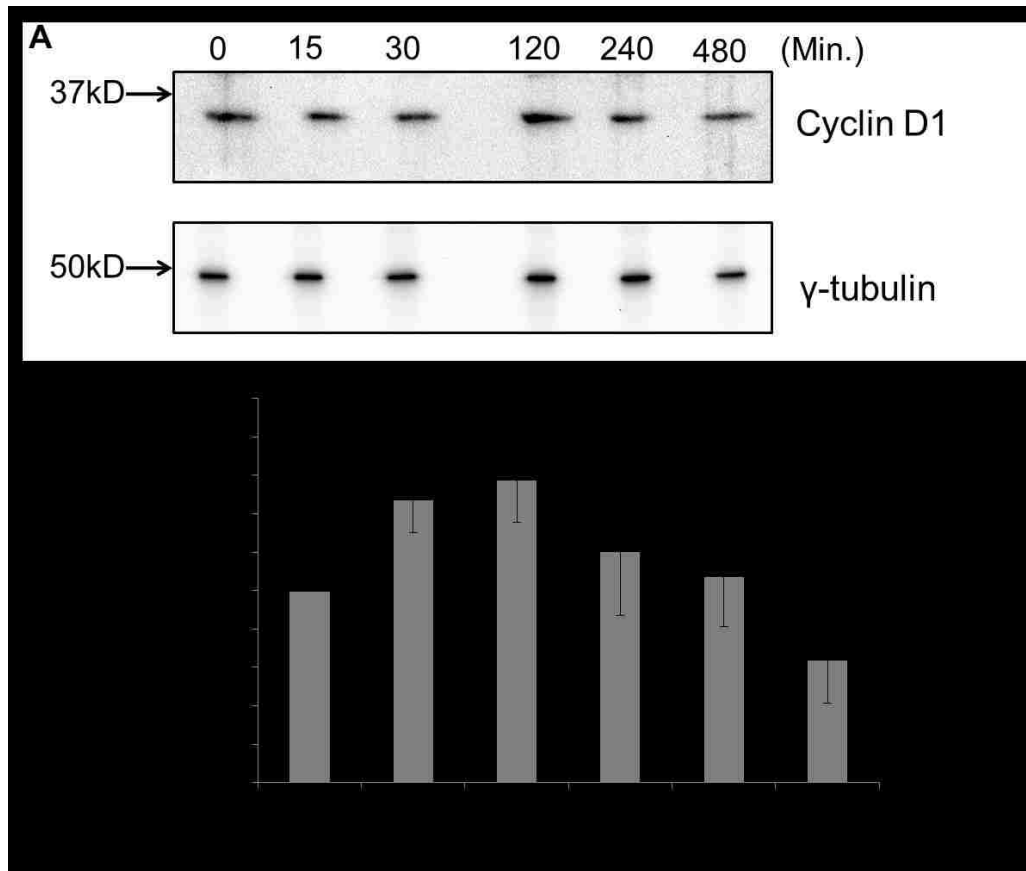
Figure 11: Nuclear expression of Cyclin D1 during G1 progression.

(A) Western blot analysis of Cyclin D1 in the nuclear extracts of G0 enriched PC-3 cells at different time points after EGF treatments using anti-Cyclin D1 antibodies. γ-tubulin was used as the loading control to analyze the relative expression. (B) Densitometric analysis of values from A normalized to 0hr.
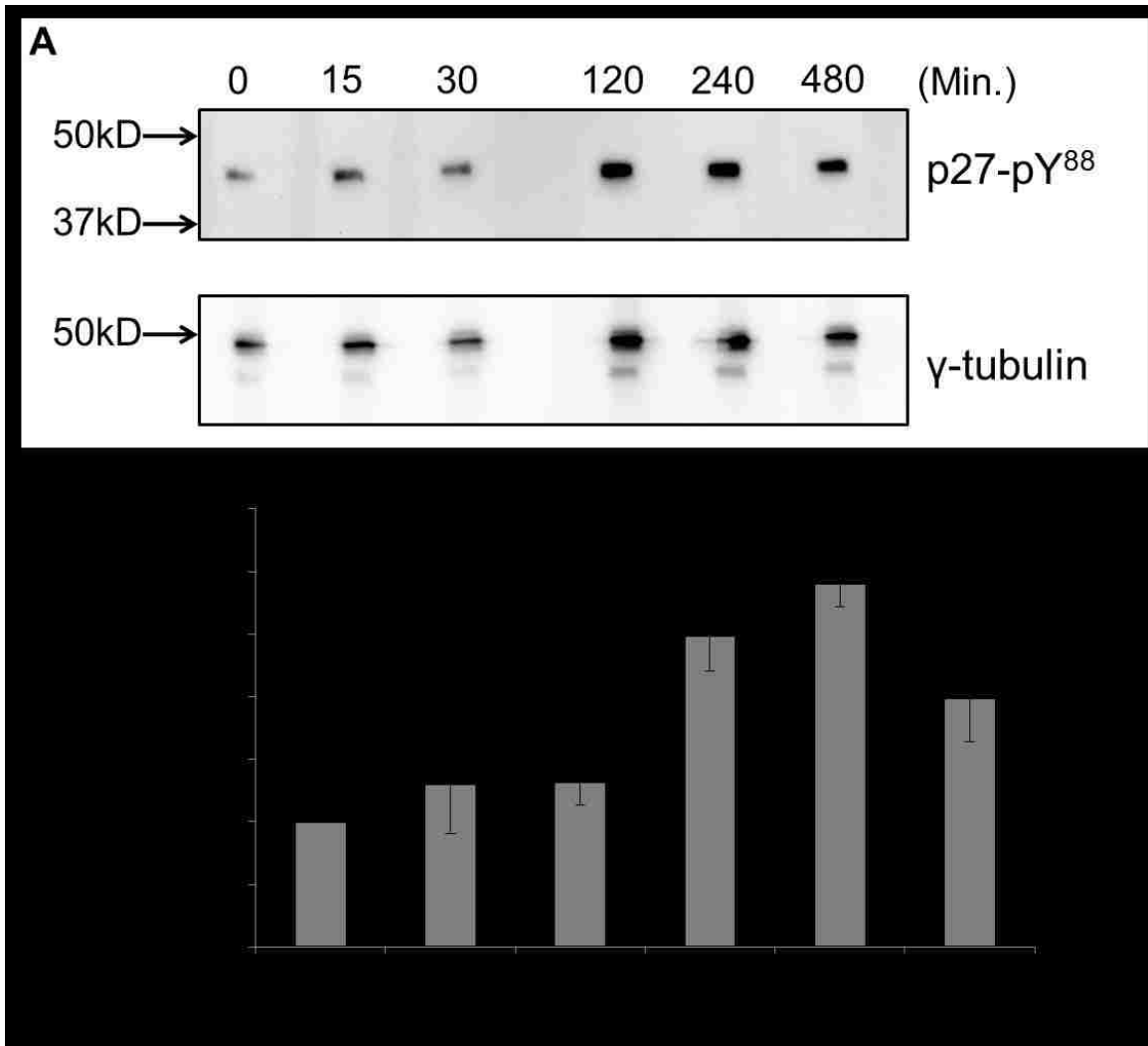
Figure 12: Nuclear expression of p27^{Kip1}-pY^{88} during G1 progression.

(A) Western blot analysis of p27^{Kip1}-pY^{88} in the nuclear extracts of G0 enriched PC-3 cells at different time points after EGF treatments using anti-p27^{Kip1}-pY^{88} antibodies. γ-tubulin was used as the loading control to analyze the relative expression. (B) Densitometric analysis of values from A normalized to 0hr.
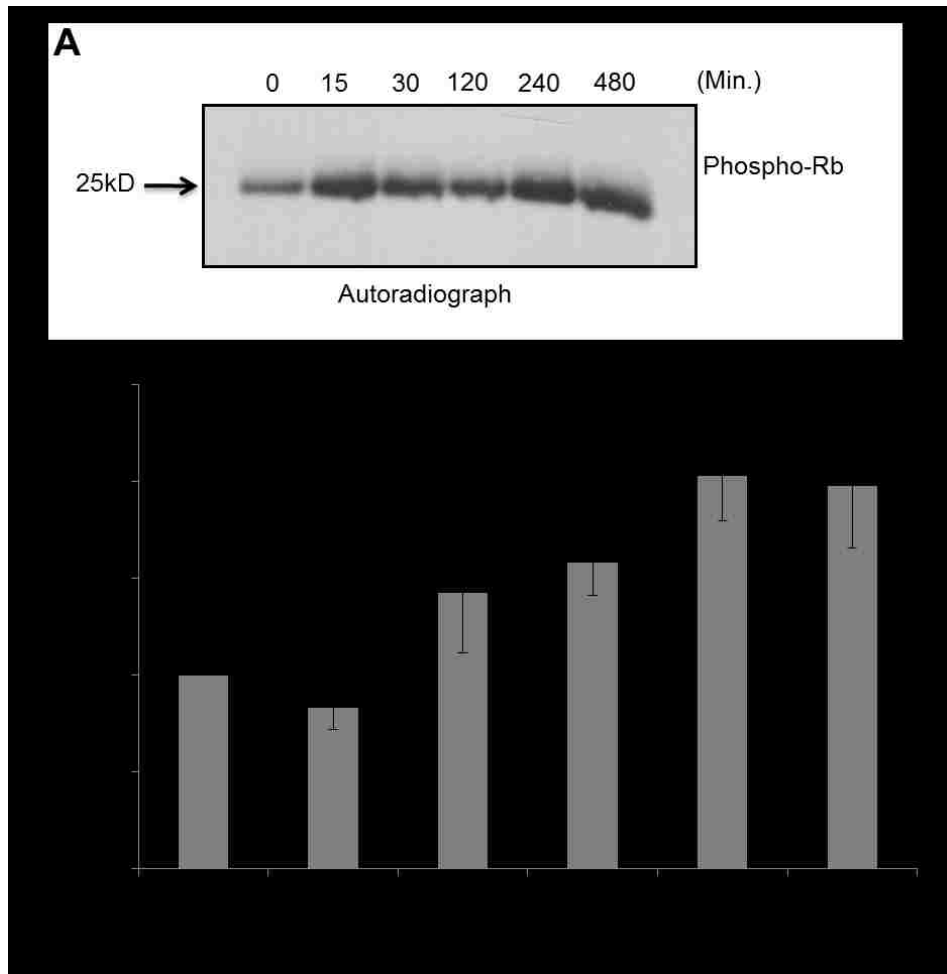
Figure 13: Kinase activity of nuclear Cdk4 during G1 progression.

(A) Autoradiograph of the immunocomplex kinase assay of nuclear Cdk4 in G0 enriched PC-3 cells at various time points after EGF treatment. (B) Densitometric analysis of the radioactive pRb bands in A normalized to 0hr.
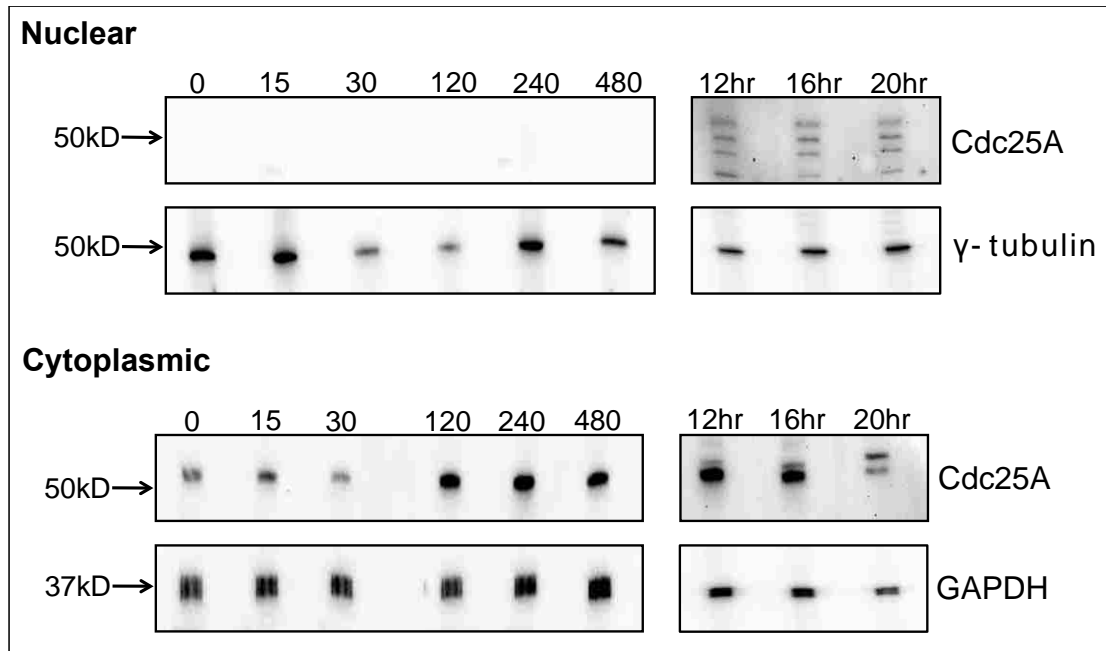
Figure 14: Nuclear and cytoplasmic expression of Cdc25A during G1 progression.

Upper panel: Western blot analysis of Cdc25A in the nuclear extracts of G0 enriched PC-3 cells at different time points after EGF treatments using anti-Cdc25A antibodies. γ-tubulin was used as the loading control to analyze the relative expression. Lower panel: Western blot analysis of Cdc25A in the cytoplasmic extracts of G0 enriched PC-3 cells at different time points after EGF treatments using anti-Cdc25A antibodies. GAPDH was used as the loading control

4.3 Discussion

Our lab has shown that overexpression of LIMK1 causes a transient G1/S arrest but the mechanism of this arrest is unknown [45]. In this study, we found overexpression of LIMK1-Flag resulted in reduced concentration of p27^{Kip1}-pY^{88}, while knockdown of LIMK1 resulted in increased levels of p27^{Kip1}-pY^{88}. Since phosphorylation at Y^{88} inactivates p27^{Kip1}, our data suggests LIMK1 overxpression delays G1 progression via induction of p27^{Kip1} functions. Alternatively, LIMK1 knockdown most likely increased G1 phase progression via increased levels of inactive p27^{Kip1} (p27^{Kip1}-pY^{88}). However, the mechanism of LIMK1 induced alterations of p27^{Kip1} expression and phosphorylation is currently unknown. LIMK1 has been shown to physically interact with p57^{Kip2} but not with p27^{Kip1}, so it is unlikely that LIMK1 is directly involved in p27^{Kip1} phosphorylation [48]. Studies have shown that overexpression of Cofilin arrests cells in G1 phase through induction of p27^{Kip1} expression [89]. The phosphorylation status of Cofilin was not examined, but LIMK1 may have a role in p27^{Kip1} induction through regulation of Cofilin phosphorylation.

We also identified the steady state nuclear expression of G1 phase regulatory proteins. We noted elevated nuclear expression of p27^{Kip1}-pY^{88} and Cdk4 activity as early as 30 minutes after EGF release, suggesting early G1 progression. Since Cdc25A was not detected or barely detected in the nuclear extracts at 20 hrs after release, it is likely that the transition into late G1/S phase took longer than 24hrs after EGF release.

CHAPTER FIVE: FUNCTIONAL COOPERATIVITY BETWEEN AURORA A KINASE AND LIM KINASE 1: IMPLICATION IN THE MITOTIC PROCESS

5.1 Introduction

Aurora A kinase (Aur-A) is a serine/threonine kinase and a member of the Aurora kinase family, which plays important roles in various but distinct mitotic processes [175], [176]. Although not a bonafide oncogene, Aur-A is overexpressed in a variety of adenocarcinomas, including cancers of the breast, skin and prostate [144], [177], [178] . Therefore, much attention has been focused on identification of Aur-A inhibitors as anticancer agents [179],[180], [181] some of which showed success in clinical trials [182]-[184] singly or in combination with EGF-R inhibitors for drug-resistant cancer or with actinomycin D in p53-based cyclotherapy [185], [186]. At the same time, an increased interest in understanding the mechanism of Aur-A activation, and identification of interacting partners and substrates that are phosphorylated by Aur-A led to a multitude of published reports in recent years [112], [187]-[189].

Aur-A activity increases in G2, with its targeting to the centrosomes by activated Plk1 [190], which then allows initiation of early mitotic events, such as centrosome maturation and separation and spindle assembly [138], [175], [176], [191], [192]. Aur-A plays a role in centrosome maturation through recruitment of γ-tubulin [67], ChToh [193], NDEL1 [134], TACC [134], and LATS2 [135] to the centrosomes and bipolar spindle assembly through interaction with microtubule associated proteins TPX2, XMAP and HURP, forming a complex [102], [137],

[194].   Aur-A phosphorylates LATS2 at a specific site (S^{380}), which allows its colocalization with the other family member, Aur-B, at the central spindle [133]. Recent studies showed that MT-binding protein TPX2 targets Aur-A to the spindle microtubules and induces autophosphorylation of Aur-A at T^{288} through a conformational change [131], [188], [195].   Binding of TPX2 prevents dephosphorylation of Aur-A-pT^{288} and promotes accumulation of activated Aur-A. Aur-A then phosphorylates a variety of substrates [196], including LIM domain containing Ajuba [123] and Plk1 [118], which allows spindle assembly and bipolarity [135].

   Ajuba interacts with centrosomal Aur-A through its LIM domain with the non-catalytic N-terminal region of Aur-A, which then induces its phosphorylation by Aur-A. This interaction and subsequent phosphorylation promotes autophosphorylation of Aur-A and its complete activation [123].   Although a number of studies indicated involvement of a variety of interacting partners of Aur-A [197], [198], some of which are responsible for inhibition of Aur-A catalytic function [132], [199], the understanding of Aur-A regulation and protein functions regulated by Aur-A during mitotic phases is far from complete.

   Recent studies on LIM domain containing protein LIMK1 showed its localization to the centrosomes and association with γ–tubulin [152]. Furthermore, LIMK1 was shown to be involved in positioning of mitotic spindles during metaphase through modulation of cortical actin through phosphorylation of cofilin [163]. LIMK1 is a LIM domain containing serine/threonine kinase, which modulates actin and microtubule dynamics and participates in a variety of cellular

processes [55], [200]. Function of LIMK1 on the actin cytoskeleton is mediated through an inactivating phosphorylation of the actin depolymerizing family protein Cofilin [53], [57] and microtubule-binding protein p25α [153]. LIMK1 has two N-terminal LIM domains, a PDZ domain and a C-terminal kinase domain. LIMK1 interacts with a variety of proteins through its LIM and PDZ domains [154], [201], [202]. LIMK1 is activated by phosphorylation at T^{508} by ROCK, PAK1 or PAK4 and phosphorylates Cofilin at S^3, rendering it inactive. LIMK1 is activated in early mitotic phases, but its inactivation is required for cytokinesis [150], [162]. Overexpression of LIMK1 leads to cytokinesis defects [150] and formation of multipolar spindles [45], which are noted in a variety of cancers [45]. Although LIMK1 needs to be phosphorylated during early prophase [162] for its targeting to the centrosomes [152], it is not known which kinase(s) phosphorylates LIMK1 during mitosis. It has been shown that LIMK1 is not phosphorylated by ROCK or PAK during mitosis [150]. In this study, we show that LIMK1 is phosphorylated by the centrosomal kinase Aur-A and also participates in phosphorylating Aur-A. We further show that functions of both LIMK1 and Aur-A are important for integrity and bipolarity of mitotic spindles.

5.2 Results

5.2.1 LIMK1 Acts as a Substrate of Aurora A in vitro

Our lab has previously shown that LIMK1 co-localizes with γ-tubulin at the centrosomes during mitosis [26], [152]. Another group found that LIMK1 dependent phosphorylation of Cofilin during mitosis is necessary for proper

61

mitotic spindle alignment [29], [163]. We sought to examine the interaction, if any, of LIMK1 with other centrosomal mitotic proteins. Aurora A is a mitotic kinase that is expressed from late G2 through mitosis and localizes to the centrosome. It is responsible for proper mitotic spindle assembly. Another lab member used immunofluorescence assays to show that Aurora A and LIMK1 colocalized at the centrosome during mitosis. To study if this colocalization results in phosphorylation of LIMK1 by Aur-A, we performed *in vitro* kinase assays with recombinant His-tagged Cofilin (Fig. 15), GST-tagged inactive LIMK1 and active GST-Aur-A (Fig. 16). The activity of recombinant LIMK1 and Aur-A was tested by their ability to phosphorylate Cofilin and MBP, respectively, which showed that LIMK1 was not active, while Aur-A retained a high level of activity. Kinase assays showed a radioactive polypeptide band corresponding to LIMK1 in the presence of GST-Aur-A. Because GST-LIMK1 was inactive, LIMK1 phosphorylation was mediated by Aur-A. We also noted autophosphorylation of Aur-A during in vitro assays.

Because Aur-A interacts with the LIM domains while phosphorylating Ajuba [34]-[36], [123], we studied if LIM domains are required for Aur-A mediated phosphorylation of LIMK1. We used recombinant His-Aur-A, inactive His-Aur-A^{K162M} (Fig. 17&18), and inactive His-tagged kinase domain of LIMK1 (LIMK1^K), which contains the known phosphorylation site T^{508}, as the substrate for kinase assays. Indeed, the kinase domain of LIMK1 was phosphorylated by Aur-A independently of the LIM domains. Since the autophosphorylated His-Aur-A was similar in size to that of His-LIMK1^K (~50 kD) (Figure 19), the specificity of

phosphorylation was confirmed using increasing amounts of His-LIMK1^K as the substrate, which showed a corresponding increase in phosphorylation (Fig. 19, lanes 4-6). No phosphorylation was detected when His-LIMK1^K was incubated with the inactive Aur-A (Aur-A^{K162M}) (Fig. 19, lanes 7-9).
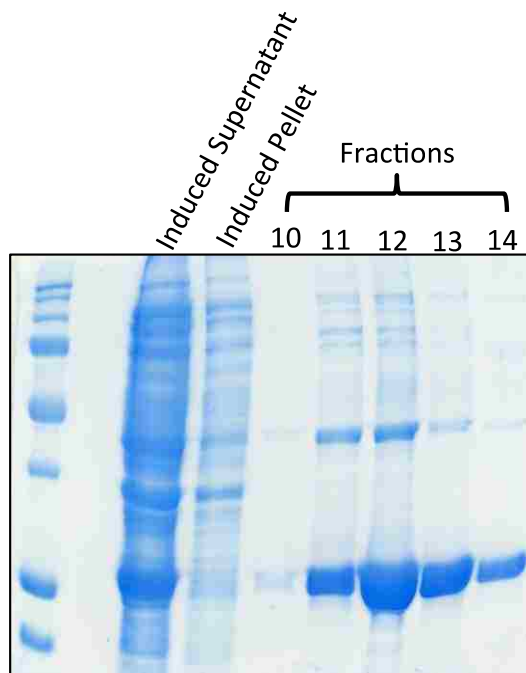
Figure 15: Purification of Recombinant His-Cofilin.

Coomassie stained SDS-PAGE of His-Cofilin expression in E.coli induced with 1mM IPTG. Lanes 2 and 3 show the expression of soluble His-Cofilin in the supernatant. Lanes 3 to 7 show retrieval of purified soluble His-Cofilin in different fractions of the affinity chromatography.
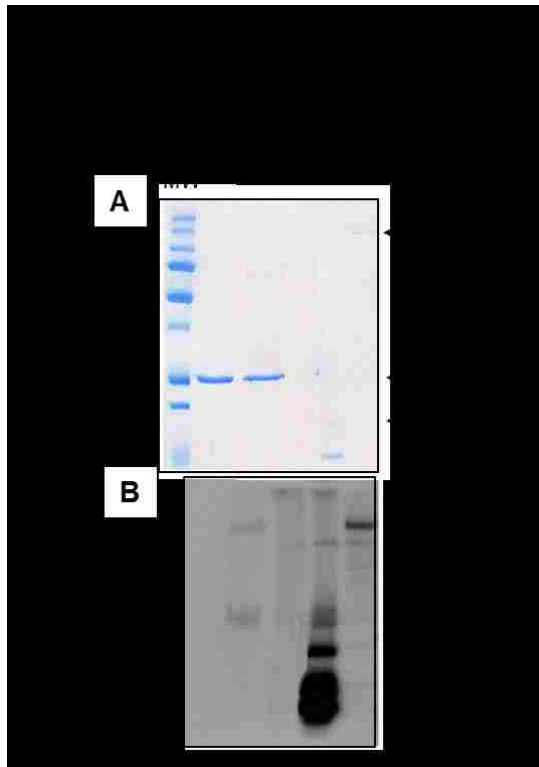
Figure 16: LIMK1 Acts as a Substrate of Aur-A

(A and B) Kinase assays with inactive GST-LIMK1 (500ng) and GST-Aur-A (50ng) kinases and His-Cofilin (1µg) or MBP (500ng) as respective substrates. (A) Coomassie stained SDS-PAGE showing location of the peptide bands. MW: molecular weight marker. (B) Autoradiogram showing no phosphorylation of His-Cofilin by GST-LIMK1 (lane 2), which confirms its inactivity. Strong phosphorylation of MBP and LIMK1 by Aur-A (lanes 4 and 5) and autophosphorylation of Aur-A (lanes 4 and 5) could be seen. Aur-A autophosphorylation seemed to be enhanced in the presence of MBP and LIMK1.
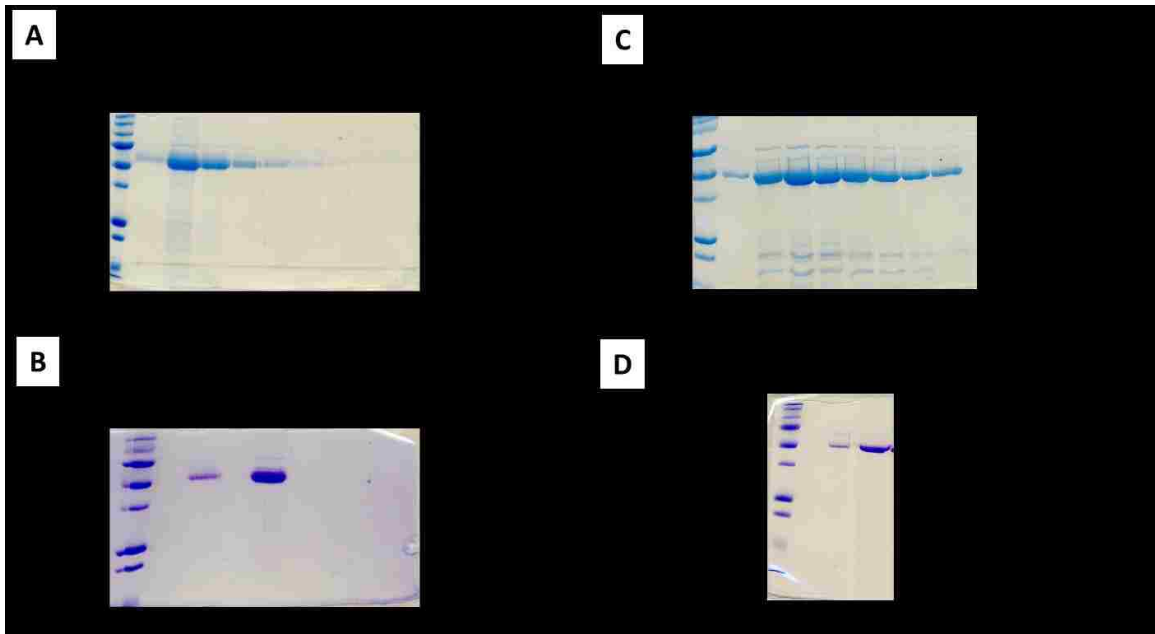
Figure 17: Expression and Affinity Purification of Recombinant His-Aurora A and His-Aurora A^{K162M}.

Coomassie stained SDS-PAGE of His-Aurora A (A&B) and His-Aurora A^{K162M} (C&D) expression in *E. coli* induced with 1mM IPTG. (A&C) Lanes 2-9 show retrival of purified soluble His-Aurora A or His-Aurora A^{K162M} in different fractions of the affinity chromatography. (B&D) Lanes 2 and 3 show 1 and 3μg of His-Aurora A or 1 and 5μg of His-Aurora A^{K162M} after buffer exchange and concentration.
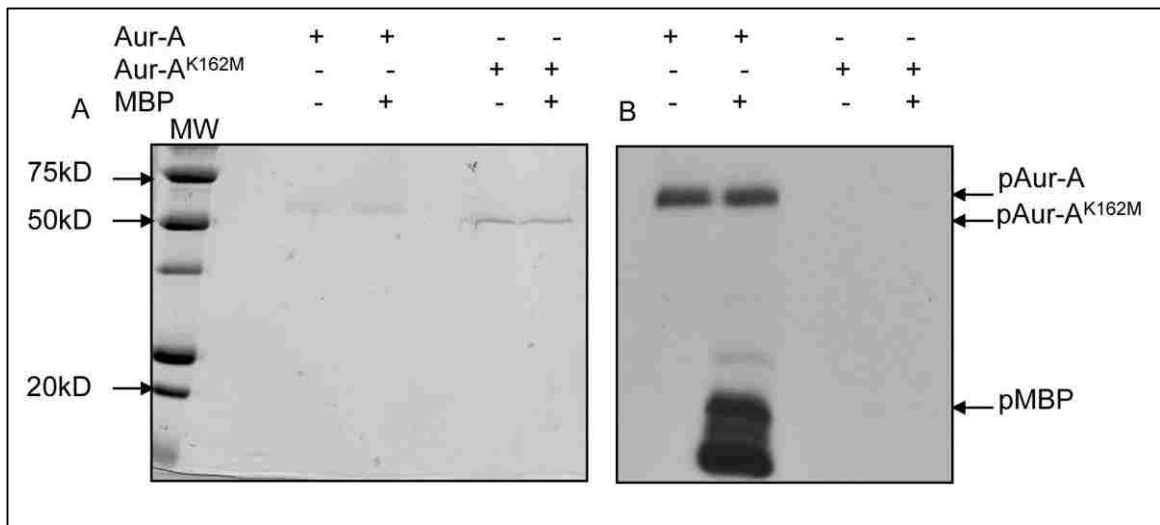
Figure 18: Kinase assays of recombinant His-Aur-A and His-Aur-A^{K162M}.

(A) Coomassie stained SDS-PAGE of kinase assay. (B) His-Aur-A (0.25µg) or His-Aur-A^{K162M} (0.25µg) was incubated with MBP (0.5µg) in kinase assay buffer containing γ-^{32}P-ATP. Phosphorylation was detected by autoradiography.
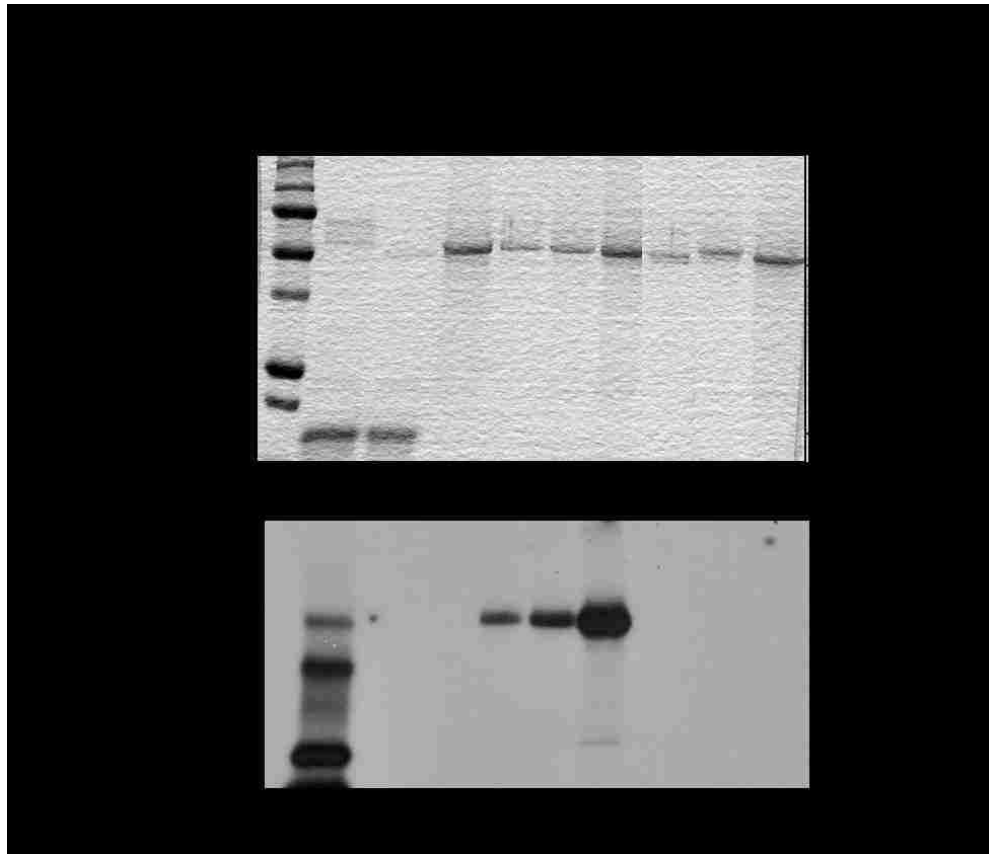
Figure 19: Aurora A Phosphorylates the Kinase Domain of Aurora-A.

(A and B) Phosphorylation of His-LIMK1[K] by active His-Aur-A. (A) Coomassie stained SDS-PAGE. (B) Autoradiogram showing increased phosphorylation intensity with increasing amounts of His-LIMK1 (0.25µg, 0.5µg, and 1µg) by active His-Aur-A (0.22µg) (lanes 4-6) but not by inactive His-Aur-A[K162M] kinase (0.22µg) (lanes 7-9). His-Aur-A[K162M] was also unable to phosphorylate MBP (1µg) (lane 2), which confirms catalytic inactivity of Aur-A[K162M] mutant. SDS-PAGE images are representative of 3-5 independent experimental repeats.

5.2.2 Aurora A Interacts with the LIM and Kinase Domains of LIMK1

The physical association between Aur-A and LIMK1 was determine by co-immunoprecipitation (CO-IP) and pull-down assays using both BPH-1 (benign prostatic hyperplasia) stable subline expressing FLAG-tagged LIMK1 (F-LIMK1) (BPHL^{CA}) and transiently transfected RWPE-1 cells expressing different domains of LIMK1 (Fig. 20). We used a construct of constitutively active phosphomimic (CA) mutant of LIMK1 (T^{508EE}) for stable expression to have fully active LIMK1. In the unphosphorylated form of LIMK1, the N-terminal LIM domains associate with the kinase domain, preventing its full activation. Phosphorylation at T^{508} disrupts this association, making the protein optimally active. Another student performed Co-IP assays followed by western blotting with Aur-A antibodies showed that Aur-A was pulled down with LIMK1 in BPHL^{CA} cells but not in the vector-only controls. There was no increase in overall expression of Aur-A in cells expressing F-LIMK1^{CA}. In a reverse experiment, LIMK1 was detected when Aur-A was immunoprecipitated from BPHL^{CA} extracts.

Experiments using extracts of PC-3 cells, which naturally overexpress LIMK1, and immobilized His-Aur-A or His-Aur-A^{K162M} (kinase dead) followed by western blotting showed that LIMK1 was pulled down with His-Aur-A and His-Aur-A^{K162M} but not the bead-only control (Fig. 21A). Densitometric analysis revealed that Aur-A^{K162M} was ~50% less efficient than Aur-A at pulling down LIMK1 (Fig. 21B). Lysates from RWPE-1 cells transiently transfected with pCMVLIMK1-FLAG (RWPE-1L) (Fig. 20) also showed pull down of LIMK1 with

His-Aur-A (Fig. 21C, top part). Next, we examined if it interacts with the LIM-domains of LIMK1. We used pCMVLIMK1^{LD}-FLAG and pCMVLIMK1^K FLAG constructs containing the LIM-domains or the kinase domain of LIMK1 (LIMK1^{LD} or LIMK1^K) (Fig. 20) and repeated the pull-down assays with extracts from RWPE-1 cells expressing these domains (RWPE-1^{LD} or RWPE-1^K). Both LIMK1^{LD} and LIMK^K were pulled down with His-Aur-A and not with the bead only control (Fig. 21C, and bottom and middle parts).
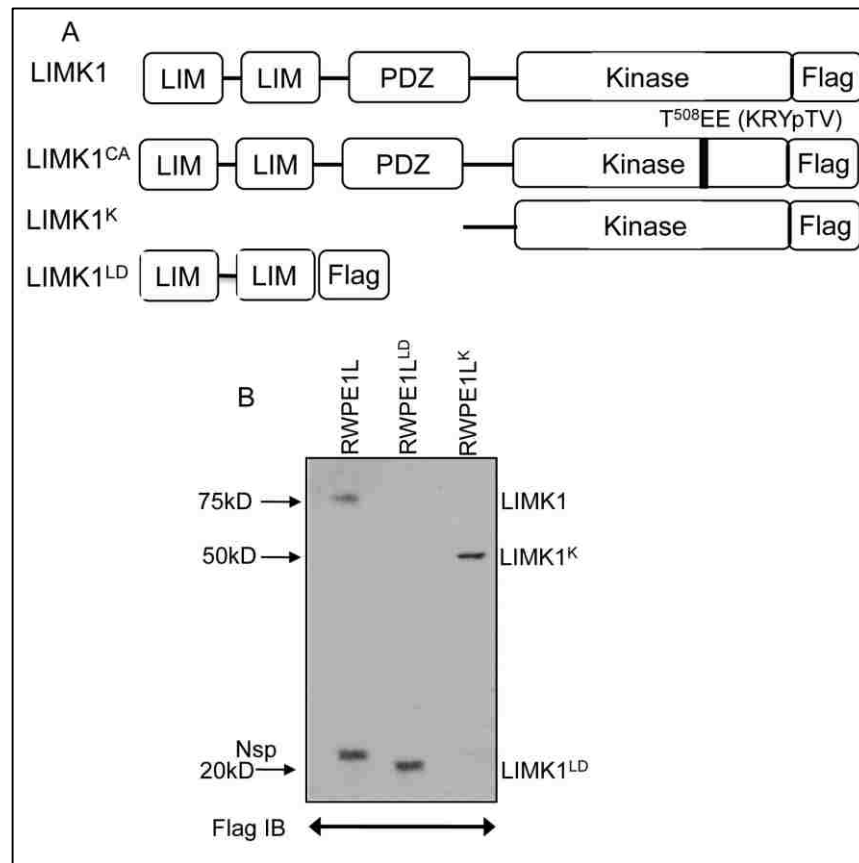
Figure 20: Expression of LIMK1-FLAG fusion proteins.

(A) Diagram of FLAG-tagged LIMK1 constructs. LIMK1: full-length, wild type LIMK1, LIMK1^{LCA}: constitutively active LIMK1 phospho-mimic, LIMK1^{K}: LIMK1 kinase domain and linking region, LIMK1^{LD}: LIMK1 LIM-domains only. (B) RWPE-1 cells were transiently transfected with LIMK1 constructs and harvested after 48 hrs. Expression of FLAGLIMK1 peptides was detected by western blotting using anti-FLAG antibodies. Nsp: nonspecific signal

71
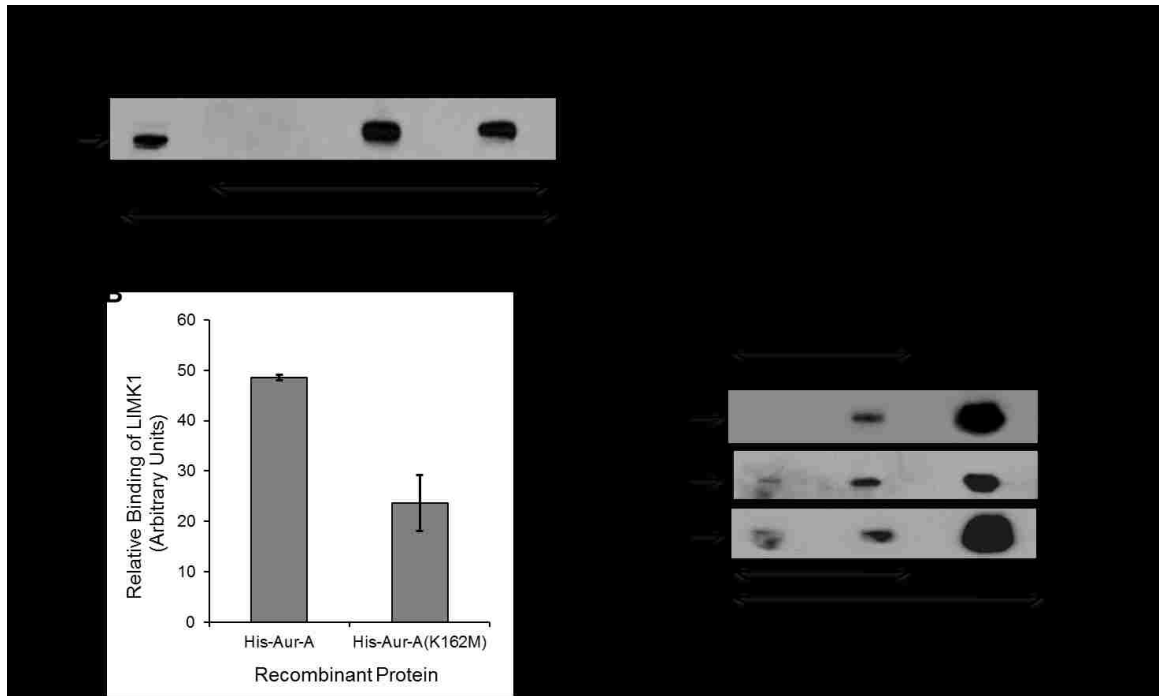
Figure 21: Aur-A physically associates with LIMK1.

(A and B) Interaction between His-Aur-A and endogenous LIMK1 affinity precipitated from PC-3 extracts. (A) Immunoblots showing binding of LIMK1 with both His-Aur-A and His-Aur-A^{K162M} (lanes 3 and 4). No nonspecific binding was noted with the beads (lane 2). (B) Densitometric analysis of the binding affinity of Aur-A and Aur-A^{K162M} to LIMK1 from equal amounts of extracts. Data shows a 50% reduction in the affinity of binding of Aur-A^{K162M} with LIMK1. Data represents a mean ± SD of three independent experiments. (C) Interaction of Aur-A with different domains of LIMK1. Total extracts of RWPE-1 cells transiently transfected with LIMK1-p3XFlag-CMV-14, LIMK1^{LD}-p3XFlag-CMV-14, or LIMK1^{K}-p3XFlag-CMV-14 were used for affinity precipitation with His Aur-A. Data shows that in addition to wild type LIMK1, Aur-A was capable of binding both LIM domains and kinase domain independently. The lane for bead control (lane 1) shows some nonspecific binding but the intensity was much lower than the beads with bound Aur-A. Data shows representative images from thee independent experiments.

5.2.3 Aurora A phosphorylates LIMK1 at S^{307}

Phosphopeptide analysis by mass spectrometry was used to identify all sites of phosphorylation of inactive LIMK1 by Aur-A. *In vitro* kinase assays were performed with His-Aur-A, His Aur-A^{K162M} and GST-LIMK1, and gel extracted LIMK1 bands were used for mass spectrometry. Phosphopeptide analysis showed that LIMK1 was phosphorylated at S^{307} by Aur-A but not at T^{508} (Fig. 22). LIMK1 was not phosphorylated at either site by inactive Aur-A (His-Aur-A^{K162M}) (data not shown). Phosphorylation of LIMK1 at S^{307} by Aur-A was confirmed by *in vitro* kinase assays using wild type (His-LIMK1) and LIMK1 with mutated serine to alanine at position 307 (His-LIMK1^{S307A}) (Fig. 23). Wild-type LIMK1 was strongly phosphorylated by Aur-A, but phosphorylation of His-LIMK1^{S307A} was barely detectable (Fig. 24). To elucidate the phosphorylation site further, nonradioactive kinase assays were performed, and phosphorylation of LIMK1 was detected using phosphospecific LIMK1 (T^{508}) antibodies (Fig. 25). Although a strong phosphorylated band of LIMK1 was noted for wild-type LIMK1, only a weak phosphorylation of T^{508} was detected for His-LIMK1^{S307A} (Fig. 25, lane 5).

Serine 307 lies within the gap region between the PDZ domain and kinase domain, an area that contains many sites of serine phosphorylation (Fig. 22). Published studies showed phosphorylation of LIMK1 at S^{307} [38], [203], [204] specifically during mitosis [40], [204] as a site of phosphorylation but functional implication of phosphorylation at this residue is unknown. Motif analysis indicated a partial homology of the S^{307} phosphorylation site to one of the motifs

that are phosphorylated by Aur-A (pS/T with a bias of L at the +1 position) (Fig. 22). Interestingly, the motif at the T^{508} phosphorylation site (KRYpTV) shows a perfect match to the motif of Aur-A phosphorylation site ([K/N/R]-R-X-[pS/pT]-V) (Fig. 20A).

To confirm Aur-A phosphorylation of LIMK1 *in vivo*, we performed *in vitro* kinase assays using whole-cell extracts and immunoprecipitated protein complex. Extracts of RWPE-1 cells expressing LIMK1 (RWPE-1L) were phosphatase treated to remove any phosphorylated residues and used for kinase assays with His-Aur-A with addition of phosphatase inhibitor. We detected phosphorylation of LIMK1/2 by Aur-A in western blotting using anti-pLIMK1/2 (pT^{508}/pT^{505}) antibodies (Fig. 26A). Phosphorylation of LIMK1 at T^{508} was further confirmed using immunoprecipitated LIMK1 from phosphatase-treated PC-3 extracts and from RWPE-1L cells using anti-FLAG antibodies (Fig. 22B&C). Strong phosphorylation at T^{508} in both assays was noted after incubation with recombinant His-Aur-A. Phosphorylated LIMK1 was not detected upon incubating with inactive Aur-A (Aur-A^{K162M}) (Fig. 26C), confirming that the phosphorylation was due to Aur-A activity rather than LIMK1 autophosphorylation. These experiments show that Aur-A also phosphorylates LIMK1 at T^{508} but requires an intact S^{307} phosphorylation site. Western blot analysis of total extract of RWPE-1 cells expressing FLAG-tagged LIMK1, LIMK1^{S307A} and LIMK1^{T508A} showed phosphorylation of LIMK1, LIMK1^{S307A} but not LIMK1^{T508} (Fig. 27) at T^{508}. This data confirms that expressed LIMK1^{S307A} could be phosphorylated by kinases other than Aur-A.

To assess the importance of this phosphorylation another student in our lab analyzed the immunolocalization of LIMK1^{S307A} and pAur-A. P69 prostate cells were transiently transfected with pCMVLIMK1-FLAG or PCMVLIMK1^{S307A}-FLAG, and colocalization of FLAG-tagged LIMK1 with pAur-A was analyzed using antibodies against FLAG and pAur-A. Although LIMK1 was colocalized with pAur-A at the centrosomes and the spindle poles, no obvious colocalization between pAur-A and LIMK1^{S307A} was noted. Analysis of Pearson's correlation coefficient confirmed the loss of colocalization between these two proteins. Furthermore, α-tubulin staining showed aster formation, but proper spindle structure was rarely seen in cells expressing LIMK1^{S307A} mutants. We have also noted loss of colocalization between LIMK1^{S307A} and γ-tubulin.
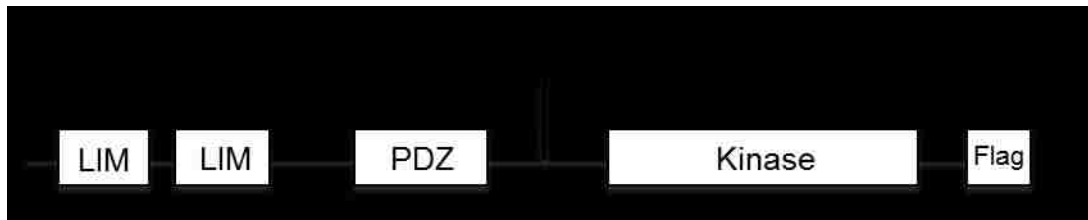
Figure 22: Aurora A Phosphorylates LIMK1 at a Site Other than T^{508}.

Phosphopeptide analysis of GST-LIMK1 after incubation with GST-Aur-A in kinase assay buffer showing phosphorylation of S^{307} at the linking region between the PDZ, and the kinase domain, which shows a partial motif for Aur-A phosphorylation (L at +1 position after phosphorylating residue).
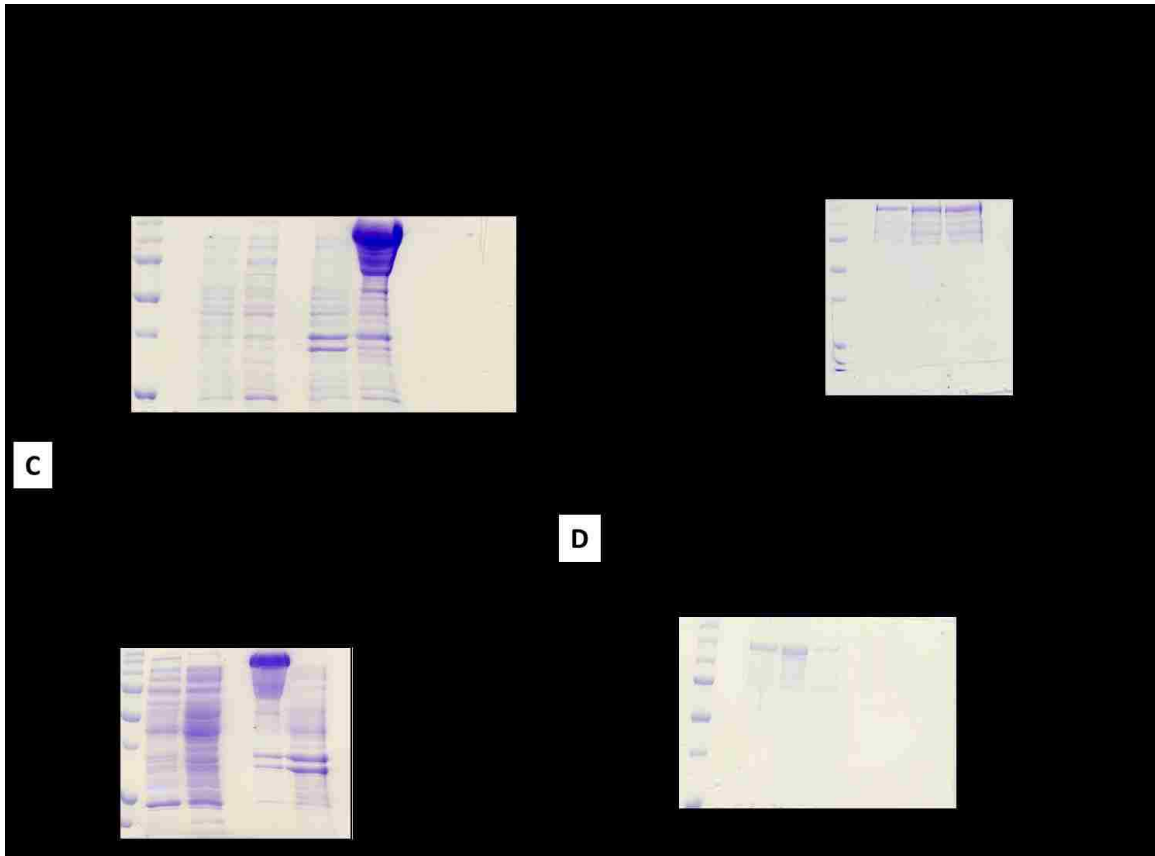
Figure 23: Solubilization of Recombinant His-LIMK1 and His-LIMK1^{S307}.

Coomassie stained SDS-PAGE of His-LIMK1 (A&B) and His-LIMK1^{S307A} (C&D) expression in *E. coli* induced with 1mM IPTG. (A&C) Lanes 2-5 show expression of insoluble His-LIMK1 and His-LIMK1^{S307A} in the pellet. (B&D) Lanes 2-4 show 5, 10, or 15µl of His-LIMK1 or His-LIMK1^{S307A} after solubilization, buffer exchange, and concentration.
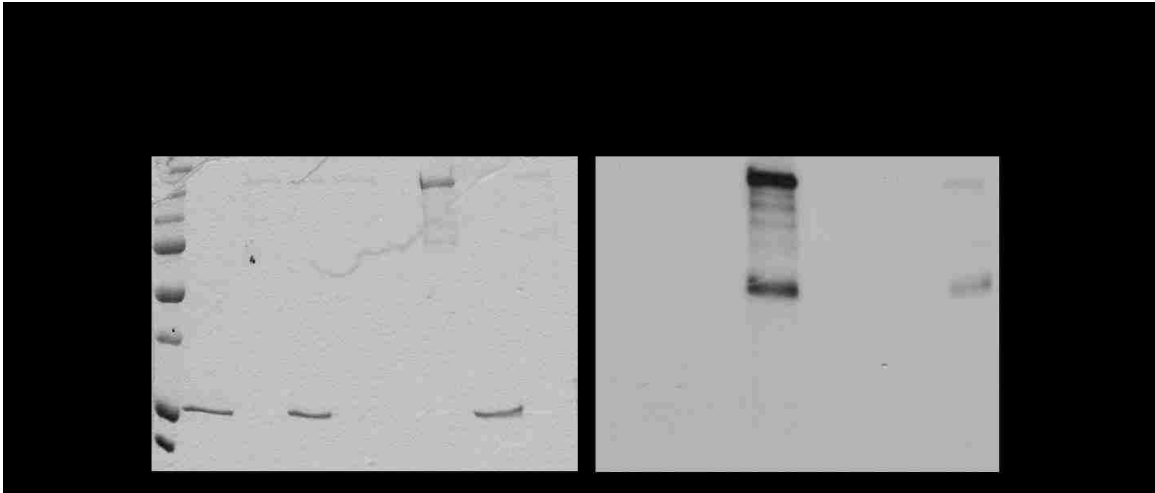
Figure 24: Aurora A Phosphorylates LIMK1 at S^{307}

(A and B) Kinase assay showing loss of phosphorylation by His-Aur-A of His-LIMK1 with S307A mutation. (A) Coomassie stained SDS-PAGE. (B) Autoradiogram of the kinase assay with His-LIMK1 (0.5ug), His-LIMK1^{S307A} (0.5ug), His-Aur-A (0.22ug) and His-Cofilin (1ug). Both His-LIMK1 and His-LIMK1^{S307A} were inactive as no His-cofilin phosphorylated polypeptide was detected (lanes 4 and 7). While strong phosphorylation of the wild type LIMK1 by His-Aur-A was noted (lane 4), very weak to no phosphorylation could be seen with LIMK1^{S307A} mutant protein (lane 8), which further confirms the unique Aur-A phosphorylation site on LIMK1
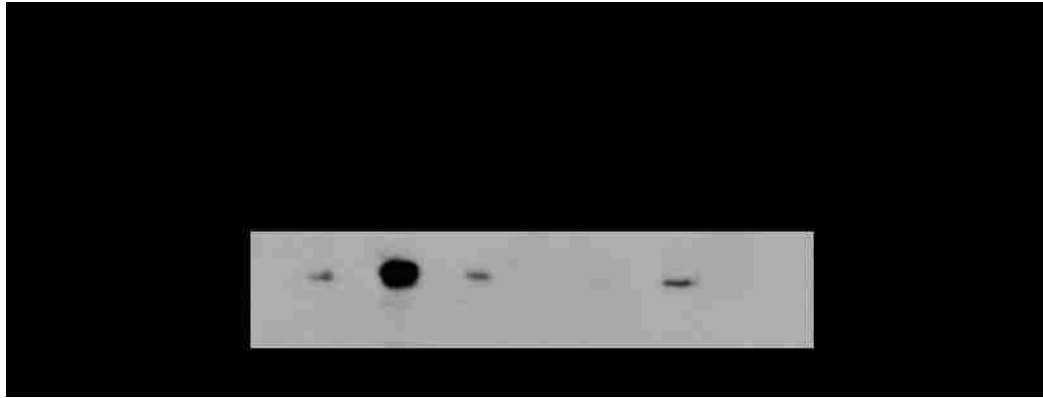
Figure 25: Phosphorylation of His-LIMK1 at S^{307} by Aur-A was essential for phosphorylation at T^{508}.

Immunoblot analysis of nonradioactive kinase assays using phosphospecific antibodies (pT^{508}) showing strong phosphorylation of wild type His-LIMK1 at T^{508} by His-Aur-A (lane 2), which was not noted with Aur-A^{K162M} (lane 3). No phosphorylation at T^{508} could be seen when His-LIMK1^{S307A} was incubated with His-Aur-A (lane 5). Some nonspecific signals were noted in lanes 1, 3, and 5. Data presented are representatives of at least 3 separate experiments.
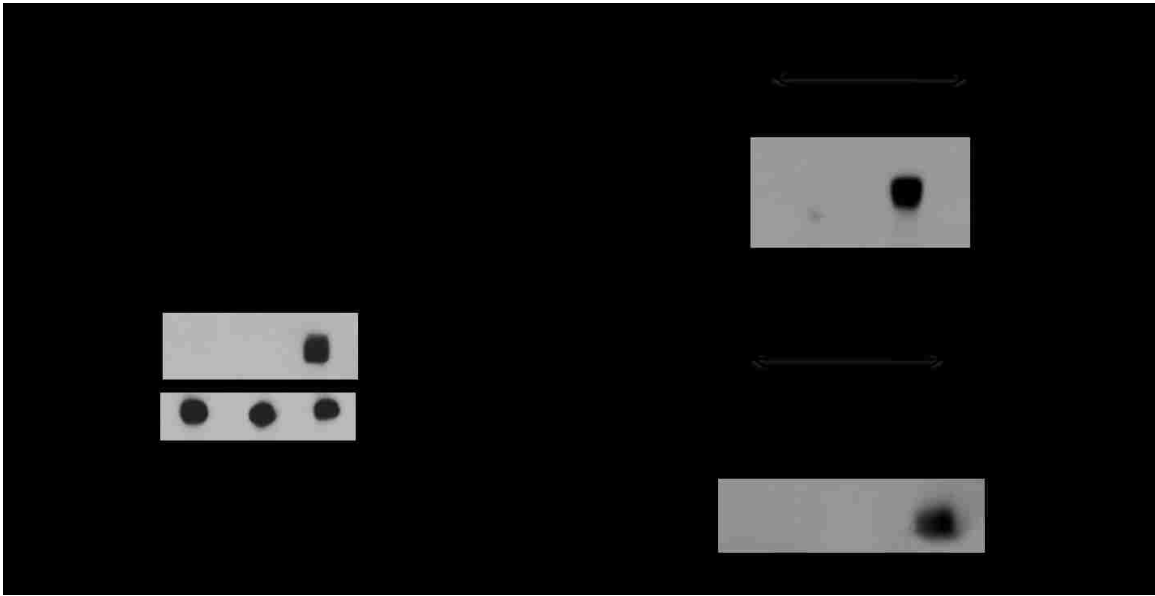
Figure 26: Aur-A allows T^{508} phosphorylation on endogenously expressed LIMK1.

(A) Nonradioactive kinase assays using calf intestinal phosphatase (CIP) (5 units) treated extracts (50µg) of RWPE- 1 cells transfected with pCMVLIMK1-FLAG. CIP treated extracts were incubated with His-Aur-A (0.22µg) with phosphatase inhibitor (PPI) (lane 3) and phosphopeptide band was detected by western blotting using anti-pT^{508}-LIMK1 antibodies. Data show strong phosphorylation at T^{508} by His-Aur-A but not without Aur-A. No phosphorylated LIMK1 (T^{508}) could be seen in the absence of PPI (lane 1). GAPDH was used as the loading control. (BC) Nonradioactive kinase assays using immunoprecipitated FLAG-tagged LIMK1 from CIP treated (100 units) transfected RWPE- 1 cell extracts (500µg) or LIMK1 from CIP treated (100 units) PC-3 cell extracts (500µg) and His-Aur-A (0.22µg). Phosphorylated LIMK1 at T^{508} was detected by immunoblotting using anti-pT^{508}-LIMK1 antibodies. (B) A strong phosphorylated band of FLAGLIMK1 at T^{508} was evident upon incubation with His-Aur-A but not in the lane without Aur-A. (C) A similar phosphorylation at T^{508} of immunoprecipitated LIMK1 by His-Aur-A was noted (lane 3) which was not seen upon incubation with Aur-A^{K162M}, which confirms the requirement of active Aur-A to achieve phosphorylation at T^{508} of LIMK1. Data show a representative image of at least 3 independent experiments.
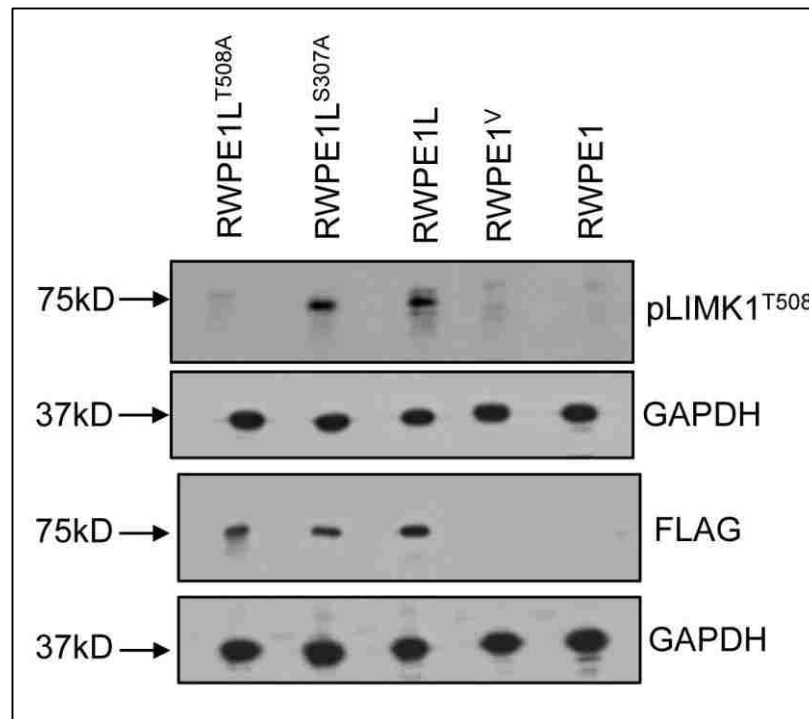
Figure 27: Western blots showing that both recombinant FLAG-tagged LIMK1 and LIMK^{S307A} are phosphorylated at T^{508} in transfected RWPE-1 cells.

Total extracts (50µg) of transiently transfected RWPE-1 cells were probed with anti-FLAG and anti-pT^{508}-LIMK1 antibodies. GAPDH was used as the loading control. Extracts expressing FLAG-tagged LIMK1^{T508A} was used as the negative control, which did not show any corresponding phosphopeptide band.

5.2.4 Functional Inactivation of Aurora A Kinase was Associated with pLIMK1 Mislocalization

Next, we studied the implication of Aur-A mediated phosphorylation on intracellular localization of LIMK1. Another student in the lab, treated PC-3 and RWPE-1 cells with a specific Aur-A inhibitor, MLN8237 [205], and studied the spindle morphology and targeting of pLIMK1 to the centrosomes. MLN8237 treatment (0.01µM) showed distinct defects in spindle morphology, multipolarity and diffused staining of pAur-A, including distinct speckles of pAur-A. Inhibition of Aur-A activity showed appearance of a stretched spindle, possibly due to defects in nuclear membrane dissolution. This observation supports studies showing a role of Aur-A in nuclear membrane breakdown [206], [207]. In RWPE-1 cells, spindles were formed but not as tightly organized as the vehicle-treated cells. Inhibition of Aur-A activity also severely disrupted localization of pLIMK1 in mitotic PC-3 and RWPE-1 cells. In MLN8237 treated PC-3 cells, pLIMK1 was not localized to the centrosomes, but located toward the cell periphery. Inhibition of Aur-A activity did not affect centrosomal localization of centrin, as two distinct spots of centrin staining were observed in PC-3 and RWPE-1 cells. MLN8237 treated RWPE-1 cells, showed similar results, with pLIMK1 localized to the edge of the cell, rather than the centrosomes, as noted in the vehicle-treated cells. Centrin staining was largely localized to the cell periphery in these cells

5.2.5 Aurora A also acts as a substrate of LIMK1 in vitro

To determine any potential reciprocal catalytic relationship between LIMK1 and Aur-A, we examined the ability of endogenous LIMK1 from PC-3 cells to phosphorylate inactive His-Aur-A^{K162M} *in vitro* using immunocomplex kinase assays. We noted that Aur-A^{K162M} was phosphorylated by LIMK1 (Fig. 28). Immunoprecipitated LIMK1 also phosphorylated His-tagged Cofilin as its bona fide substrate. Importantly, LIMK1-mediated phosphorylation was not at T^{288}, the Aur-A autophosphorylation site, as anti-Aur-A phosphospecific (pT^{288}) antibodies failed to recognize the phosphorylated Aur-A polypeptide band in western blots (Fig. 29). Phosphospecific Aur-A-pT^{288} antibodies were able to recognize autophosphorylation of Aur-A in kinase assays, which was not seen for inactive Aur-A. This observation suggests that LIMK1 phosphorylates Aur-A at a site different than the activating autophosphorylation site.
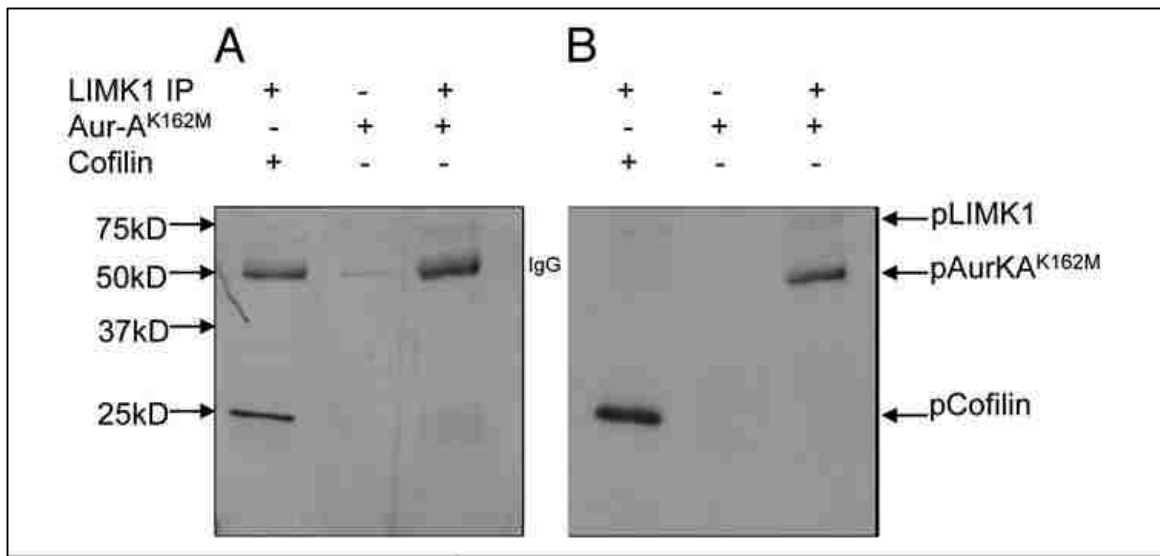
Figure 28. LIMK1 phosphorylates Aur-A.

(A and B) Kinase assays using immunoprecipitated LIMK1 and His-Aur-A[K162M] and His-cofilin as the substrates. (A) Coomassie stained SDS-PAGE of the kinase assays. (B) Autoradiogram of the SDS-PAGE showing phosphorylation of His-Aur-A[K162M] (lane 3) and His-Cofilin (lane 1) by LIMK1. LIMK1 was immunoprecipitated from PC-3 cells using anti-LIMK1 antibodies and incubated with His-Aur-A[K162M] or His-Cofilin in kinase assay buffer with γ-^{32}P-ATP.

His-Aur-A	-	-	-	+
His-Aur-A^{K162M}	+	+	-	-
LIMK1 IP	-	+	+	-

50kD →
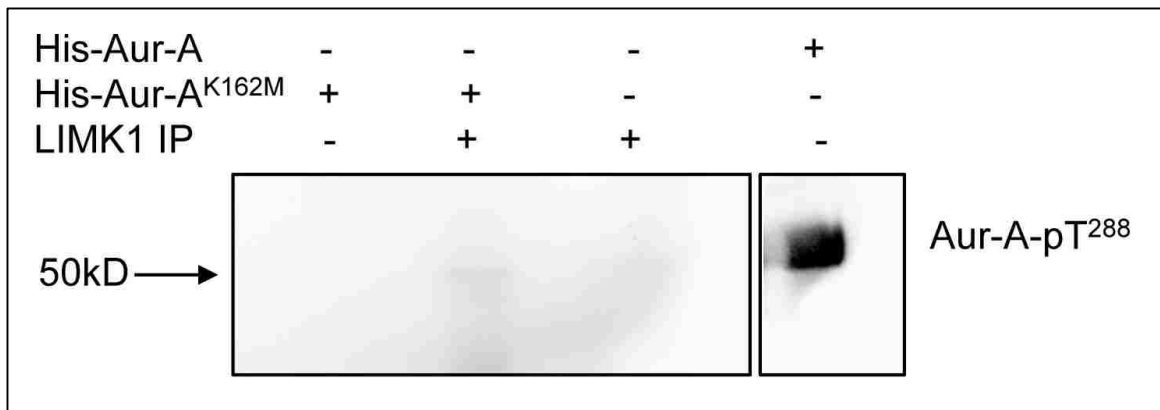
Aur-A-pT^{288}

Figure 29. Non-radioactive immunocomplex kinase assays showing LIMK1 mediated phosphorylation of Aur-A was not at T^{288}.

Western blot analysis of phosphorylated Aur-A using anti-p-Aur-A-pT^{288} antibodies in kinase assays with immunoprecipitated LIMK1 (500µg extracts) and His-Aur-A^{K162M} (0.25µg). Anti-pAur-A antibodies recognized autophosphorylation of His-Aur-A (0.25µg) (lane 4). No phosphorylated bands were seen in lanes with LIMK1 (lanes 2 and 3). The image is the representative of two separate assays.

5.2.6 Knockdown of LIMK1 was Associated with Decreased pAur-A (pT^{288}) Levels, Mislocalized pAur-A and Abnormal Spindle Structures

To elucidate the implication of Aur-A phosphorylation by LIMK1, we examined the effect of knockdown of LIMK1 on the levels of pAur-A (pT^{288}). Another student in the lab, transfected PC-3 cells with LIMK1 shRNA constructs, and 72 hr post-transfection, total pAur-A levels were examined by western blotting. A substantial decrease in the overall pT^{288}-Aur-A levels in LIMK1 shRNA transfected cells compared with nonspecific shRNA transfected cells was noted. Densitometric quantification showed that inhibition of expression of LIMK1 resulted in a ~40–50% decrease in pAur-A levels compared with the control cells, while total Aur-A levels were unaltered. Knockdown of LIMK1 also interfered with localization of pAur-A in mitotic PC-3 cells, which was more diffused compared with control cells. The majority of pAur-A remained associated with α-tubulin, which appears to be organized in astral microtubules. The overall spindle structure was disorganized and not as tight and uniform as noted in nonspecific shRNA expressing cells. Knockdown of LIMK1 expression interfered with centrosome separation and spindle bipolarity, although it did not inhibit centrosomal localization of pAur-A. To verify the effect of LIMK1 knockdown on spindle structure, we quantified the number of transfected cells containing mitotic spindle abnormalities. There was a significant increase (2.4-fold) in the number of cells with abnormal spindles for LIMK1 shRNA expressing cells compared with the scrambled shRNA expressing cells. Taken together, these results suggest

that LIMK1 may regulate mitotic spindle organization and bipolarity through localization of pAur-A.

5.3 Discussion

The findings presented in this study suggest that a functional cooperation between Aur-A and LIMK1 is important in the early mitotic phase, specifically during mitotic spindle formation. This study also partly explains our recent observation showing localization of pLIMK1[T508] to the centrosomes during prophase through telophase [152]. In this study, we noted that pLIMK1[T508] colocalizes with Aur-A to the centrosomes during mitosis. At the centrosomes, upon activation through autophosphorylation at T^{288}, Aur-A phosphorylates a number of proteins, including LATS2 [133], NDEL [134] for centrosome maturation, kinesin motor protein Eg5 [66], MCAK [141] for spindle bipolarity and ASAP [208] for spindle formation. It is speculated that activated Aur-A maintains continued activation of centrosomal LIMK1 throughout its localization to the spindle poles. The requirement of sustained activation of LIMK1 at the spindle poles is supported by studies showing that LIMK1-induced Cofilin phosphorylation is essential for accurate spindle orientation during metaphase through stabilization of cortical actin network [163].

Our observation that pLIMK1[T508] colocalized with Aur-A and γ-tubulin [152] to the centrosomes during prophase suggests that recruitment of LIMK1 to the centrosomes is necessary for proper spindle formation through modulation of actin filaments. We noted that Aur-A binds to the LIM domains and the kinase

domain of LIMK1 independently and phosphorylates LIMK1 *in vitro*. Published studies showing similar interaction of Aur-A with the LIM domains of Ajuba and subsequent phosphorylation of Ajuba and autophosphorylation suggest that Aur-A exhibits preference for binding to LIM domain containing proteins [123], [209].

Our data further show that Aur-A phosphorylates LIMK1 primarily at S^{307}, which lies outside the kinase domain of LIMK1, and that interaction between LIMK1 and Aur-A results in phosphorylation of LIMK1 at T^{508}. We speculate that once S^{307} is phosphorylated, a possible change in conformation makes the T^{508} residue accessible for phosphorylation as the secondary site. Results from *in vitro* kinase assays and immunoprecipitation followed by immunoblot analysis suggest that Aur-A-mediated phosphorylation at S^{307} is essential for its phosphorylation at T^{508} by Aur-A. Active Aur-A was unable to phosphorylate inactive recombinant LIMK1^{S307A} at T^{508}. It is possible that the conformational change induced by S^{307} phosphorylation could either (1) allow Aurora A to directly phosphorylate at T^{508} or (2) allow LIMK1 to autophosphorylate at T^{508}. Earlier, it was shown that LIMK1 becomes hyperphosphorylated upon initiation of mitosis at a site other than T^{508}, but the site was not identified [150]. Our data shows phosphorylation of LIMK1 at an additional site S^{307} by the mitotic kinase Aur-A and colocalization of these two proteins to the centrosomes. Treatment with Aur-A inhibitor MLN8237 showed a diffused accumulation of pLIMK1 (T^{508}) in the cytoplasm. It could be speculated that LIMK1 is phosphorylated at T^{508} by other kinases in the absence of functional Aur-A, but pLIMK1 was not recruited to the centrosomes. This suggests that targeting of LIMK1 to the centrosomes

requires Aur-A-mediated phosphorylation at S^{307}. This speculation is further supported by our result showing that LIMK1^{S307A} does not colocalize with Aur-A in mitotic cells.

Unlike interaction of Aur-A with Ajuba, association of Aur-A with LIMK1 also induces phosphorylation of Aur-A, but not at the autophosphorylation site (T^{288}). LIMK1-mediated phosphorylation of Aur-A was at a site other than T^{288}, as phosphospecific (T^{288}) Aur-A antibodies did not recognize the resulting phosphopeptide. Catalytic activation of Aur-A is through T-loop phosphorylation at T^{288} directly by PAK1 [198] or mainly through autophosphorylation by Aur-A. Nevertheless, the possibility of a kinase that phosphorylates Aur-A *in vivo* and sensitizes it for autophosphorylation cannot be ruled out. Immunoprecipitated LIMK1 effectively phosphorylated kinase-dead His-Aur-A, suggesting that active LIMK1 was capable of such phosphorylation. This observation is in support of the report showing that cell extracts immunodepleted of pT^{288} Aur-A retained the ability of T^{288} phosphorylation of GST-fused Aur-A activation loop peptide [210]. Depletion of LIMK1 resulted in 40–50% reduced levels of pT^{288} Aur-A, which suggests an indirect regulatory role of LIMK1 in Aur-A phosphorylation at T^{288}. Furthermore, knockdown of LIMK1 indicated a physiological consequence in centrosome separation and spindle bipolarity. Inhibition of LIMK1 did not inhibit Aur-A targeting to the centrosomes and actually favored microtubular localization of pAur-A. However, knockdown of LIMK1 expression interfered separation of asters needed for spindle bipolarity. Additionally, a 2.4-fold increase in the number of abnormal mitotic spindles was noted in PC-3 cells following

knockdown of LIMK1. Based on our observation, we speculate that decreased phosphorylation of Aur-A at T^{288} could occur by two different mechanisms. First, upon binding to LIMK1, Aur-A may autophosphorylate at T^{288}, as it does upon interaction with Ajuba. Second, LIMK1 knockdown disrupts proper Aur-A subcellular localization whereby it may prevent interaction of Aur-A with interacting proteins that stimulate direct phosphorylation or autophosphorylation at T^{288}. Nonetheless, LIMK1 induced phosphorylation of Aur-A may be important for optimal activation of Aur-A at the microtubule organization center (MTOC), and regulation of spindle bipolarity. It is known that activated Aur-A mediates formation of bipolar spindles through regulation of microtubule dynamics by inactivating phosphorylation of MCAK at the center of the aster [141].

In this study, we presented a novel functional relationship between Aur-A and LIMK1. This functional relationship seems to be mediated through reciprocal phosphorylation of one another. Our data show that small-molecule inhibitors alter mitotic progression not only through direct inhibition of Aur-A, but also through altered LIMK1 localization and function. Although Aur-A regulates functions of a variety of proteins, not many kinases that regulate Aur-A function are known to date. Our study provides evidence of a new mechanism whereby the function of Aur-A is regulated and that Aur-A has an additional regulatory function during mitosis. Additionally, our data suggests that development of small-molecule inhibitors targeted toward LIMK1 may have the added benefit of disrupting Aur-A function.

CHAPTER SIX: AURORA A KINASE MODULATES ACTIN CYTOSKELETON THROUGH PHOSPHORYLATION OF COFILIN: IMPLICATION IN THE MITOTIC PROCESS

6.1 Introduction

Aurora A (Aur-A) is a member of the family of Aurora serine/threonine kinases, which play important roles in the mitotic process. Expression of Aur-A is significantly increased during late G2 when it is targeted to the centrosomes. Aur-A is responsible for centrosomal maturation and separation by recruiting γ-tubulin, centrosomin, NDEL1, TACC, and LATS2 to the centrosome [67], [133], [134], [193]. Aur-A also regulates mitotic spindle assembly through interactions with LIMK1, TPX2, Eg5, Hurp, and XMAP215 [102], [137], [194], [211]. Although the function of Aur-A is essential during early prophase, spindle pole localization of Aur-A is sustained through the mitotic phases, suggesting its involvement in later mitotic events. Recent studies showed a cooperative function of Aur-A and Aur-B on anaphase microtubule dynamics [212]. Aur-A expression is tightly regulated and altered expression of Aur-A results in mitotic spindle defects. Inhibition of Aur-A expression resulted in chromosome misalignment and multinucleated cells [213], whereas overexpression of Aur-A induced generation of supernumerary centrosomes, multipolar spindles, and aneuploidy. Importantly, overexpression of Aur-A is seen a variety of cancers including, breast, ovarian and prostate [103], [149], which may lead to development of aneuploidy in the cancerous cells.

In addition to its regulation of microtubule dynamics and chromosome segregation during mitosis, Aur-A has been implicated in the regulation of actin cytoskeleton. Activation of Drosophila Aur-A has been suggested to play a role in actin dependent asymmetric protein localization during mitosis [78]. Overexpression of Aur-A was shown to induce up-regulation of SSH-1 leading to dephosphorylation and activation of the actin depolymerizing protein, Cofilin [214]. Aur-A also interacts with LIMK1 and Ajuba, proteins that are involved in reorganization of the actin cytoskeleton [123], [211]. Recent studies showed an indirect relationship between Aur-A and regulation of actin-dependent processes through phosphorylation of Rho kinases in Drosophila [215]. Nonetheless, the role of Aur-A regulation of the actin cytoskeleton has not been clearly defined.

Although not widely studied, actin has an important function throughout mitosis. During G2 phase, the actin cytoskeleton is involved in centrosome separation [216], [217]. Cortical actin plays a role in the anchoring and orientation of the mitotic spindle [218], [219]. Additionally, regulation of actin dynamics is essential for completion of cytokinesis through formation of the contractile ring [220], [221]. The dynamics of the actin cytoskeleton is regulated by the actin depolymerizing protein, Cofilin. Kinases, such as LIMK1/2 and TESK1/2, regulate Cofilin activity through phosphorylation, which prevents its binding to actin [53], [80], [81], [222], [223]. However, functionally active Cofilin is essential for completion of cytokinesis. Also, LIMK1 mediated inactivating phosphorylation of Cofilin during mitosis is necessary for proper mitotic spindle orientation [163], however, the exact function of Cofilin during mitosis has yet to

be determined. In this study, we identified Cofilin as a novel substrate of Aur-A. Aur-A regulates Cofilin activity through phosphorylation, thereby regulating actin polymerization. Additionally, we found that Aur-A is involved the regulation of Cofilin phosphorylation during mitosis.

6.2 Results

6.2.1 Cofilin Acts as a Substrate of Aurora A

LIMK1/2 act as the bona-fide kinases for inactivating phosphorylation of Cofilin but treatment with BMS-5, a specific inhibitor of LIMK1/2 catalytic activity did not completely inhibit Cofilin phosphorylation. Although a significantly decreased phosphorylation of Cofilin was noted after treatment with BMS-5 compared to the vehicle control, DMSO (Fig. 30A) a small amount of phosphorylated Cofilin was still detectable. This suggests that either the kinase activity of LIMK1 is not completely blocked by BMS-5 or a different kinase, may be responsible for Cofilin phosphorylation. In our previous studies we identified a novel interaction between LIMK1 and Aur-A at the centrosomes, which prompted us to investigate if Aur-A is responsible for the remaining Cofilin phosphorylation. To determine if Cofilin is a substrate of Aur-A, we performed *in vitro* kinase assays with recombinant His-tagged Cofilin and Aur-A (Fig. 30C). A radioactive polypeptide band corresponding to the size of Cofilin was detected after incubation with Aur-A (Fig. 30B, lane 3). To further confirm that Cofilin is a substrate of Aur-A, we performed an immunocomplex kinase assay (Fig. 30D&E). Endogenous Aur-A was immunoprecipitated from asynchronous PC-3

cell lysate with anti-Aur-A antibodies and incubated with recombinant His-tagged Cofilin and γ-^{32}P-ATP (Fig. 30D&E). Results showed phosphorylation of recombinant Cofilin by the immunoprecipitated Aur-A (Fig. 30E, lane 2). However, our previous studies showed that LIMK1 co-precipitates with Aur-A so it is possible that the phosphorylation seen may be due to a combination of both LIMK1 and Aur-A activity on Cofilin. Together, this data confirms that Cofilin acts as a substrate of Aur-A.
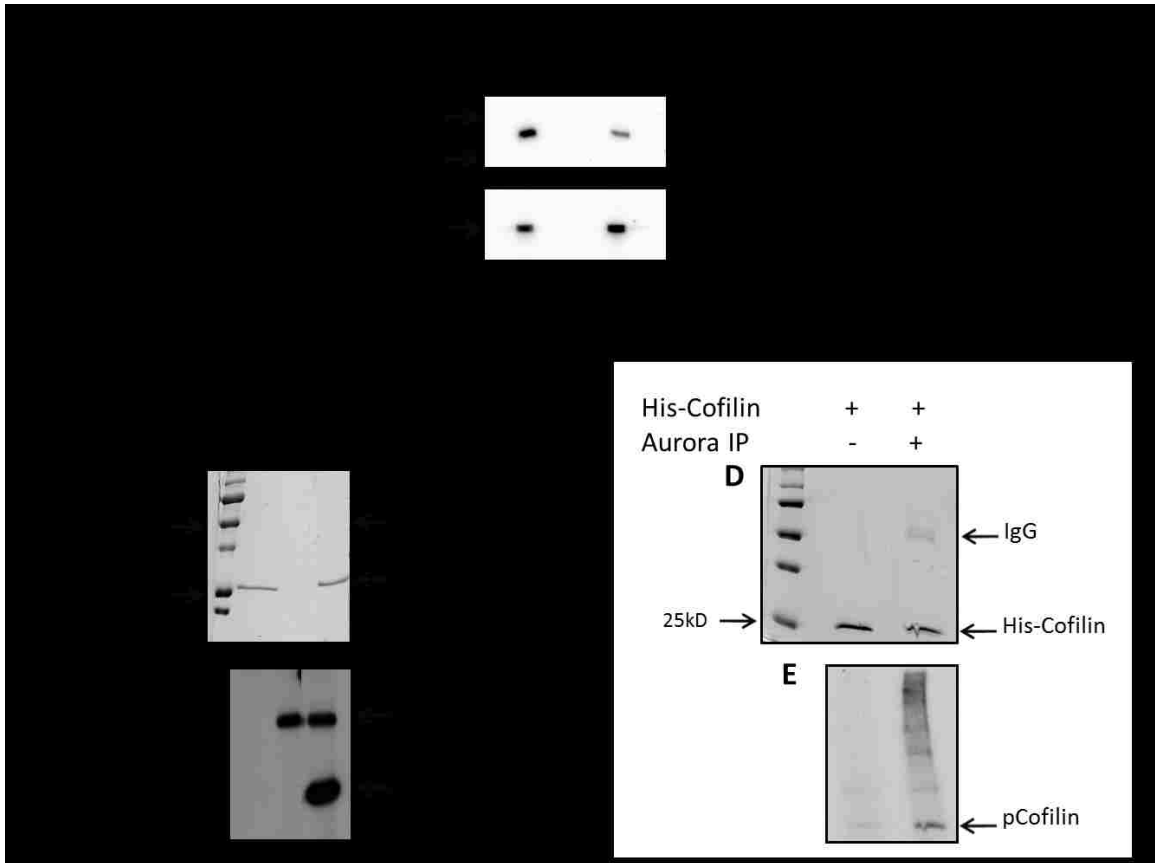
Figure 30: Phosphorylation of Cofilin by Aurora A:

(A) Western blot analysis of PC3 cells treated with either DMSO or BMS-5 (5µM) (LIMK1/2 inhibitor) for 24 hr. Immunoblotting with anti-pS³-Cofilin and anti-GAPDH (loading control) antibodies show reduced cofilin phosphorylation after treatment with BMS-5 compared to the DMSO control. (B & C) *In vitro* kinase assays with recombinant His-Cofilin (1µg) and His-Aurora A (0.22µg). (B) Coomassie stained SDS-PAGE showing location of polypeptide bands. (C) Autoradiogram showing phosphorylation of His-Cofilin. (D&E) Immunocomplex kinase assays of immunoprecipitated Aur-A and His-Cofilin (1µg). Aurora A was immunoprecipitated from PC3 whole cell lysates (500µg) with anti-Aur-A antibodies and used in a kinase assay with recombinant His-Cofilin. (D) Coomassie stained SDS-PAGE showing location and loading of Cofilin polypeptides. (E) Autoradiogram of phosphorylated Cofilin.

6.2.2 Aurora A Phosphorylated Cofilin at S^3, S^8, and T^{25}

Cofilin activity is regulated by phosphorylation/dephosphorylation of its main phosphorylation site, S^3. To determine if Aur-A phosphorylates Cofilin at S^3, we performed *in vitro* kinase assays with a nonphosphorylatable S3A mutant Cofilin (Cofilin[S3A]) (Fig. 31). Phosphorylation of recombinant His-Cofilin[S3A] by His-Aur-A (lane 2) was reduced compared to phosphorylation of wild-type His-Cofilin, suggesting that S^3 is a site of phosphorylation by Aur-A (Fig. 32). Because phosphorylation of Cofilin[S3A] was reduced compared to wild-type Cofilin but not eliminated, it can be speculated that Aur-A phosphorylates Cofilin at additional residue(s). To identify the additional sites of phosphorylation, we performed phosphopeptide analysis of recombinant wild type full-length Cofilin subjected to *in vitro* non-radioactive kinase assays with recombinant wild type His-tagged Aur-A or catalytically inactive His-Aur-A[K162M]. Mass spectrometric analysis detected two phosphopeptides containing the phosphorylated residues S^3, S^8, and T^{25} in the sample incubated with active Aur-A (Fig. 33). Phosphorylation at these sites was not detected in the sample incubated with inactive Aur-A[K162M] (data not shown). To confirm these results, we expressed recombinant His-tagged triple mutant Cofilin (Cofilin[S3A/S8A/T25A]) in which these three residues were mutated to Alanine (Fig. 34) and used for *in vitro* kinase assays (Fig. 35). Results showed Cofilin[S3A/S8A/T25A] was still phosphorylated by Aur-A (Fig. 35, lane 3), which was not detected when incubated with inactive Aur-A[K162M] (lane 7). Phosphorylation of Cofilin[S3A/S8A/T25A] by Aur-A was reduced

compared to phosphorylation of Cofilin^{S3A}, suggesting that these sites are phosphorylated by Aur-A but additional site(s) may also be phosphorylated by Aur-A. To broadly identify Cofilin fragments containing other possible phosphorylation sites, we expressed recombinant His-tagged C-terminal fragment of Cofilin containing amino acids 90-166 (Cofilin$^{90-166}$) and used for *in vitro* kinase assays. Our results showed that Cofilin$^{90-166}$ was not phosphorylated by Aur-A (Fig. 35, lane 4), suggesting that putative additional phosphorylation sites in Cofilin are between amino acids 1-89. Other than S^3, S^8, T^{25}, possible additional phosphorylation sites within this region are S^{23}, S^{24}, S^{41}, T^{63}, T^{70}, and T^{88} (Fig. 36).
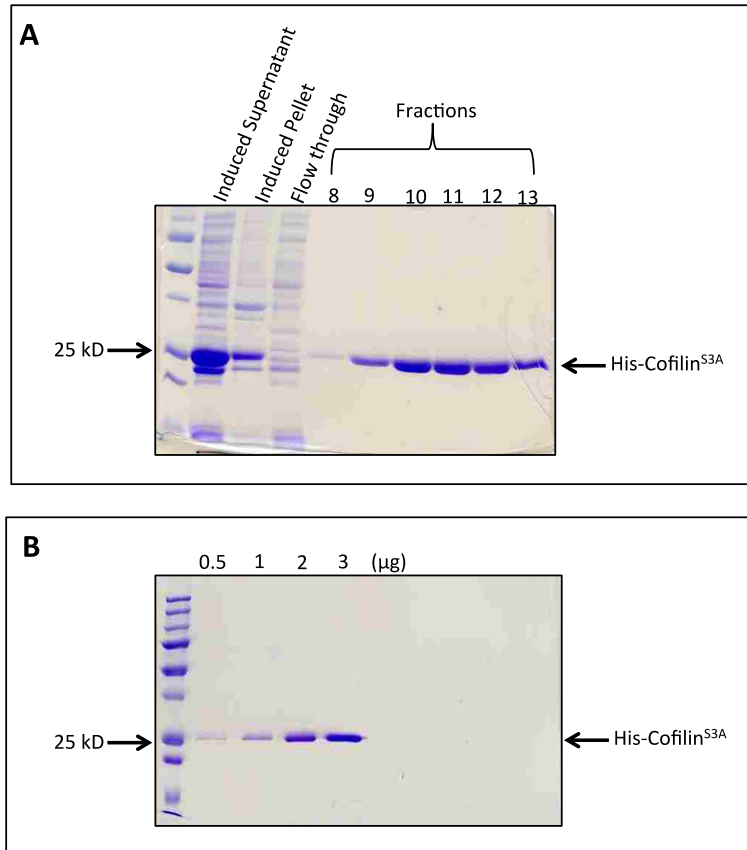
Figure 31: Expression and Affinity Purification of Recombinant His-Cofilin^{S3A}.

Coomassie stained SDS-PAGE of His-Cofilin^{S3A}expression in *E. coli* induced with 1mM IPTG. (A) Lanes 2 and 3 show expression of His-Cofilin^{S3A} in the supernatant. Lanes 4-10 show retrival of purified soluble His-Cofilin^{S3A} in different fractions of the affinity chromatography. (B) Lanes 2-5 show 0.5, 1, 2, and 3μg of His-Cofilin^{S3A} after buffer exchange and concentration.
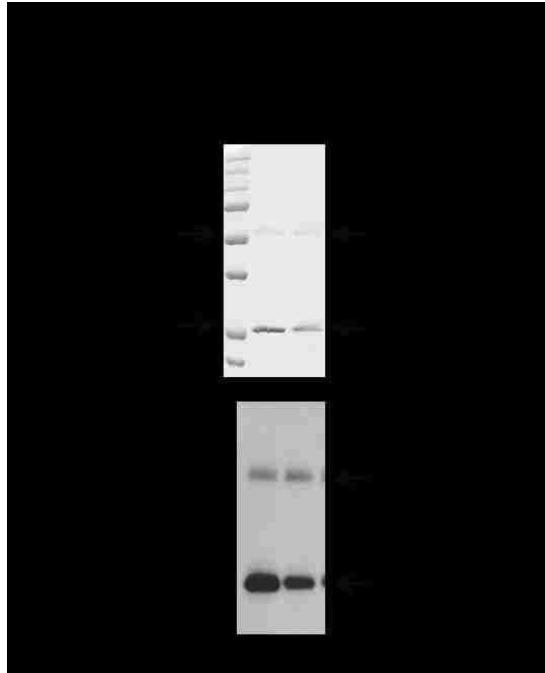
Figure 32: Aurora A Phosphorylates Cofilin at S^3

Aurora A Phosphorylated Cofilin at Specific Sites: (A & B) *In vitro* kinase assays with recombinant His-Cofilin, His-Cofilin^{S3A} mutant, and His-Aur-A. (A) Coomassie stained SDS-PAGE showing protein location and loading. (B) Autoradiogram showing reduced phosphorylation of His-Cofilin^{S3A} compared to His-Cofilin.

Figure 33 : Aurora A Phosphorylates Cofilin at S^3, S^8, T^{25}

Phosphopeptide analysis of phosphorylated Cofilin by mass spectroscopy. Two phosphopeptides were detected containing a total of three sites phosphorylated by Aur-A.
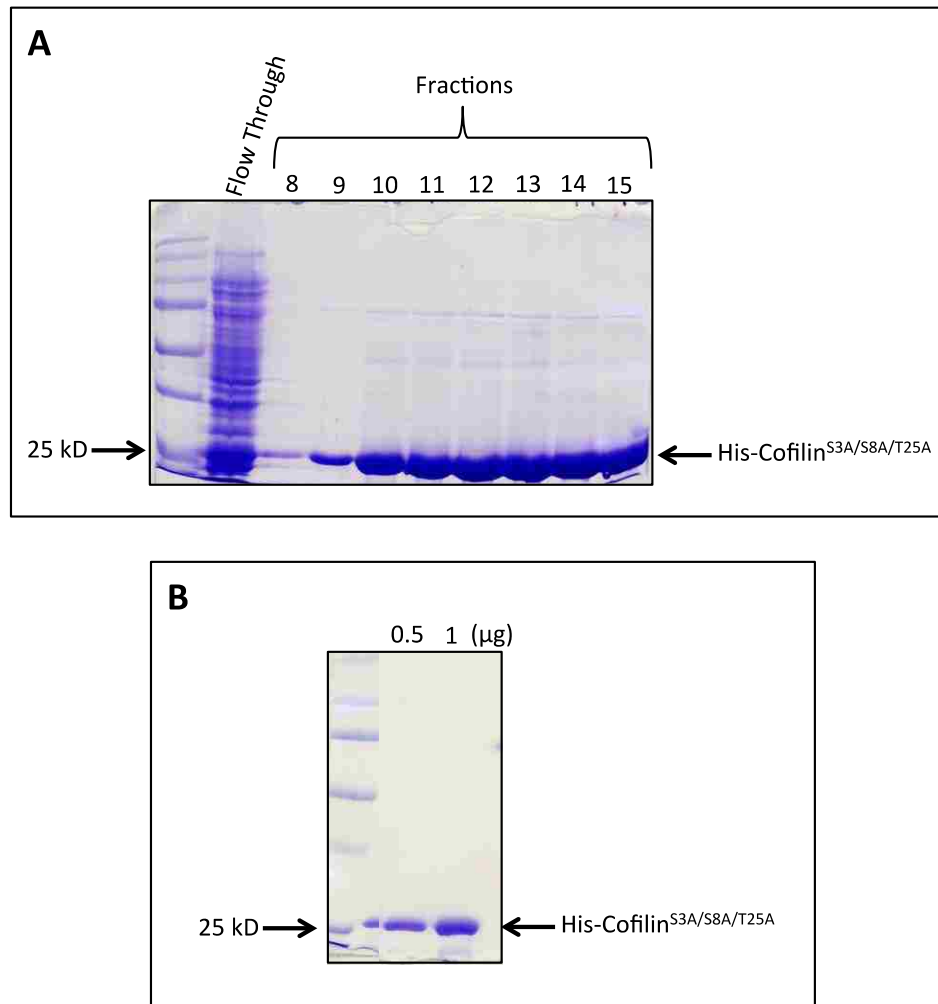
Figure 34: Expression and Affinity Purification of Recombinant His-Cofilin^S3A/S8A/T25A.

Coomassie stained SDS-PAGE of His-Cofilin$^{S3A/S8A/T25A}$ expression in *E. coli* induced with 1mM IPTG. (A) Lanes 2-10 show retrival of purified soluble His-Cofilin$^{S3A/S8A/T25A}$ in different fractions of the affinity chromatography. (B) Lanes 1 and 2 show 0.5 and 1µg of His-Cofilin$^{S3A/S8A/T25A}$ after buffer exchange and concentration.
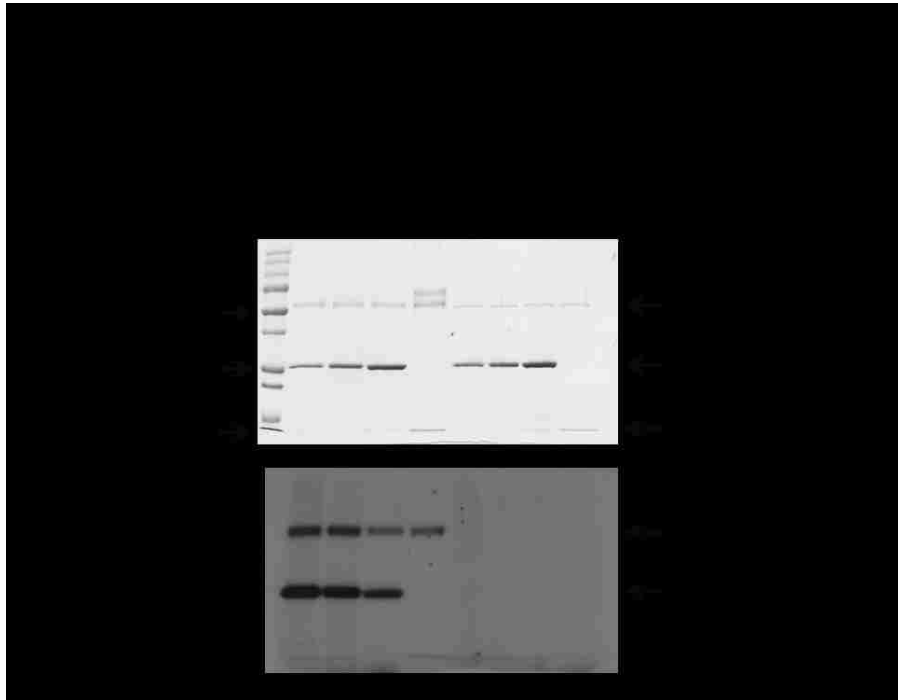
Figure 35: Aurora A Phosphorylates Sites in Addition to S³, S⁸, and T²⁵

(A&B) *In vitro* kinase assays of recombinant wild type His-Cofilin and His-Cofilin^{S3A}, His-Cofilin$^{S3A/S8A/T25A}$, and His-Cofilin$^{90-166}$ mutants using His-Aurora A or His-Aurora A^{K162M} mutant.   (A) Coomassie stained SDS-PAGE showing protein location and loading. (B) Autoradiogram showing phosphorylation of His-Cofilin, His-Cofilin^{S3A}, and His-Cofilin$^{S3A/S8A/T25A}$.   No phosphorylation of His-Cofilin$^{90-166}$ could be detected.

MA**S³**GVAV**S⁸**DGVIKVFNDMKVRK**S²³S²⁴T²⁵**PEEVKKRKKAVLF CL**S⁴¹**EDKKNIILEEGKEILVGDVGQ**T⁶³**VDDPYA**T⁷⁰**FVKMLPDKD CRYALYDA**T⁸⁸**Y

Figure 36: Possible phosphorylation sites in Cofilin by Aurora A

Possible sites of phosphorylation are in bold.   Sites identified by mass spectroscopy are underlined.

6.2.3 Phosphorylation by Aurora A Reduced the Actin Depolymerizing Activity of Cofilin

To examine the effect of phosphorylation of Cofilin by Aur-A on its actin modulatory function, we performed actin polymerization assays to assess the functional status of Cofilin. Wild-type recombinant His-Cofilin depolymerized F-actin as reduced Phalloidin staining and reduced length of F-actin were noted compared to the actin only control (Fig. 37A). Next, we examined the depolymerizing activity of His-Cofilin, His-Cofilin^{S3A}, and His-Cofilin$^{S3A/S8A/T25A}$ after phosphorylation by His-Aur-A (Fig. 37B&C). His-Cofilin incubated with inactive His-Aur-A^{K162M} was more active than His-Cofilin incubated with His-Aur-A as noted by the reduced length of F-actin and the reduced intensity of Phalloidin staining. Phosphorylation of His-Cofilin^{S3A} by His-Aur-A reduced its activity compared to His-Cofilin^{S3A} incubated with His-Aur-A^{K162M}. Additionally, His-Cofilin$^{S3A/S8A/T25A}$ incubated with His-Aur-A was significantly more active than His-Cofilin^{S3A} incubated with Aur-A, suggesting that phosphorylation at S^8 or T^{25} may regulate Cofilin activity. Together, this data suggests that phosphorylation by Aur-A negatively regulates Cofilin activity via phosphorylation.
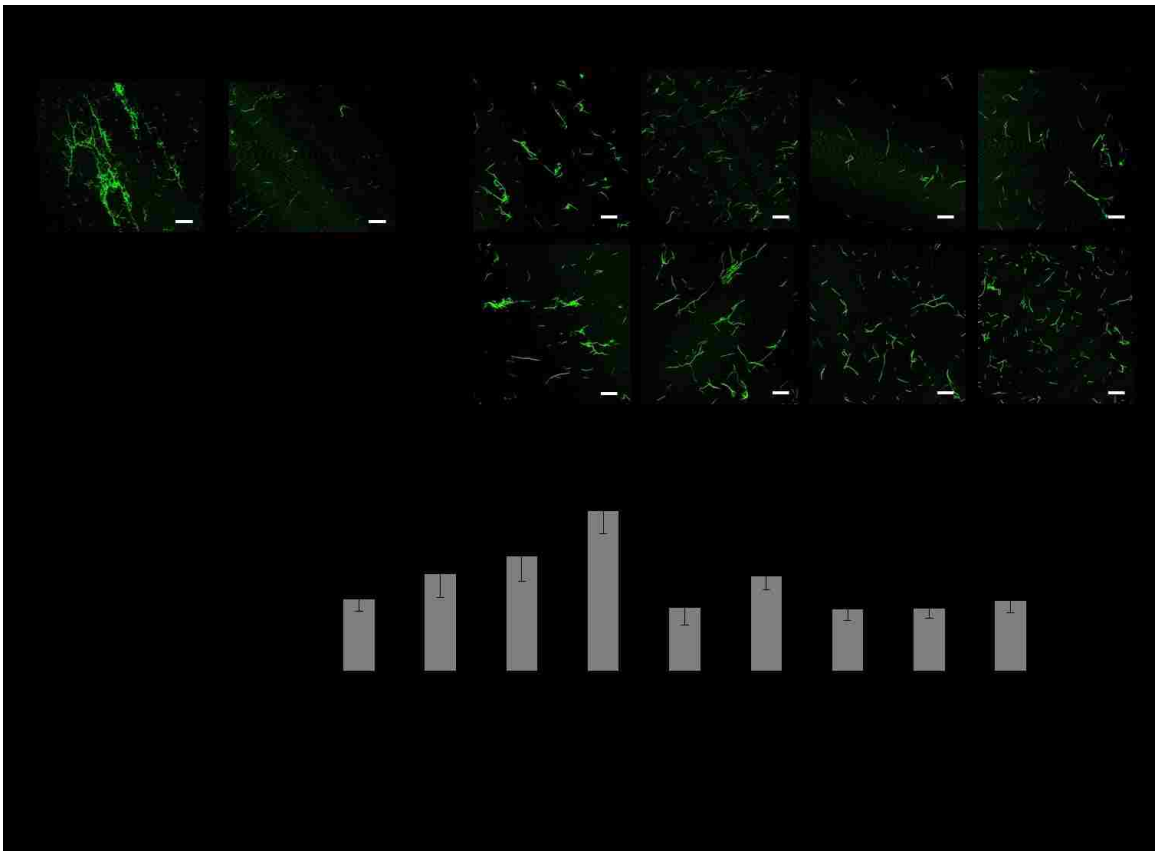
Figure 37: Phosphorylation by Aurora A Reduced Actin Depolymerizing Activity of Cofilin.

(A) Images showing depolymerization of actin by Cofilin. Decreased Phalloidin staining of F-actin could be noted in the presence of His-Cofilin. (B) Recombinant His-Cofilin, His-Cofilin^{S3A}, or His-Cofilin$^{S3A/S8A/T25A}$ mutants were *in vitro* phosphorylated by His-Aur-A^{K162M} (top panels) or His-Aur-A (bottom panels) and incubated with polymerized actin and stained with Phalloidin. (C) Quantification of actin filament length from B. Incubation with phosphorylated His-Cofilin or His-Cofilin^{S3A} mutant by inactive Aur-A reduced Phalloidin staining compared to His-cofilin or His-Cofilin^{S3A} phosphorylated with active Aur-A. Incubation with phosphorylated His-Cofilin$^{S3A/S8A/T25A}$ by active Aur-A partially retained Cofilin activity as noted by shorter fragments of Phalloidin stained F actin compared to His-Cofilin or His-Cofilin^{S3A}. Data is representative of ten longest actin filaments each in 15 fields of two independent experiments. Scale bar: 25μm, *p<0.05

6.2.4 Inhibition of Aurora Kinases Decreased the Distribution of F-Actin

Next, we wanted to examine the effect of Aurora A activity on actin polymerization *in vivo.* MCF7 cells were treated with the pan-Aurora inhibitor, VX-680, or the vehicle and F-actin status was monitored by staining with Phalloidin (Fig. 38A-C). The mean intensity of F-actin was reduced to ~50% in cells treated with VX-680 compared to vehicle treated cells. This data suggests that actin depolymerizing activity of Cofilin was higher in cells treated with VX-680.
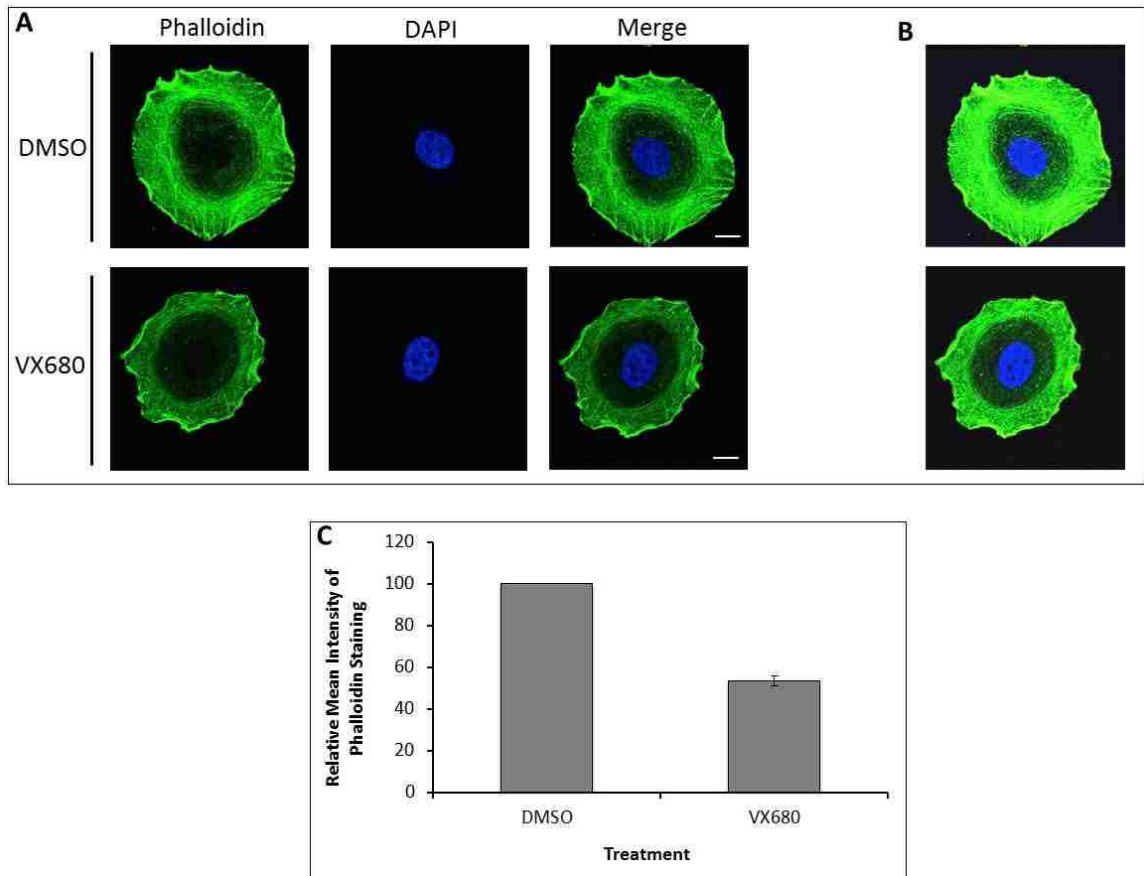
Figure 38: Inhibition of Aurora Kinases Reduced the Levels of F-Actin.

(A) Immunofluoresence analysis of MCF7 cells treated with either VX-680 (100nM) or DMSO for 24 hrs. F-actin (green) was visualized by staining with Phalloidin. DNA was stained with DAPI (blue). (B) Phalloidin staining from cells in A was imaged after increasing exposure time to show actin staining in detail within the cell. (C) Quantitation of the mean intensity of Phalloidin staining. Data is representative of 150 cells from two independent experiments. Scale bar: 10µm.

6.2.5 Mutation of Aurora A Phosphorylation Sites on Cofilin Caused Mislocalization of Cofilin

To examine the effect of phosphorylation at S^3, S^8, and T^{25} by Aur-A we prepared a mammalian expression construct of non-phosphorylatable RFP-tagged Cofilin in which all three phosphorylation sites were mutated to alanines (Cofilin$^{S3A/S8A/T25A}$-RFP). M12 cells were transfected with either wild type RFP-tagged Cofilin (Cofilin-RFP) (Fig. 39A) or RFP-tagged Cofilin$^{S3A/S8A/T25A}$ (Fig. 39B) for 48 hours. In cells expressing lower amounts of Cofilin-RFP (top panel), Cofilin-RFP localized primarily to the perinuclear region (white arrows). In cells expressing higher amounts of Cofilin-RFP (bottom panel), the expressed protein was also localized throughout the cell although in some areas accumulation of Cofilin-RFP could be seen. Cofilin$^{S3A/S8A/T25A}$-RFP, however, did not show specific localization to the perinuclear region (bottom panels). Cells expressing lower amounts of Cofilin$^{S3A/S8A/T25A}$-RFP (top panel) showed punctate localization of the expressed Cofilin throughout the cytoplasm while in cells with higher amounts of expressed protein (bottom panel), diffuse localization of Cofilin$^{S3A/S8A/T25A}$-RFP throughout the cytoplasm could be noted. Both proteins colocalized with F-actin (yellow arrows), but to a lesser extent for Cofilin$^{S3A/S8A/T25A}$-RFP. This data suggests phosphorylation by Aur-A regulates subcellular localization of Cofilin.
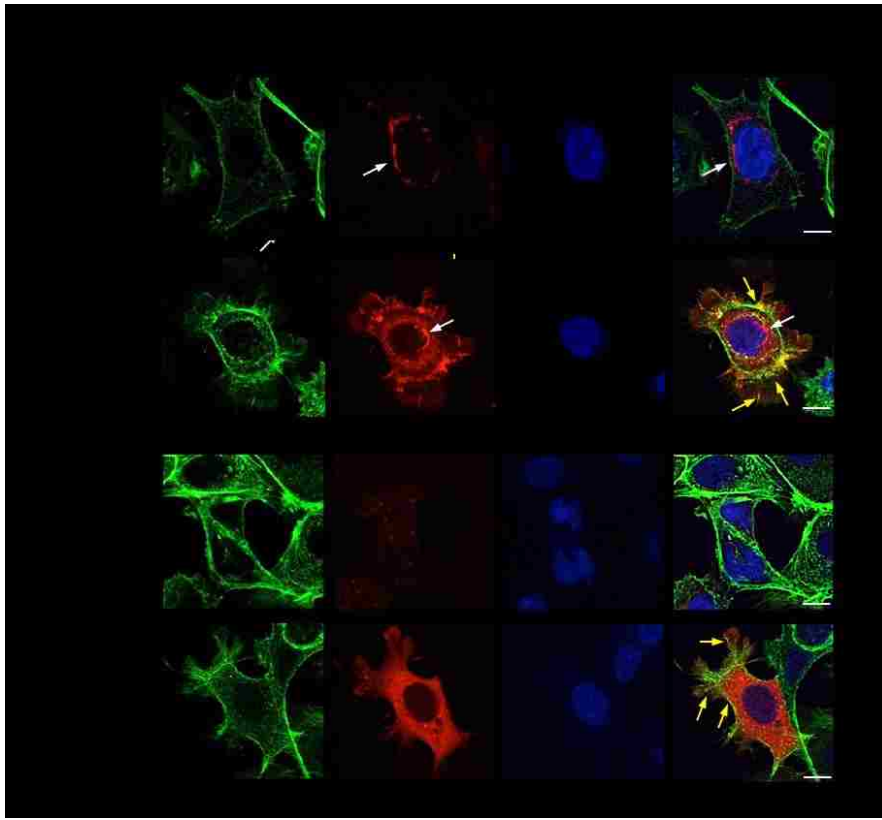
Figure 39: Mutation of Aurora A Phosphorylation Sites Resulted in Mislocalization of Cofilin.

Immunofluorescence analysis of M12 cells transfected with Cofilin-RFP (A) or Cofilin$^{S3A/S8A/T25A}$-RFP (B). F-actin was stained with Phalloidin-488 (green) and DNA was stained with DAPI (blue). Cofilin-RFP localized to the perinuclear region (white arrows) while Cofilin$^{S3A/S8A/T25A}$-RFP showed diffuse staining throughout the cell. Colocalization of the wild type Cofilin and the mutant Cofilin with F-actin could be noted (yellow arrows). Scale bar: 10μm. Top panel: cells expressing lower amounts of Cofilin RFP or Cofilin$^{S3A/S8A/T25A}$-RFP; bottom panel: cells expressing higher amounts of Cofilin-RFP or Cofilin$^{S3A/S8A/T25A}$-RFP.

6.2.6 Aurora A Physically Associates with Cofilin During Mitosis

Aur-A is primarily expressed from late G2 throughout mitosis. In our next experiment, we wanted to examine if Aur-A and Cofilin interact during mitosis. M12 cells synchronized at the G2/M boundary were isolated by shake off and released into mitosis for 0, 30, and 60 mins. Aur-A was immunoprecipitated from mitotic cell extracts using anti-Aur-A antibodies and co-precipitated Cofilin was detected by immunoblotting. Cofilin was precipitated equally in all time points, which suggests that Cofilin and Aur-A interact throughout the early mitotic phases (Fig. 40A). The interaction was confirmed using NIH-3T3 cell extracts in which Cofilin was precipitated with Aur-A in all time points (Fig. 40B). Specificity of the antibodies was detected by immunoprecipitating Cofilin and Aurora from Nocodazole treated extracts. Immunorecipitated antigens were detected by immunoblotting with anti-Cofilin or anti-Aurora A antibodies (Fig. 41). This result suggests that Aur-A may play a role in regulation of Cofilin activity during mitosis.
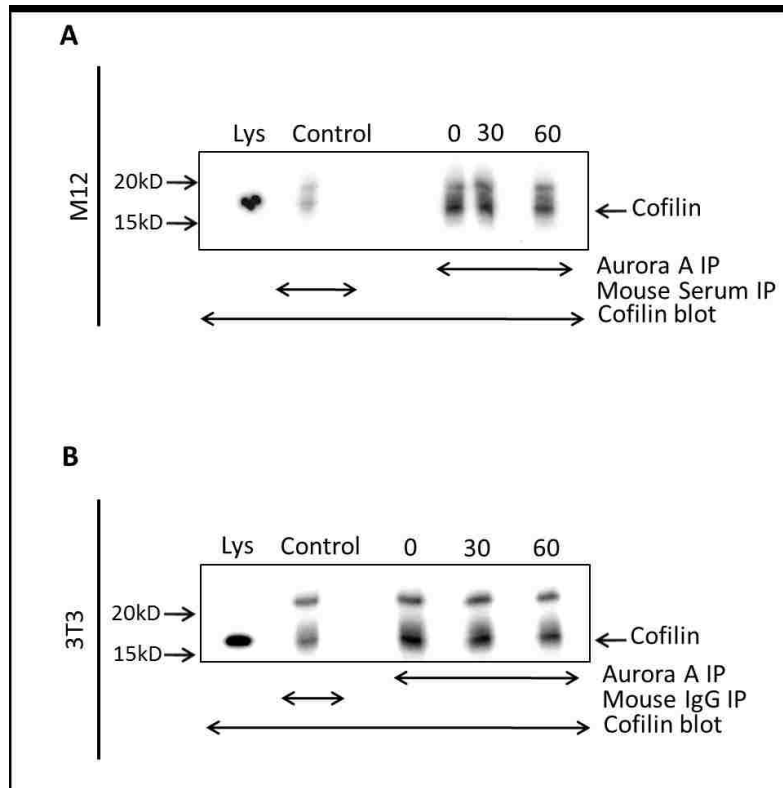
Figure 40: Interaction of Aurora A with Cofilin During Mitosis

Coimmunoprecipitation of Cofilin with Aur-A in Nocodazole treated M12 (A) or NIH-3T3 (B) cell extracts harvested at different times after release. Aur-A was immunoprecipitated using anti-Aurora A antibodies, and Cofilin was detected by immunoblotting using anti-Cofilin antibodies. Mouse IgG was used as a control. Data represents the results of three independent experiments.
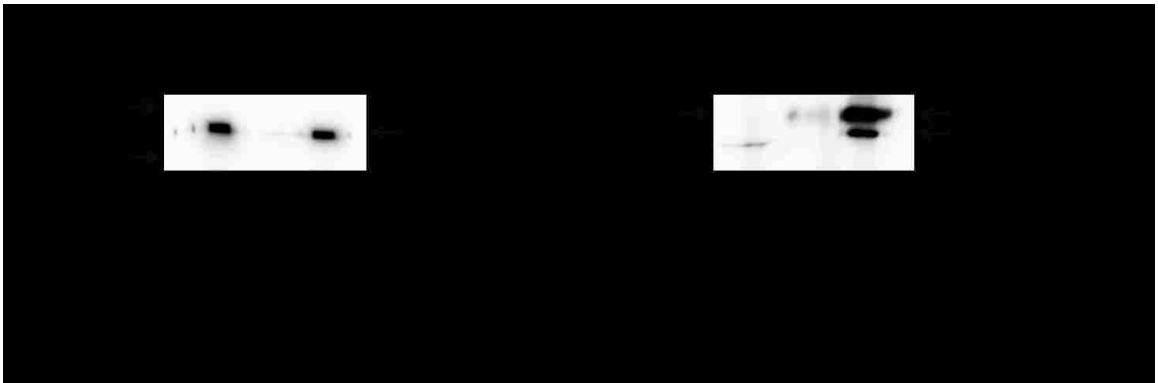
Figure 41: Confirmation of antibody specificity.

Immunoprecipation of Cofilin (A) or Aurora A (B) from Nocodazole treated M12 cell extracts. Cofilin or Aur-A was immunoprecipitated and immunoblotted with anti-Cofilin and anti-Aur-A antibodies. Rabbit IgG and mouse serum were used as controls.

6.2.7 Inhibition of Aurora A Activity Altered Cofilin Phosphorylation During Mitosis

Next, we examined the association of Aur-A catalytic activity with Cofilin phosphorylation during mitosis. M12 cells were treated with the Aur-A specific inhibitor, MLN8237, or DMSO and synchronized at the G2/M boundary with nocodazole. Mitotic cells were collected and released for 0, 30, and 60 mins. Phosphorylated-Cofilin (pS^3) and total Cofilin were detected in mitotic cell extracts by immunoblotting (Fig. 42A&B). Total Cofilin levels in DMSO and MLN8237 treated cells remained relatively constant in all time points but phospho-Cofilin levels fluctuated. In DMSO treated cells, Cofilin phosphorylation was highest at 30 mins (~1.5-fold increase compared to 0 hr) and barely detectable at 60 mins (~0.5-fold decrease compared to 0 hr). This is in support of an earlier study showing Cofilin phosphorylation during mitosis [166]. Interestingly, MLN8237 treated cells had low levels of phospho-Cofilin at 0 hr, but a > 4-fold increased levels at 30 and 60 mins. Total Cofilin decreased slightly at 30 and 60 mins in MLN8237 treated cells compared to DMSO treated cells (Fig. 42C). MLN8237 treated cells contained ~70% less phospho-Cofilin compared to DMSO treated cells at 0 hr (Fig.42C). From 0 to 30 mins, Cofilin phosphorylation increased ~4-fold in MLN8237 treated cells to a level about equal to that in DMSO treated cells. However, between 30 to 60 mins Cofilin phosphorylation in DMSO treated cells decreased while phosphorylation in MLN8237 treated cells did not change, causing ~2.5-fold difference in phosphorylation between the two

113

treatments. This data suggests that Aur-A plays a role in regulation of Cofilin activity during mitosis.

To coordinate the mitotic phases with Cofilin phosphorylation, we evaluated the stages of mitosis in MLN8237 treated cells as Aur-A inhibition has been shown to cause a mitotic delay [213]. We used immunofluorescence analysis to quantify the distribution of cells released in fresh medium in each mitotic phase at each time point in MLN8237 treated cells (Fig. 43A-D and Table 7&8). DMSO treated cells had a higher percentage of cells in mitosis (~40% at each time point) compared to MLN8237 treated cells (~20% of cells at each time point) (Fig. 43C and Table 7). In DMSO treated cells, quantitative analysis of mitotic phases in DMSO treated cells showed that ~30.2%, ~68.48%, ~1.86%, and 0% of cells were in prophase, metaphase, anaphase, and telophase respectively, at 30 mins. At 60 mins, cells progressed to anaphase and telophase as evident from ~25.41%, ~59.61%, ~7.93%, and ~7.06% of cells in prophase, metaphase, anaphase, and telophase, respectively (Fig. 43D & Table 8). Treatment with Aur-A inhibitor caused a delay in mitotic progression as evident from ~77.54% and ~22.46% of cells at 30 mins and ~78.34% and ~19.84% of cells at 60 mins in prophase and metaphase, respectively. No cells in anaphase or telophase were noted at 60 mins. This data suggests that alteration of Cofilin phosphorylation may be associated with the mitotic delay induced by the inhibition of Aur-A activity.

114
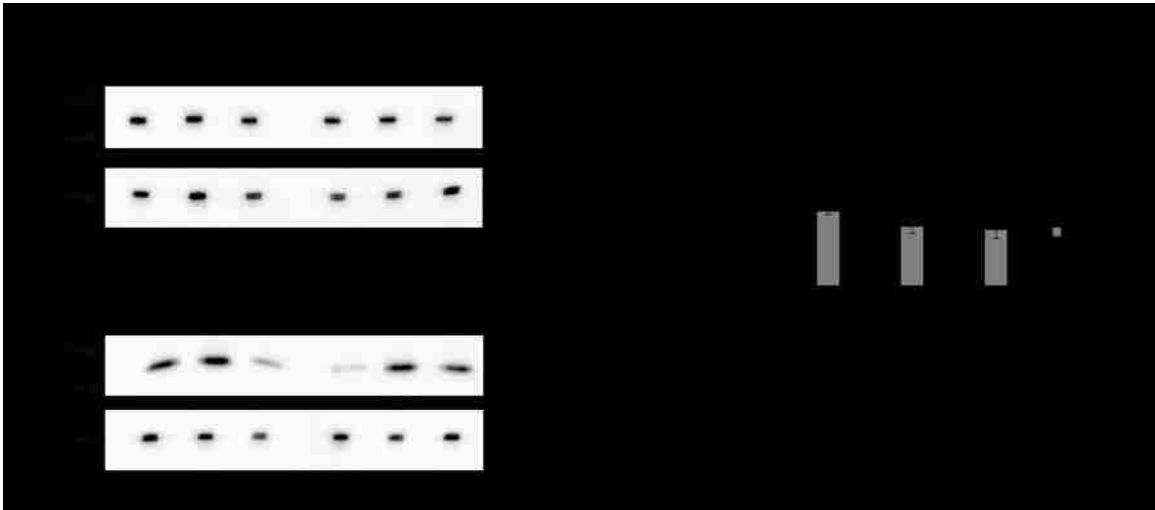
Figure 42: Inhibition of Aurora A Activity Altered Cofilin Phosphorylation.

Western blot analysis of endogenous Cofilin (A) and phospho-Cofilin (pS^3) (B) in nocodazole treated M12 cell extracts released at different times with treatment with MLN8237 (100nM) or the vehicle. Anti-Cofilin and anti-phospho-Cofilin antibodies were used for the immunoblots. GAPDH expression was used as the loading control. Values below each figure indicates relative protein levels normalized to 0 minute expression (not released from G2/M boundary). (C) Densitometric analysis of Cofilin and phospho-Cofilin in MLN8237 treated cells compared to DMSO treated cells. Data shows mean±SD of three independent experiments.

±
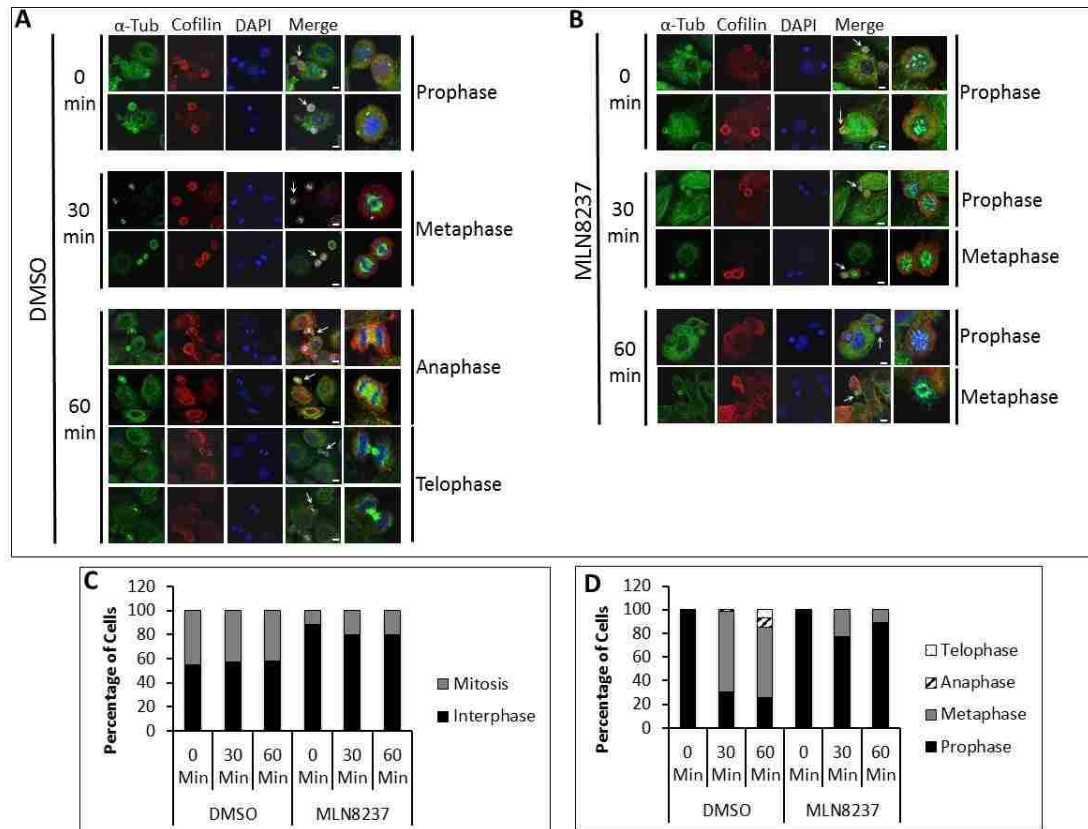
Figure 43: Treatment with Aur-A Inhibitor Delayed Progression of Cells Through Prophase.

Immunofluorescence analysis of DMSO (A) or MLN8237 (100nM) (B) treated and nocodazole synchronized M12 cells released into mitosis for 0, 30, or 60 mins. α-tubulin (green) and Cofilin (red) were visualized by staining with anti-α-tubulin and anti-Cofilin antibodies. DNA was stained with DAPI (blue). Representative enlarged mitotic cells are shown in the extreme right column in each row. White arrows show the cells selected for the enlarges images. (C) Quantitation of the percent of cells in interphase or mitosis. Data shows average numbers of cells counted in 20 fields each from two separate experiments. (D) Quantitation of the percent of cells in each mitotic phase. Data shows average number of cells counted in 20 random fields each from two separate experiments. Scale bar: 10μm.

116

Table 7. Distribution of cells in interphase and mitotic phases

	DMSO			MLN8237		
	0 Min	30 Min	60 Min	0 Min	30 Min	60 Min
Interphase	55.07±12.56	56.97±10.24	57.84±11.11	88.10±9.23	80.04±7.88	80.06±11.42
Mitosis	44.93±11.76	43.03±9.84	42.16±8.65	11.90±8.83	19.96±7.13	19.94±11.88

Table 8. Distribution of cells in different mitotic phases

	DMSO			MLN8237		
	0 Min	**30 Min**	**60 Min**	**0 Min**	**30 Min**	**60 Min**
Prophase	100±0	30.20±8.99	25.41±6.50	100±0	77.54±18.43	78.34±4.12
Metaphase	0	68.48±7.12	59.61±15.36	0	22.46±18.42	19.84±1.54
Anaphase	0	1.86±1.11	7.93±6.46	0	0	0
Telophase	0	0	7.06±2.39	0	0	0

6.2.8 Inhibition of Aurora A Activity Altered Slingshot-1 Expression During Mitosis

It has been shown that overexpression of Aur-A can increase the expression of slingshot-1 phosphatase (SSH-1) [214]. Hence, we wanted to examine if inhibition of Aur-A altered expression of SSH-1. M12 cells were treated with either MLN8237 or DMSO and synchronized to the G2/M boundary with nocodazole. Mitotic cells were isolated by mitotic shake off and released into mitosis with fresh media containing either MLN8237 or DMSO. SSH-1 expression was detected in mitotic extracts by immunoblotting (Fig. 44). In DMSO treated cells, SSH-1 expression increased through 60 mins. SSH-1 expression in MLN8237 treated cells followed a similar trend but expression was significantly lower in all time points compared to DMSO treated cells. Together, this data confirms that Aur-A modulates SSH-1 expression during early mitotic phases.
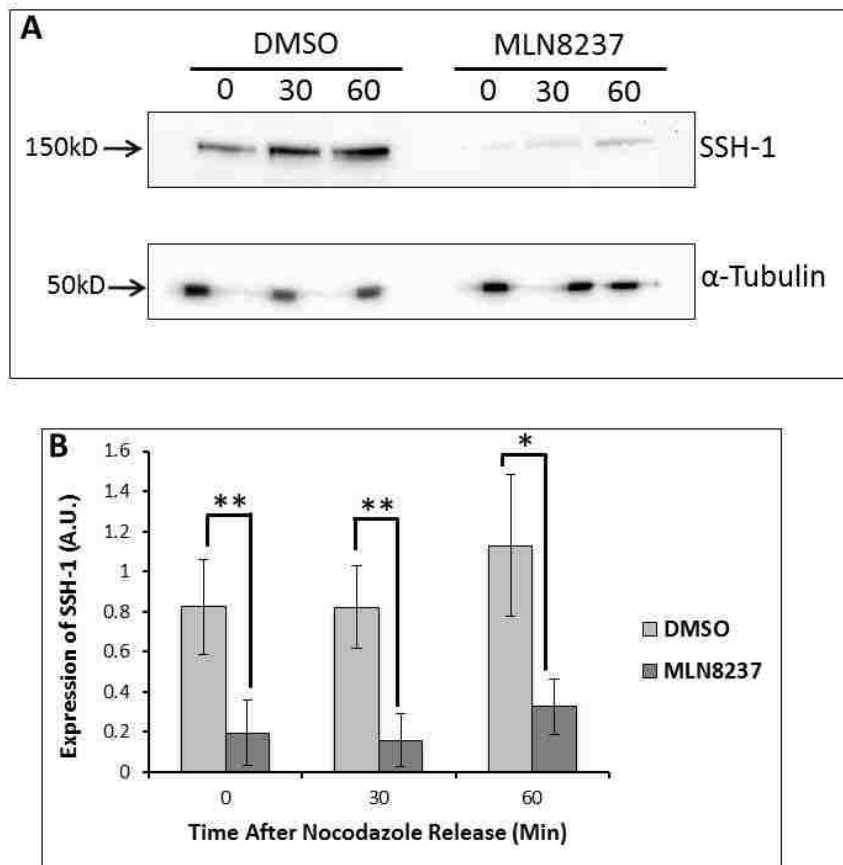
Figure 44: Inhibition of Aurora A Activity Altered Slingshot-1 Expression

(A) Western blot analysis of SSH-1 expression in nocodazole treated M12 extracts released at different times with treatment of MLN8237 (100nM) or vehicle. Anti-SSH-1 antibodies were used for the immunoblots and α-tubulin expression was used as the loading control. (B) Densitometric analysis of SSH-1 expression in MLN8237 and DMSO treated cells. Data is representative of at least three independent experiments. *p=<0.05. **p=<0.005.

6.2.9 Both Aurora A and LIMK1 Contribute to Cofilin Phosphorylation in the Early Mitotic Phase

Recently, a bidirectional functional relationship between Aur-A and LIMK1 during mitosis has been demonstrated [211]. Earlier it was shown that LIMK1 phosphorylates Cofilin during mitosis [166]. To determine the contribution of LIMK1/2 in maintaining phospho-Cofilin levels during early mitotic phases, we examined the effect of the LIMK1/2 inhibitor BMS-5 on Cofilin phosphorylation by western blot analysis. We noted a significant reduction in phospho-Cofilin (pS^3) levels in all time points in released M12 cells treated with BMS-5, which was further reduced to undetectable levels upon combination treatment of BMS-5 and MLN8237 (Fig. 45). Because Aur-A phosphorylates and activates LIMK1 [211], we examined the activation status of LIMK1 during mitosis in cells treated with MLN8237. It could be noted from our results that phosphorylated LIMK1/2 was barely detectable in DMSO treated cells but was undetectable in MLN8237 treated cells (Fig. 46). Since, low levels of pLIMK1/2 were detected in DMSO treated cells it is more likely that pLIMK1/2 is further lowered in MLN8237 treated cells rather than completely absent. Together, this data suggests both LIMK and Aur-A participate in the regulation of Cofilin phosphorylation during mitosis.
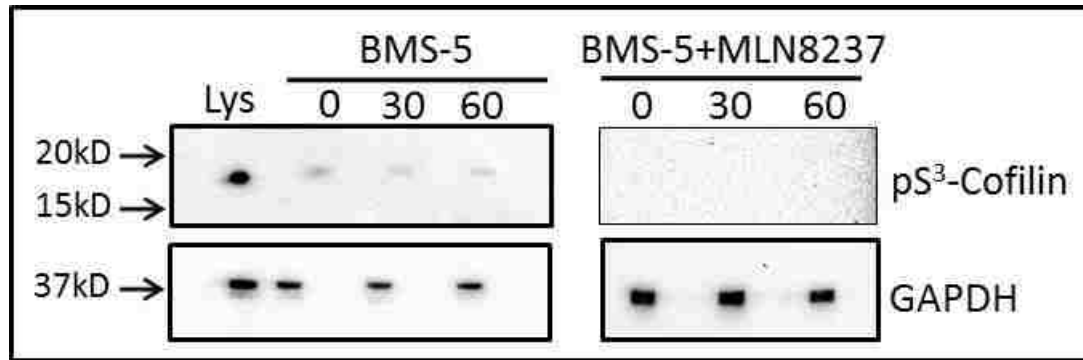
Figure 45: Both Aurora A and LIMK1 Contribute to Cofilin Phosphorylation During Mitosis.

Western blot analysis of pS^3-Cofilin in extracts of nocodazole synchronized M12 cells treated with BMS-5 (5µM) singly or in combination with MLN8237 (100nM) using anti-pS^3-Cofilin antibodies. Cells were released into mitosis and harvested at different times. GAPDH expression was used as the loading control Lys: untreated whole cell lysate.
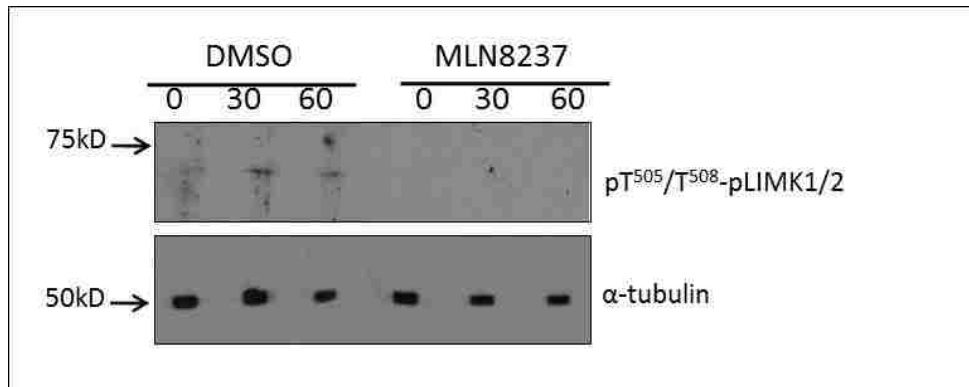
Figure 46: MLN8237 Treatment Reduced pLIMK1/2 levels in Mitotic Cells.

Western blot analysis of phospho-LIMK1/2 in MLN8237 or DMSO treated G2/M synchronized M12 cells released into mitosis for 0, 30, or 60 minutes. Cell extracts were used for immunoblots using anti-p-T^{505}/T^{508}-LIMK1/2 antibodies. α-tubulin was used as the loading control

6.3 Discussion

In this study, we show a novel interaction between Aur-A and Cofilin. Our study identified that Cofilin acts as a substrate of Aur-A, which phosphorylates Cofilin at multiple sites including S^3, S^8, and T^{25}. Phosphorylation at S^3 renders Cofilin inactive by blocking its binding to actin. Therefore, one role of Aur-A phosphorylation is to regulate the activity of Cofilin. Serine^8 phosphorylation has been mentioned in two proteomics studies [56], [166] but has never been experimentally confirmed therefore, the consequence of this phosphorylation is unknown. Threonine^{25} phosphorylation has also been noted in a number of proteomics studies [56], [224], [225] including a mitotic phase proteomics study [226], but the function of this phosphorylation is also unknown.

In vitro phosphorylation of the Cofilin$^{S3A/S8A/T25A}$ mutant suggested additional residues are phosphorylated by Aur-A. Because the C-terminal fragment of Cofilin (residues 90-166) was not phosphorylated by Aur-A, the additional phosphorylation sites most likely lie between amino acids 1-89. Two putative residues are S^{23} and S^{24} (RK**SS**T) because they share a partial homology with the Aur-A phosphorylation motif ([K/N/R]-R-X-[pS/pT]-V) with a bias at the n+1 position. Interestingly the phosphorylation motif of Aur-A maintains that the n+1 position must not be a proline residue while T^{25} precedes a proline residue. Additionally, T^{63} and T^{70} may be phosphorylated by Aur-A but their phosphorylation would not have been detected by mass spectroscopy because the tryptic digestion would not have produced a peptide containing

124

these residues. Serine[41] and T[88] are two residues that could have been the additional phosphorylation sites but were not detected by mass spectrometry.

Phosphorylation by Aur-A negatively regulates Cofilin activity as noted in actin polymerization assays. Phosphorylation at S^3 inactivates Cofilin by preventing its ability to bind actin filaments. Therefore, reduced actin depolymerization by wild-type recombinant Cofilin incubated with His-Aur-A may be due to phosphorylation specifically at this site. Importantly, His-Cofilin^{S3A} activity was also noticeably reduced by phosphorylation by His-Aur-A, while His-Cofilin$^{S3A/S8A/T25A}$ retained a significantly higher level of activity when incubated with His-Aur-A. This data suggests phosphorylation at residues in addition to S^3 are involved in regulation of the depolymerization activity of Cofilin. Since S^8 is in close proximity to S^3, phosphorylation at that site may result in a similar conformational change that would prevent binding to actin. Inhibition of Aurora activity was also correlated with the reduced levels of F-actin *in vivo*. Taking this result into account with our early data, it is likely that the alteration in F-actin by Aur-A was mediated through Cofilin.

Aur-A phosphorylation of Cofilin also influences intracellular localization of Cofilin. Wild type Cofilin-RFP and Cofilin$^{S3A/S8A/T25A}$-RFP showed distinct differences in subcellular localization. Cofilin has been reported to localize to the Golgi to aid in cargo sorting and fission of carrier vesicles [227]-[229]. Aur-A may regulate Cofilin localization to this area through phosphorylation.

Our results also showed that Aur-A and Cofilin interact during mitosis and that this interaction is maintained during mitotic progression from prophase to

telophase. However, the activation status of Cofilin through phosphorylation changes as cells progress through the mitotic phases. Phospho-Cofilin levels are at the peak when cells are mostly in prophase and metaphase between 0 to 30 minutes after Nocodazole release, but declined significantly as the cells start to progress to anaphase between 30-60 minutes. It can be speculated that actin depolymerization is required as the spindles start to change shape and elongate during anaphase possibly through interaction with cortical actin. Interestingly, inhibition of Aur-A activity through MLN8237 resulted in a sustained increase in phospho-Cofilin levels as noted in 60 minutes after release, which is counterintuitive of decreased phospho-Cofilin as a result of inactivation of Aur-A. Importantly, MLN8237 treated cells showed a delayed progression of mitosis, as the majority of the cells are in prophase and only a small percentage of cells in metaphase. It can be speculated that inhibition of Aur-A activity induced mitotic delay is partly mediated by the failure of Cofilin-mediated deploymerization of actin. However, the question is how phospho-Cofilin levels increased upon inhibition of Aur-A kinase activity. We speculate that LIMK1 and SSH-1 phosphatase mediated Cofilin phosphorylation/dephosphorylation is responsible for the optimum phospho-Cofilin levels during mitosis. We have previously reported that Aur-A phosphorylates LIMK1 during mitosis, activating the protein and regulating its localization to the centrosomes [211]. An earlier report from another group showed that Aur-A regulates SSH-1 expression, as Aur-A overexpression led to increased expression of SSH-1 and dephosphorylation of

126

Cofilin [214]. Our data supported this previous finding as SSH-1 expression was significantly reduced after treatment with MLN8237.

Based on these observations we propose a Cofilin phosphorylation model during mitosis (Fig. 47). In early mitotic phases, LIMK1 and Aur-A phosphorylate and inactivate Cofilin (Fig. 47D and A) while at the later stages SSH-1 inactivates LIMK1 by removing the phosphate group at T^{508} [230](Fig. 47G), and additionally, dephosphorylates and activates Cofilin (Fig. 47F) [214]. Aur-A being a key regulator of early mitotic phases is participating in maintenance of phospho-Cofilin levels through activation of LIMK1, and SSH-1 as a negative feedback loop (Fig. 47B and E), which possibly resulted in decreased phospho-Cofilin levels as cells start to progress to anaphase. Hence, we speculate the possible scenario for increased phosphorylation of Cofilin following MLN8237 treatment. Inhibition of Aur-A may decrease the level of SSH-1 (Fig. 47E), thereby increasing the amount of phosphorylated/inactive Cofilin (Fig. 47F). Earlier studies showed that LIMK1 dependent phosphorylation of Cofilin is necessary for proper mitotic spindle orientation [163]. Treatment of cells with the Aur-A specific inhibitor, MLN8237, causes multipolar spindles and abnormal spindle morphology [211]. Therefore, in conclusion, our data suggests that regulation of spindle morphology and orientation by Aur-A in the early mitotic phases may be mediated, in part, through its control over Cofilin activity and actin polymerization.
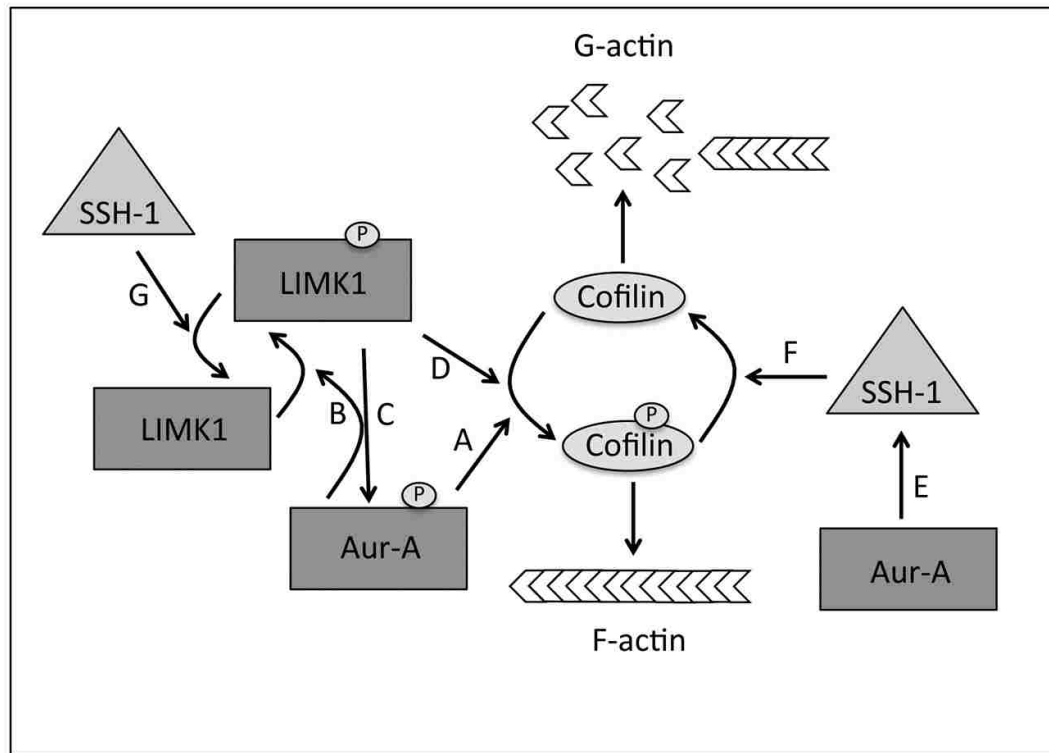
Figure 47: Model of the Regulation of Cofilin Phosphorylation.

(A) Aur-A phosphorylates Cofilin, causing inactivation of the protein leading to accumulation of F-actin. (B) Aur-A phosphorylates LIMK1 at S^{307} priming it for full activation by phosphorylation at T^{508}. (C) Interaction with LIMK1 allows for activation of Aur-A through autophosphorylation at T^{288}.   (D) LIMK1 phosphorylates Cofilin and inactivates it.   (E) Overexpression of Aur-A up regulates SSH-1. (F) SSH-1 activates Cofilin in late mitosis through dephosphorylation leading to depolymerization of F-actin. (G) SSH-1 inactivates LIMK1 in late mitosis by dephosphorylation at T^{508}.

CHAPTER SEVEN: GENERAL DISCUSSION AND CONCLUSION

The aim of this dissertation was to examine the role of LIMK1 and its substrates in cell cycle progression. We found that LIMK1 contributes to cell cycle progression in the following ways: 1) LIMK1 expression altered p27^{Kip1} expression during G1 phase, 2) LIMK1 regulates the activation and localization of Aurora A and vice versa during mitosis, 3) LIMK1 and Aurora A both regulate phosphorylation Cofilin during mitosis. Our findings are further discussed in the following sections.

7.1 The Role of LIMK1 in G1 Phase Progression

Prior to this study, little was known about the role of LIMK1 during G1 progression. We had previously found that overexpression of LIMK1 caused a transient G1/S phase arrest [45], but the mechanism of this arrest was unknown. In this study, we found overexpression of LIMK1 resulted in lower levels of p27^{Kip1} and its phosphorylated forms p27^{Kip1}-Y^{88}, and p27^{Kip1}-S^{10}. This observation was confirmed by knock down experiments, which showed elevated levels of p27^{Kip1} and p27^{Kip1}-Y^{88} in cells with inhibition of LIMK1 expression. Our data suggests that ectopic expression of LIMK1 induces G1/S phase arrest through decreased levels of p27^{Kip1}-pY^{88} (inactive p27^{Kip1}). Further studies will need to be performed to identify the mechanism behind the alteration in p27^{Kip1} levels.

7.2 The Role of LIMK1 and its substrates, Aurora A and Cofilin, in Mitosis

LIMK1 becomes highly phosphorylated during the early stages of mitosis, but it was not known which kinase was responsible for this phosphorylation. Inhibition ROCK or Pak did not effect LIMK1 phosphorylation [150], but treatment with the Cdk inhibitor, roscovitine, reduced LIMK1 phosphorylation [162]. Additionally, this phosphorylation was found to be at a site other than T^{508}. In this study, we found that Aurora A is responsible for the early mitotic phosphorylation of LIMK1. Aurora A phosphorylates LIMK1 at S^{307}, which then primes LIMK1 to be phosphorylated at T^{508} by Aurora A. Since Aurora A is activated by Cdk1, it is likely that roscovitine reduced LIMK1 phosphorylation through Aurora A inactivation [112].

Phosphorylation of LIMK1 at T^{508} regulates the centrosomal localization of LIMK1 during mitosis [152]. We found that phosphorylation at S^{307} is necessary for LIMK1 localization to the centrosome. Additionally, catalytic inhibition of Aurora A resulted in mislocalization of LIMK1. Based on this observation, it can be speculated that Aurora A regulates the centrosomal localization of LIMK1 during mitosis.

The phosphorylation pattern of Cofilin during mitosis has been well established. Cofilin is phosphorylated during metaphase by LIMK1 and dephosphorylated during the late stages of mitosis by Slingshot-1 [166]. In this study, we noted dual inhibition of LIMK1 and Aurora A reduced phospho-Cofilin levels more than single inhibition of either kinase. Therefore, it is likely that both

LIMK1 and Aurora A contribute directly to the phosphorylation of Cofilin during mitosis. Additionally, Aurora A also exerts regulation on Cofilin phosphorylation indirectly through the regulation of Slingshot-1 expression.

Previous studies have shown that regulation of the actin cytoskeleton is necessary for proper centrosome separation and maintenance of centrosome integrity. Knockdown of LIMK1 results in a loss of centrosome integrity causing defocused/diffused centrosomes [165]. Enrichment of F-actin at the cell cortex maintains cell rigidity which is necessary for proper spindle orientation and placement of the cleavage furrow [231] Therefore, centrosome defocusing after LIMK1 knockdown was attributed to a loss in cortical rigidity. Additionally, mutation of Twinstar, *Drosophila* homolog of Cofilin resulted in abnormal accumulation of F-actin leading to defects in centrosome separation [232]. Our study showed that LIMK1 knockdown resulted in loss of centrosome integrity, mislocalization of Aurora A, and decreased levels of Aurora A-pT^{288}. Therefore, in addition to regulation of the actin cytoskeleton, LIMK1 may regulate centrosome separation and integrity through its interaction with Aurora A.

Studies in *Drosophila* have suggested Aurora A may be involved in actin-dependent protein localization [78]. Our study supports this finding since Aurora A regulates LIMK1 and Cofilin during mitosis. Additionally, Aurora A may exert additional control over centrosome separation through the regulation of LIMK1 and Cofilin.

The actin cytoskeleton is essential for proper mitotic spindle orientation. Disruption of the actin cytoskeleton with the actin polymerization inhibitors,

Latrunculin B or Cytochalasin D, resulted in random orientation of the mitotic spindles [219]. Cells treated with Lat-A did not elongate during anaphase and many cells were unable to undergo cytokinesis [163]. siRNA knockdown of LIMK1 or treatment with Lat-A resulted in weakened astral microtubules as assessed by decreased staining of α-tubulin [163]. Additionally, LIMK1 mediated phosphorylation of Cofilin is necessary for proper mitotic spindle orientation [163]. Therefore, Aurora A may indirectly regulate microtubule dynamics through actin cytoskeletal modulation via interaction with LIMK1 and Cofilin.

In addition to regulation of the actin cytoskeleton, LIMK1 is involved in the regulation of microtubule dynamics. LIMK1 interaction with thrombin in endothelial cells induces actin polymerization and microtubule depolymerization [164] . Phosphorylation of p25α/TPPP by LIMK1 prevents tubulin polymerization [153]. This study presents a novel role for LIMK1 in maintenance of microtubule dynamics through interaction with Aurora A. Our study identified LIMK1 as a protein cofactor of Aurora A necessary for Aurora A localization to the centrosomes. siRNA knockdown of LIMK1 resulted in diffuse Aurora A localization and also abnormal mitotic spindles. Our findings and published studies suggest that both LIMK1 and Aurora A may be involved in regulating microtubule dynamics.

Overexpression of LIMK1 results in an increased number of multinucleated cells [150]. The formation of multinucleated cells has been attributed to cytokinesis defects caused by F-actin accumulation at the contractile ring [154]. Although Aurora A has been studied primarily during early mitosis,

our data suggests that Aurora A may play a role in the regulation of the later stages of mitosis. Based on our observation it can be speculated that Aurora A may participate in the regulation of cytokinesis through the regulation of LIMK1 and Cofilin activation, and hence the actin cytoskeleton,

Both Aurora A and LIMK1 are overexpressed in a multitude of cancer types, including breast and prostate [71], [72], [144], [156]. Therefore, identifying interacting partners for these proteins and understanding their mechanism of action during mitosis has become a highly studied area. Additionally, identifying small molecule inhibitors of Aurora A and LIMK1 as anticancer therapeutics is of high importance. Although inhibitors of Aurora A are widely available, very few LIMK1 inhibitors are available, none of which show therapeutic potential. Our data suggests that inhibition of LIMK1 or Aurora A in combination, would have the added benefit of inhibition of cell cycle progression.

LIST OF REFERENCES

[1] Y. Li, M. Chopp, C. Powers, and N. Jiang, "Apoptosis and protein expression after focal cerebral ischemia in rat.," *Brain Res.*, vol. 765, no. 2, pp. 301–312, Aug. 1997.

[2] H. Osuga, S. Osuga, F. Wang, R. Fetni, M. J. Hogan, R. S. Slack, A. M. Hakim, J. E. Ikeda, and D. S. Park, "Cyclin-dependent kinases as a therapeutic target for stroke.," *Proc. Natl. Acad. Sci. U.S.A.*, vol. 97, no. 18, pp. 10254–10259, Aug. 2000.

[3] B. Zhivotovsky and S. Orrenius, "Cell cycle and cell death in disease: past, present and future.," *J. Intern. Med.*, vol. 268, no. 5, pp. 395–409, Nov. 2010.

[4] O. Ibraghimov-Beskrovnaya, "Targeting dysregulated cell cycle and apoptosis for polycystic kidney disease therapy.," *Cell Cycle*, vol. 6, no. 7, pp. 776–779, Apr. 2007.

[5] V. Baldin, J. Lukas, M. J. Marcote, M. Pagano, and G. Draetta, "Cyclin D1 is a nuclear protein required for cell cycle progression in G1.," *Genes Dev.*, vol. 7, no. 5, pp. 812–821, May 1993.

[6] A. Brehm, E. A. Miska, D. J. McCance, J. L. Reid, A. J. Bannister, and T. Kouzarides, "Retinoblastoma protein recruits histone deacetylase to repress transcription.," *nature*, vol. 391, no. 6667, pp. 597–601, Feb. 1998.

[7] A. Harel-Bellan, L. Magnaghi-Jaulin, R. Groisman, I. Naguibneva, P. Robin, S. Lorain, J. P. Le Villain, F. Troalen, and D. Trouche, "Retinoblastoma protein represses transcription by recruiting a histone deacetylase : Abstract : Nature," *Nature*, vol. 391, no. 6667, pp. 601–605, Feb. 1998.

[8] R. X. Luo, A. A. Postigo, and D. C. Dean, "Rb Interacts with Histone Deacetylase to Repress Transcription," *Cell*, 1998.

[9] J. A. Lees, M. Saito, M. Vidal, M. Valentine, T. Look, E. Harlow, N. Dyson, and K. Helin, "The retinoblastoma protein binds to a family of E2F transcription factors.," *Mol. Cell. Biol.*, vol. 13, no. 12, pp. 7813–7825, Dec. 1993.

[10 K. Helin, E. Harlow, and A. Fattaey, "Inhibition of E2F-1 transactivation by direct binding of the retinoblastoma protein.," *Mol. Cell. Biol.*, vol. 13, no. 10, pp. 6501–6508, Oct. 1993.

[11] G. Leone, J. DeGregori, Z. Yan, L. Jakoi, S. Ishida, R. S. Williams, and J. R. Nevins, "E2F3 activity is regulated during the cell cycle and is required for the induction of S phase.," *Genes Dev.*, vol. 12, no. 14, pp. 2120–2130, Jul. 1998.

[12] T. Soucek, O. Pusch, E. Hengstschläger-Ottnad, P. D. Adams, and M. Hengstschläger, "Deregulated expression of E2F-1 induces cyclin A- and E-associated kinase activities independently from cell cycle position.," *Oncogene*, vol. 14, no. 19, pp. 2251–2257, May 1997.

[13] B. D. Dynlacht, O. Flores, J. A. Lees, and E. Harlow, "Differential regulation of E2F transactivation by cyclin/cdk2 complexes.," *Genes Dev.*, vol. 8, no. 15, pp. 1772–1786, Aug. 1994.

[14] J. W. Ludlow, C. L. Glendening, D. M. Livingston, and J. A. DeCarprio, "Specific enzymatic dephosphorylation of the retinoblastoma protein.," *… and cellular biology*, 1993.

[15] A. B. Pardee, "A restriction point for control of normal animal cell proliferation.," *Proc. Natl. Acad. Sci. U.S.A.*, vol. 71, no. 4, pp. 1286–1290, Apr. 1974.

[16] J. Nourse, E. Firpo, W. M. Flanagan, S. Coats, K. Polyak, M. H. Lee, J. Massagué, G. R. Crabtree, and J. M. Roberts, "Interleukin-2-mediated elimination of the p27Kip1 cyclin-dependent kinase inhibitor prevented by rapamycin.," *nature*, vol. 372, no. 6506, pp. 570–573, Dec. 1994.

[17] M. H. Lee, I. Reynisdóttir, and J. Massagué, "Cloning of p57KIP2, a cyclin-dependent kinase inhibitor with unique domain structure and tissue distribution.," *Genes Dev.*, vol. 9, no. 6, pp. 639–649, Mar. 1995.

[18] N. Rivard, G. L'Allemain, J. Bartek, and J. Pouysségur, "Abrogation of p27Kip1 by cDNA Antisense Suppresses Quiescence (G0 State) in Fibroblasts," *Journal of Biological …*, 1996.

[19] N. K, O. K, O. I, and M. K, "LIMK-1 and LIMK-2, two members of a LIM motif-containing protein kinase family.," *Oncogene*, vol. 11, no. 4, pp. 701–710, Aug. 1995.

[20] H. Toyoshima and T. Hunter, "p27, a novel inhibitor of G1 cyclin-Cdk protein kinase activity, is related to p21," *Cell*, vol. 78, no. 1, pp. 67–74, Jul. 1994.

[21] K. Mizuno, I. Okano, K. Ohashi, K. Nunoue, K. Kuma, T. Miyata, and T. Nakamura, "Identification of a human cDNA encoding a novel protein kinase with two repeats of the LIM/double zinc finger motif.," *Oncogene*,

vol. 9, no. 6, pp. 1605–1612, Jun. 1994.

[22] A. A. Russo, P. D. Jeffrey, A. K. Patten, J. Massagué, and N. P. Pavletich, "Crystal structure of the p27Kip1 cyclin-dependent-kinase inhibitor bound to the cyclin A-Cdk2 complex.," *nature*, vol. 382, no. 6589, pp. 325–331, Jul. 1996.

[23] K. Ohashi, K. Nagata, M. Maekawa, T. Ishizaki, S. Narumiya, and K. Mizuno, "Rho-associated Kinase ROCK Activates LIM-kinase 1 by Phosphorylation at Threonine 508 within the Activation Loop," *Journal of Biological Chemistry*, vol. 275, no. 5, pp. 3577–3582, Feb. 2000.

[24] N. Ishida, T. Hara, T. Kamura, M. Yoshida, K. Nakayama, and K. I. Nakayama, "Phosphorylation of p27Kip1 on serine 10 is required for its binding to CRM1 and nuclear export.," *J. Biol. Chem.*, vol. 277, no. 17, pp. 14355–14358, Apr. 2002.

[25] G. M. Bokoch, D. C. Edwards, L. C. Sanders, and G. N. Gill, "Activation of LIM-kinase by Pak1 couples Rac/Cdc42 GTPase signalling to actin cytoskeletal dynamics," *Nat. Cell Biol.*, vol. 1, no. 5, pp. 253–259, Jul. 1999.

[26] A. Besson, M. Gurian-West, X. Chen, K. S. Kelly-Spratt, C. J. Kemp, and J. M. Roberts, "A pathway in quiescent cells that controls p27Kip1 stability, subcellular localization, and tumor suppression.," *Genes Dev.*, vol. 20, no. 1, pp. 47–64, Jan. 2006.

[27] C. Dan, "Cytoskeletal Changes Regulated by the PAK4 Serine/Threonine Kinase Are Mediated by LIM Kinase 1 and Cofilin," *Journal of Biological Chemistry*, vol. 276, no. 34, pp. 32115–32121, Jun. 2001.

[28] A. J. Ridley, H. F. Paterson, C. L. Johnston, D. Diekmann, and A. Hall, "The small GTP-binding protein rac regulates growth factor-induced membrane ruffling.," *Cell*, vol. 70, no. 3, pp. 401–410, Aug. 1992.

[29] A. R. Mohanty, Q. Kan, S. Srivastava, B. Uranbileg, S. Arakawa-Takeuchi, N. Fujita, and H. Okayama, "Successive phosphorylation of p27(KIP1) protein at serine-10 and C terminus crucially controls its potency to inactivate Cdk2.," *J. Biol. Chem.*, vol. 287, no. 26, pp. 21757–21764, Jun. 2012.

[30] C. D. Nobes and A. Hall, "Rho, Rac, and Cdc42 GTPases regulate the assembly of multimolecular focal complexes associated with actin stress fibers, lamellipodia, and filopodia," *Cell*, 1995.

[31 R. Kozma, S. Ahmed, A. Best, and L. Lim, "The Ras-related protein Cdc42Hs

and bradykinin promote formation of peripheral actin microspikes and filopodia in Swiss 3T3 fibroblasts.," *Mol. Cell. Biol.*, vol. 15, no. 4, pp. 1942–1952, Apr. 1995.

[32] M. Amano, K. Chihara, K. Kimura, Y. Fukata, N. Nakamura, Y. Matsuura, and K. Kaibuchi, "Formation of actin stress fibers and focal adhesions enhanced by Rho-kinase.," *Science*, vol. 275, no. 5304, pp. 1308–1311, Feb. 1997.

[33] J. Soosairajah, S. Maiti, O. Wiggan, P. Sarmiere, N. Moussi, B. Sarcevic, R. Sampath, J. R. Bamburg, and O. Bernard, "Interplay between components of a novel LIM kinase–slingshot phosphatase complex regulates cofilin," *EMBO J.*, vol. 24, no. 3, pp. 473–486, Jan. 2005.

[34] R. J. Sheaff, M. Groudine, M. Gordon, J. M. Roberts, and B. E. Clurman, "Cyclin E-CDK2 is a regulator of p27Kip1.," *Genes Dev.*, vol. 11, no. 11, pp. 1464–1478, Jun. 1997.

[35] A. C. Carrano, E. Eytan, A. Hershko, and M. Pagano, "SKP2 is required for ubiquitin-mediated degradation of the CDK inhibitor p27 : Abstract : Nature Cell Biology," *Nat. Cell Biol.*, vol. 1, no. 4, pp. 193–199, Jun. 1999.

[36] H. Nguyen, D. M. Gitig, and A. Koff, "Cell-Free Degradation of p27 kip1 , a G1 Cyclin-Dependent Kinase Inhibitor, Is Dependent on CDK2 Activity and the Proteasome," *Mol. Cell. Biol.*, 1999.

[37] M. Kobayashi, M. Nishita, T. Mishima, K. Ohashi, and K. Mizuno, "MAPKAPK-2-mediated LIM-kinase activation is critical for VEGF-induced actin remodeling and cell migration.," *EMBO J.*, vol. 25, no. 4, pp. 713–726, Feb. 2006.

[38] M. K. James, A. Ray, D. Leznova, and S. W. Blain, "Differential modification of p27Kip1 controls its cyclin D-cdk4 inhibitory activity.," *Mol. Cell. Biol.*, vol. 28, no. 1, pp. 498–510, Jan. 2008.

[39] R. Li, J. Soosairajah, D. Harari, A. Citri, J. Price, H. L. Ng, C. J. Morton, M. W. Parker, Y. Yarden, and O. Bernard, "Hsp90 increases LIM kinase activity by promoting its homo-dimerization," *The FASEB Journal*, vol. 20, no. 8, pp. 1218–1220, Jun. 2006.

[40] M. Grimmler, Y. Wang, T. Mund, Z. Cilensek, E.-M. Keidel, M. B. Waddell, H. Jäkel, M. Kullmann, R. W. Kriwacki, and L. Hengst, "Cdk-inhibitory activity and stability of p27Kip1 are directly regulated by oncogenic tyrosine kinases.," *Cell*, vol. 128, no. 2, pp. 269–280, Jan. 2007.

[41] R. N. Booher, P. S. Holman, and A. Fattaey, "Human Myt1 Is a Cell Cycle-regulated Kinase That Inhibits Cdc2 but Not Cdk2 Activity," *Journal of Biological Chemistry*, 1997.

[42] G. J. Den Haese, N. Walworth, A. M. Carr, and K. L. Gould, "The Wee1 protein kinase regulates T14 phosphorylation of fission yeast Cdc2.," *Molecular biology of the cell*, vol. 6, no. 4, pp. 371–385, Apr. 1995.

[43] Y. Gu, J. Rosenblatt, and D. O. Morgan, "Cell cycle regulation of CDK2 activity by phosphorylation of Thr160 and Tyr15.," *EMBO J.*, vol. 11, no. 11, pp. 3995–4005, Nov. 1992.

[44] I. Blomberg and I. Hoffmann, "Ectopic Expression of Cdc25A Accelerates the G1/S Transition and Leads to Premature Activation of Cyclin E- and Cyclin A-Dependent Kinases," *Mol. Cell. Biol.*, 1999.

[45] M. Davila, D. Jhala, D. Ghosh, W. E. Grizzle, and R. Chakrabarti, "Expression of LIM kinase 1 is associated with reversible G1/S phase arrest, chromosomal instability and prostate cancer.," *Molecular Cancer*, vol. 6, p. 40, 2007.

[46] I. B. Dawid, J. J. Breen, and R. Toyama, "LIM domains: multiple roles as adapters and functional modifiers in protein interactions.," *Trends Genet.*, vol. 14, no. 4, pp. 156–162, Apr. 1998.

[47] A. S. Fanning and J. M. Anderson, "Protein–protein interactions: PDZ domain networks," *Curr. Biol.*, vol. 6, no. 11, pp. 1385–1388, Nov. 1996.

[48] T. Yokoo, "p57Kip2 Regulates Actin Dynamics by Binding and Translocating LIM-kinase 1 to the Nucleus," *J. Biol. Chem.*, vol. 278, no. 52, pp. 52919–52923, Oct. 2003.

[49] N. Yang, O. Higuchi, and K. Mizuno, "Cytoplasmic localization of LIM-kinase 1 is directed by a short sequence within the PDZ domain.," *Experimental Cell Research*, vol. 241, no. 1, pp. 242–252, May 1998.

[50] N. Yang and K. Mizuno, "Nuclear export of LIM-kinase 1, mediated by two leucine-rich nuclear-export signals within the PDZ domain.," *Biochem. J.*, vol. 338, pp. 793–798, Mar. 1999.

[51] P. Goyal, D. Pandey, and W. Siess, "Phosphorylation-dependent regulation of unique nuclear and nucleolar localization signals of LIM kinase 2 in endothelial cells.," *J. Biol. Chem.*, vol. 281, no. 35, pp. 25223–25230, Sep. 2006.

[52] P. Vlachos and B. Joseph, "The Cdk inhibitor p57Kip2 controls LIM-kinase 1

activity and regulates actin cytoskeleton dynamics," *Oncogene*, vol. 28, no. 47, pp. 4175–4188, Sep. 2009.

[53] P. Caroni, S. Arber, F. A. Barbayannis, H. Hanser, C. Schneider, C. A. Stanyon, and O. Bernard, "Regulation of actin dynamics through phosphorylation of cofilin by LIM-kinase ," *Nature*, vol. 393, no. 6687, pp. 805–809, Jun. 1998.

[54] E. Nishida, S. Maekawa, and H. Sakai, "Cofilin, a protein in porcine brain that binds to actin filaments and inhibits their interactions with myosin and tropomyosin.," *Biochemistry*, vol. 23, no. 22, pp. 5307–5313, Oct. 1984.

[55] O. Bernard, "Lim kinases, regulators of actin dynamics," *International Journal of Biochemistry and Cell Biology*, vol. 39, no. 6, pp. 1071–1076, 2007.

[56] R. Nagaoka, H. Abe, and T. Obinata, "Site-directed mutagenesis of the phosphorylation site of cofilin: Its role in cofilin-actin interaction and cytoplasmic localization," *Cell Motil. Cytoskeleton*, vol. 35, no. 3, pp. 200–209, 1996.

[57] N. Yang, O. Higuchi, K. Ohashi, K. Nagata, and A. Wada, "Cofilin phosphorylation by LIM-kinase 1 and its role in Rac-mediated actin reorganization," *Nature*, pp. 1–4, Jun. 1998.

[58] K. Nagata, K. Ohashi, N. Yang, and K. Mizuno, "The N-terminal LIM domain negatively regulates the kinase activity of LIM-kinase 1.," *Biochem. J.*, vol. 343, pp. 99–105, Oct. 1999.

[59] S.-E. Chow, J.-S. Wang, M.-R. Lin, and C. L. Lee, "Downregulation of p57kip2 promotes cell invasion via LIMK/cofilin pathway in human nasopharyngeal carcinoma cells," *J. Cell. Biochem.*, vol. 112, no. 11, pp. 3459–3468, Oct. 2011.

[60] E. A. Nigg, "Mitotic kinases as regulators of cell division and its checkpoints.," *Nature reviews. Molecular cell biology*, vol. 2, no. 1, pp. 21–32, Jan. 2001.

[61] K. S. Nadella, M. Saji, N. K. Jacob, E. Pavel, M. D. Ringel, and L. S. Kirschner, "Regulation of actin function by protein kinase A-mediated phosphorylation of Limk1," *EMBO Rep*, vol. 10, no. 6, pp. 599–605, May 2009.

[62] T.-C. TSENG, S.-H. CHEN, Y.-P. P. HSU, and T. K. TANG, "Protein Kinase Profile of Sperm and Eggs: Cloning and Characterization of Two Novel Testis-Specific Protein Kinases (AIE1, AIE2) Related to Yeast and Fly Chromosome Segregation Regulators," *DNA Cell Biol.*, vol. 17, no. 10,

pp. 823–833, Oct. 1998.

[63] H. M. Hu, C. K. Chuang, M. J. Lee, T. C. Tseng, and T. K. Tang, "Genomic organization, expression, and chromosome localization of a third aurora-related kinase gene, Aie1.," *DNA Cell Biol.*, vol. 19, no. 11, pp. 679–688, Nov. 2000.

[64] M. Kimura, Y. Matsuda, T. Yoshioka, and Y. Okano, "Cell cycle-dependent expression and centrosome localization of a third human aurora/Ipl1-related protein kinase, AIK3.," *J. Biol. Chem.*, vol. 274, no. 11, pp. 7334–7340, Mar. 1999.

[65] O. Higuchi, G. H. Baeg, T. Akiyama, and K. Mizuno, "Suppression of fibroblast cell growth by overexpression of LIM-kinase 1.," *FEBS Lett.*, vol. 396, no. 1, pp. 81–86, Oct. 1996.

[66] R. Giet, R. Uzbekov, F. Cubizolles, K. Le Guellec, and C. Prigent, "The Xenopus laevis aurora-related protein kinase pEg2 associates with and phosphorylates the kinesin-related protein XlEg5.," *Journal of Biological Chemistry*, vol. 274, no. 21, pp. 15005–15013, May 1999.

[67] E. Hannak, M. Kirkham, A. A. Hyman, and K. Oegema, "Aurora-A kinase is required for centrosome maturation in Caenorhabditis elegans," *The Journal of cell …*, 2001.

[68] Y. Terada, Y. Uetake, and R. Kuriyama, "Interaction of Aurora-A and centrosomin at the microtubule-nucleating site in Drosophila and mammalian cells," *The Journal of Cell Biology*, 2003.

[69] R. Giet, "Drosophila Aurora A kinase is required to localize D-TACC to centrosomes and to regulate astral microtubules," *The Journal of Cell Biology*, vol. 156, no. 3, pp. 437–451, Feb. 2002.

[70] C. A. Kemp, K. R. Kopish, P. Zipperlen, J. Ahringer, and K. F. O'Connell, "Centrosome maturation and duplication in C. elegans require the coiled-coil protein SPD-2.," *Dev. Cell*, vol. 6, no. 4, pp. 511–523, Apr. 2004.

[71] R. Bagheri-Yarmand, A. Mazumdar, A. A. Sahin, and R. Kumar, "LIM kinase 1 increases tumor metastasis of human breast cancer cellsvia regulation of the urokinase-type plasminogen activator system," *Int. J. Cancer*, vol. 118, no. 11, pp. 2703–2710, 2006.

[72] M. Davila, "LIM Kinase 1 Is Essential for the Invasive Growth of Prostate Epithelial Cells: IMPLICATIONS IN PROSTATE CANCER," *J. Biol. Chem.*, vol. 278, no. 38, pp. 36868–36875, Jul. 2003.

140

[73] K. Yoshioka, V. Foletta, O. Bernard, and K. Itoh, "A role for LIM kinase in cancer invasion," *Proceedings of the National Academy of Sciences*, vol. 100, no. 12, pp. 7247–7252, May 2003.

[74] I. Okamoto, C. Pirker, M. Bilban, W. Berger, D. Losert, C. Marosi, O. A. Haas, K. Wolff, and H. Pehamberger, "Seven novel and stable translocations associated with oncogenic gene expression in malignant melanoma.," *Neoplasia*, vol. 7, no. 4, pp. 303–311, Apr. 2005.

[75] H. Akagawa, A. Tajima, Y. Sakamoto, B. Krischek, T. Yoneyama, H. Kasuya, H. Onda, T. Hori, M. Kubota, T. Machida, N. Saeki, A. Hata, K. Hashiguchi, E. Kimura, C.-J. Kim, T.-K. Yang, J.-Y. Lee, K. Kimm, and I. Inoue, "A haplotype spanning two genes, ELN and LIMK1, decreases their transcripts and confers susceptibility to intracranial aneurysms.," *Hum. Mol. Genet.*, vol. 15, no. 10, pp. 1722–1734, May 2006.

[76] V. C. Foletta, M. A. Lim, J. Soosairajah, A. P. Kelly, E. G. Stanley, M. Shannon, W. He, S. Das, J. Massagué, and O. Bernard, "Direct signaling by the BMP type II receptor via the cytoskeletal regulator LIMK1," *The Journal of cell …*, 2003.

[77] C. C. Hoogenraad, A. Akhmanova, N. Galjart, and C. I. De Zeeuw, "LIMK1 and CLIP-115: linking cytoskeletal defects to Williams syndrome," *Bioessays*, vol. 26, no. 2, pp. 141–150, 2004.

[78] D. Berdnik, "ScienceDirect.com - Current Biology - Drosophila Aurora-A Is Required for Centrosome Maturation and Actin-Dependent Asymmetric Protein Localization during Mitosis," *Curr. Biol.*, pp. 1–8, 2002.

[79] N. Yonezawa, E. Nishida, and H. Sakai, "pH control of actin polymerization by cofilin.," *Journal of Biological Chemistry*, 1985.

[80] J. Toshima, J. Y. Toshima, T. Amano, N. Yang, S. Narumiya, and K. Mizuno, "Cofilin Phosphorylation by Protein Kinase Testicular Protein Kinase 1 and Its Role in Integrin-mediated Actin Reorganization and Focal Adhesion Formation," *Molecular biology of the cell*, vol. 12, no. 4, pp. 1131–1145, Apr. 2001.

[81] J. Toshima, "Cofilin Phosphorylation and Actin Reorganization Activities of Testicular Protein Kinase 2 and Its Predominant Expression in Testicular Sertoli Cells," *Journal of Biological Chemistry*, vol. 276, no. 33, pp. 31449–31458, Jun. 2001.

[82] R. Niwa, K. Nagata-Ohashi, M. Takeichi, and K. Mizuno, "Control of Actin Reorganization by Slingshot, a Family of Phosphatases that Dephosphorylate ADF/Cofilin," *Cell*, 2002.

[83] T. Y. Huang, C. DerMardirossian, and G. M. Bokoch, "Cofilin phosphatases and regulation of actin dynamics," *Current Opinion in Cell Biology*, 2006.

[84] Y. Yoo, H. J. Ho, C. Wang, and J.-L. Guan, "Tyrosine phosphorylation of cofilin at Y68 by v-Src leads to its degradation through ubiquitin-proteasome pathway.," *Oncogene*, vol. 29, no. 2, pp. 263–272, Jan. 2010.

[85] R. Assoian, "Cell anchorage and the cytoskeleton as partners in growth factor dependent cell cycle progression," *Current Opinion in Cell Biology*, vol. 9, no. 1, pp. 93–98, 1997.

[86] R. K. Assoian, "Control of the G1 phase cyclin-dependent kinases by mitogenic growth factors and the extracellular matrix.," *Cytokine Growth Factor Rev.*, vol. 8, no. 3, pp. 165–170, Sep. 1997.

[87] S. Huang, C. S. Chen, and D. E. Ingber, "Control of Cyclin D1, p27Kip1, and Cell Cycle Progression in Human Capillary Endothelial Cells by Cell Shape and Cytoskeletal Tension," *Molecular biology of the cell*, vol. 9, no. 11, pp. 3179–3193, Nov. 1998.

[88] M. Fasshauer, M. Iwig, and D. Glaesser, "Synthesis of proto-oncogene proteins and cyclins depends on intact microfilaments.," *Eur. J. Cell Biol.*, vol. 77, no. 3, pp. 188–195, Nov. 1998.

[89] R. K. Assoian, "Anchorage-dependent Cell Cycle Progression," *The Journal of Cell Biology*, vol. 136, no. 1, pp. 1–4, Jan. 1997.

[90] C.-H. Tsai, S.-J. Chiu, C.-C. Liu, T.-J. Sheu, C.-H. Hsieh, P. C. Keng, and Y.-J. Lee, "Regulated expression of cofilin and the consequent regulation of p27(kip1) are essential for G(1) phase progression.," *Cell Cycle*, vol. 8, no. 15, pp. 2365–2374, Aug. 2009.

[91] S. Nicholson-Dykstra, H. N. Higgs, and E. S. Harris, "Actin dynamics: growth from dendritic branches.," *Curr. Biol.*, vol. 15, no. 9, pp. R346–57, May 2005.

[92] S. H. Zigmond, "Formin-induced nucleation of actin filaments.," *Current Opinion in Cell Biology*, vol. 16, no. 1, pp. 99–105, Feb. 2004.

[93] J. Condeelis, "How is actin polymerization nucleated in vivo?," *Trends in Cell Biology*, vol. 11, no. 7, pp. 288–293, Jul. 2001.

[94] H. Yamaguchi, J. Wyckoff, and J. Condeelis, "Cell migration in tumors," *Current Opinion in Cell Biology*, 2005.

[95] J. Condeelis and J. E. Segall, "Intravital imaging of cell movement in tumours.," *Nat Rev Cancer*, vol. 3, no. 12, pp. 921–930, Dec. 2003.

[96] W. L. Lingle, W. H. Lutz, J. N. Ingle, N. J. Maihle, and J. L. Salisbury, "Centrosome hypertrophy in human breast tumors: Implications for genomic stability and cell polarity," *Proceedings of the …*, 1998.

[97] H. Zhou, J. Kuang, L. Zhong, W. L. Kuo, J. W. Gray, A. Sahin, B. R. Brinkley, and S. Sen, "Tumour amplified kinase STK15/BTAK induces centrosome amplification, aneuploidy and transformation.," *Nat. Genet.*, vol. 20, no. 2, pp. 189–193, Oct. 1998.

[98] T. Tanaka, M. Kimura, K. Matsunaga, D. Fukada, H. Mori, and Y. Okano, "Centrosomal kinase AIK1 is overexpressed in invasive ductal carcinoma of the breast.," *Cancer Res.*, vol. 59, no. 9, pp. 2041–2044, May 1999.

[99] S. Sen, H. Zhou, R.-D. Zhang, D. S. Yoon, F. Vakar-Lopez, S. Ito, F. Jiang, D. Johnston, H. B. Grossman, A. C. Ruifrok, R. L. Katz, W. Brinkley, and B. Czerniak, "Amplification/overexpression of a mitotic kinase gene in human bladder cancer.," *J. Natl. Cancer Inst.*, vol. 94, no. 17, pp. 1320–1329, Sep. 2002.

[100] F. Jiang, N. P. Caraway, A. L. Sabichi, H. Z. Zhang, A. Ruitrok, H. B. Grossman, J. Gu, S. P. Lerner, S. Lippman, and R. L. Katz, "Centrosomal abnormality is common in and a potential biomarker for bladder cancer.," *Int. J. Cancer*, vol. 106, no. 5, pp. 661–665, Sep. 2003.

[101] O. J. Gruss, R. E. Carazo-Salas, C. A. Schatz, G. Guarguaglini, J. Kast, M. Wilm, N. Le Bot, I. Vernos, E. Karsenti, and I. W. Mattaj, "Ran Induces Spindle Assembly by Reversing the Inhibitory Effect of Importin α on TPX2 Activity," *Cell*, vol. 104, no. 1, pp. 83–93, Jan. 2001.

[102] T. A. Kufer, H. H. W. Silljé, R. Körner, O. J. Gruss, P. Meraldi, and E. A. Nigg, "Human TPX2 is required for targeting Aurora-A kinase to the spindle.," *J Cell Biol*, vol. 158, no. 4, pp. 617–623, Aug. 2002.

[103] J. R. Bischoff, L. Anderson, Y. Zhu, K. Mossie, L. Ng, B. Souza, B. Schryver, P. Flanagan, F. Clairvoyant, C. Ginther, C. S. Chan, M. Novotny, D. J. Slamon, and G. D. Plowman, "A homologue of Drosophila aurora kinase is oncogenic and amplified in human colorectal cancers.," *EMBO J.*, vol. 17, no. 11, pp. 3052–3065, Jun. 1998.

[104] R. R. Adams, M. Carmena, and W. C. Earnshaw, "Chromosomal

passengers and the (aurora) ABCs of mitosis," *Trends in Cell Biology*, vol. 11, no. 2, pp. 49–54, Feb. 2001.

[105] K. B. Shannon and E. D. Salmon, "Chromosome dynamics: new light on Aurora B kinase function.," *Curr. Biol.*, vol. 12, no. 13, pp. R458–60, Jul. 2002.

[106] R. Giet and C. Prigent, "Aurora/Ipl1p-related kinases, a new oncogenic family of mitotic serine-threonine kinases.," *Journal of Cell Science*, vol. 112, pp. 3591–3601, Nov. 1999.

[107] J. R. Brown, K. K. Koretke, M. L. Birkeland, P. Sanseau, and D. R. Patrick, "Evolutionary relationships of Aurora kinases: implications for model organism studies and the development of anti-cancer drugs.," *BMC Evol. Biol.*, vol. 4, p. 39, Oct. 2004.

[108] Q. Liu, "Aurora A, mitotic entry, and spindle bipolarity," *Proceedings of the National Academy of Sciences*, vol. 103, no. 15, pp. 5811–5816, Apr. 2006.

[109] J. Du and G. Hannon, "Suppression of p160ROCK bypasses cell cycle arrest after Aurora-A/STK15 depletion," *Proceedings of the National Academy of Sciences*, vol. 101, no. 24, pp. 8975–8980, Jun. 2004.

[110] H. Yang, T. Burke, J. Dempsey, B. Diaz, E. Collins, J. Toth, R. Beckmann, and X. Ye, "Mitotic requirement for aurora A kinase is bypassed in the absence of aurora B kinase.," *FEBS Lett.*, vol. 579, no. 16, pp. 3385–3391, Jun. 2005.

[111] A. Lindqvist, V. Rodriguez-Bravo, and R. H. Medema, "The decision to enter mitosis: feedback and redundancy in the mitotic entry network," *The Journal of Cell Biology*, vol. 185, no. 2, pp. 193–202, Apr. 2009.

[112] R. D. Van Horn, S. Chu, L. Fan, T. Yin, J. Du, R. Beckmann, M. Mader, G. Zhu, J. Toth, K. Blanchard, and X. S. Ye, "Cdk1 activity is required for mitotic activation of aurora A during G2/M transition of human cells.," *J. Biol. Chem.*, vol. 285, no. 28, pp. 21849–21857, Jul. 2010.

[113] Y. W. Qian, E. Erikson, and J. L. Maller, "Mitotic effects of a constitutively active mutant of the Xenopus polo-like kinase Plx1.," *Mol. Cell. Biol.*, vol. 19, no. 12, pp. 8625–8632, Dec. 1999.

[114] O. Kelm, M. Wind, W. D. Lehmann, and E. A. Nigg, "Cell Cycle-regulated Phosphorylation of the XenopusPolo-like Kinase Plx1," 2002.

[115] Y. J. Jang, "Phosphorylation of Threonine 210 and the Role of Serine 137

in the Regulation of Mammalian Polo-like Kinase," *Journal of Biological Chemistry*, vol. 277, no. 46, pp. 44115–44120, Aug. 2002.

[116] K. S. Lee and R. L. Erikson, "Plk is a functional homolog of Saccharomyces cerevisiae Cdc5, and elevated Plk activity induces multiple septation structures.," *Mol. Cell. Biol.*, vol. 17, no. 6, pp. 3408–3417, Jun. 1997.

[117] Y.-J. Jang, C.-Y. Lin, S. Ma, and R. L. Erikson, "Functional studies on the role of the C-terminal domain of mammalian polo-like kinase," *Proceedings of the …*, 2002.

[118] A. Seki, J. A. Coppinger, C.-Y. Jang, J. R. Yates, and G. Fang, "Bora and the kinase Aurora a cooperatively activate the kinase Plk1 and control mitotic entry," *Science Signaling*, vol. 320, no. 5883, p. 1655, 2008.

[119] E. H. Y. Chan, A. Santamaria, H. H. W. Silljé, and E. A. Nigg, "Plk1 regulates mitotic Aurora A function through betaTrCP-dependent degradation of hBora.," *Chromosoma*, vol. 117, no. 5, pp. 457–469, Oct. 2008.

[120] L. Macůrek, A. Lindqvist, D. Lim, M. A. Lampson, R. Klompmaker, R. Freire, C. Clouin, S. S. Taylor, M. B. Yaffe, and R. H. Medema, "Polo-like kinase-1 is activated by aurora A to promote checkpoint recovery," *nature*, vol. 455, no. 7209, pp. 119–123, 2008.

[121] A. Kumagai and W. G. Dunphy, "Purification and molecular cloning of Plx1, a Cdc25-regulatory kinase from Xenopus egg extracts.," *Science*, vol. 273, no. 5280, pp. 1377–1380, Sep. 1996.

[122] N. Watanabe, H. Arai, Y. Nishihara, M. Taniguchi, T. Hunter, and H. Osada, "M-phase kinases induce phospho-dependent ubiquitination of somatic Wee1 by SCF -TrCP," *Proceedings of the National Academy of Sciences*, vol. 101, no. 13, pp. 4419–4424, Mar. 2004.

[123] T. Hirota, N. Kunitoku, T. Sasayama, T. Marumoto, D. Zhang, M. Nitta, K. Hatakeyama, and H. Saya, "Aurora-A and an Interacting Activator, the LIM Protein Ajuba, Are Required for Mitotic Commitment in Human Cells," *Cell*, vol. 114, no. 5, pp. 585–598, Sep. 2003.

[124] A. Hutterer, D. Berdnik, F. Wirtz-Peitz, M. Žigman, A. Schleiffer, and J. A. Knoblich, "Mitotic Activation of the Kinase Aurora-A Requires Its Binding Partner Bora," *Dev. Cell*, vol. 11, no. 2, pp. 147–157, Aug. 2006.

[125] A. S. Nikonova, I. Astsaturov, I. G. Serebriiskii, R. L. Dunbrack, and E. A. Golemis, "Aurora A kinase (AURKA) in normal and pathological cell division.," *Cell. Mol. Life Sci.*, vol. 70, no. 4, pp. 661–687, Feb. 2013.

[126] A. O. Walter, W. Seghezzi, W. Korver, J. Sheung, and E. Lees, "The mitotic serine/threonine kinase Aurora2/AIK is regulated by phosphorylation and degradation.," *Oncogene*, vol. 19, no. 42, pp. 4906–4916, Jan. 2000.

[127] L. E. Littlepage, H. Wu, T. Andresson, J. K. Deanehan, L. T. Amundadottir, and J. V. Ruderman, "Identification of phosphorylated residues that affect the activity of the mitotic kinase Aurora-A.," *Proc. Natl. Acad. Sci. U.S.A.*, vol. 99, no. 24, pp. 15440–15445, Nov. 2002.

[128] Y. Arlot-Bonnemains, A. Klotzbucher, R. Giet, R. Uzbekov, R. Bihan, and C. Prigent, "Identification of a functional destruction box in the Xenopus laevis aurora-A kinase pEg2.," *FEBS Lett.*, vol. 508, no. 1, pp. 149–152, Nov. 2001.

[129] A. Castro, S. Vigneron, C. Bernis, J.-C. Labbé, C. Prigent, and T. Lorca, "The D-Box-activating domain (DAD) is a new proteolysis signal that stimulates the silent D-Box sequence of Aurora-A.," *EMBO Rep*, vol. 3, no. 12, pp. 1209–1214, Dec. 2002.

[130] L. E. Littlepage and J. V. Ruderman, "Identification of a new APC/C recognition domain, the A box, which is required for the Cdh1-dependent destruction of the kinase Aurora-A during mitotic exit.," *Genes Dev.*, vol. 16, no. 17, pp. 2274–2285, Sep. 2002.

[131] R. Bayliss, T. Sardon, I. Vernos, and E. Conti, "Structural Basis of Aurora-A Activation by TPX2 at the Mitotic Spindle," *Molecular Cell*, 2003.

[132] P. A. Eyers, E. Erikson, L. G. Chen, and J. L. Maller, "A novel mechanism for activation of the protein kinase Aurora A.," *Curr. Biol.*, vol. 13, no. 8, pp. 691–697, Apr. 2003.

[133] S. Toji, N. Yabuta, T. Hosomi, S. Nishihara, T. Kobayashi, S. Suzuki, K. Tamai, and H. Nojima, "The centrosomal protein Lats2 is a phosphorylation target of Aurora-A kinase," *Genes Cells*, vol. 9, no. 5, pp. 383–397, May 2004.

[134] D. Mori, Y. Yano, K. Toyo-oka, N. Yoshida, M. Yamada, M. Muramatsu, D. Zhang, H. Saya, Y. Y. Toyoshima, K. Kinoshita, A. Wynshaw-Boris, and S. Hirotsune, "NDEL1 Phosphorylation by Aurora-A Kinase Is Essential for Centrosomal Maturation, Separation, and TACC3 Recruitment," *Mol. Cell. Biol.*, vol. 27, no. 1, pp. 352–367, Dec. 2006.

[135] Y. Abe, M. Ohsugi, K. Haraguchi, J. Fujimoto, and T. Yamamoto, "LATS2-Ajuba complex regulates gamma-tubulin recruitment to centrosomes and spindle organization during mitosis.," *FEBS Lett.*, vol. 580, no. 3,

pp. 782–788, Feb. 2006.

[136] M. J. Lee, F. Gergely, K. Jeffers, S. Y. Peak-Chew, and J. W. Raff, "Msps/XMAP215 interacts with the centrosomal protein D-TACC to regulate microtubule behaviour.," *Nat. Cell Biol.*, vol. 3, no. 7, pp. 643–649, Jul. 2001.

[137] M. D. Koffa, C. M. Casanova, R. Santarella, T. Köcher, M. Wilm, and I. W. Mattaj, "HURP is part of a Ran-dependent complex involved in spindle formation.," *Curr. Biol.*, vol. 16, no. 8, pp. 743–754, Apr. 2006.

[138] M. Carmena and W. C. Earnshaw, "The cellular geography of aurora kinases," *Nature reviews. Molecular cell biology*, vol. 4, no. 11, pp. 842–854, Nov. 2003.

[139] L. S. Kiat, K. M. Hui, and G. Gopalan, "Aurora-A kinase interacting protein (AIP), a novel negative regulator of human Aurora-A kinase.," *J. Biol. Chem.*, vol. 277, no. 47, pp. 45558–45565, Nov. 2002.

[140] J. Wong, R. Lerrigo, C.-Y. Jang, and G. Fang, "Aurora A regulates the activity of HURP by controlling the accessibility of its microtubule-binding domain.," *Molecular biology of the cell*, vol. 19, no. 5, pp. 2083–2091, May 2008.

[141] X. Zhang, S. C. Ems-McClung, and C. E. Walczak, "Aurora A phosphorylates MCAK to control ran-dependent spindle bipolarity.," *Molecular biology of the cell*, vol. 19, no. 7, pp. 2752–2765, Jul. 2008.

[142] V. Horn, J. Thélu, A. Garcia, C. Albigès-Rizo, M. R. Block, and J. Viallet, "Functional interaction of Aurora-A and PP2A during mitosis.," *Molecular biology of the cell*, vol. 18, no. 4, pp. 1233–1241, Apr. 2007.

[143] S. Kitajima, Y. Kudo, I. Ogawa, M. Tatsuka, H. Kawai, M. Pagano, and T. Takata, "Constitutive phosphorylation of aurora-a on ser51 induces its stabilization and consequent overexpression in cancer.," *PLoS ONE*, vol. 2, no. 9, p. e944, 2007.

[144] H. M. Buschhorn, R. R. Klein, S. M. Chambers, M. C. Hardy, S. Green, D. Bearss, and R. B. Nagle, "Aurora-A over-expression in high-grade PIN lesions and prostate cancer.," *Prostate*, vol. 64, no. 4, pp. 341–346, Sep. 2005.

[145] Y. M. Jeng, "Overexpression and Amplification of Aurora-A in Hepatocellular Carcinoma," *Clinical Cancer Research*, vol. 10, no. 6, pp. 2065–2071, Mar. 2004.

[146] S.-B. Yang, X.-B. Zhou, H.-X. Zhu, L.-P. Quan, J.-F. Bai, J. He, Y.-N. Gao, S.-J. Cheng, and N.-Z. Xu, "Amplification and overexpression of Aurora-A in esophageal squamous cell carcinoma," *Oncology Reports*, vol. 17, no. 5, pp. 1083–1088, 2007.

[147] S. Sen, A. R. White, and Z. Hongyi, "A putative serine/threonine kinase encoding gene BTAK on chromosome 20q13 is amplified and overexpressed in human breast cancer cell lines.," *Oncogene*, vol. 14, no. 18, pp. 2195–2200, Jun. 1997.

[148] J. Gu, Y. Gong, M. Huang, C. Lu, M. R. Spitz, and X. Wu, "Polymorphisms of STK15 (Aurora-A) gene and lung cancer risk in Caucasians.," *Carcinogenesis*, vol. 28, no. 2, pp. 350–355, Feb. 2007.

[149] D. Li, J. Zhu, P. F. Firozi, J. L. Abbruzzese, D. B. Evans, K. Cleary, H. Friess, and S. Sen, "Overexpression of oncogenic STK15/BTAK/Aurora A kinase in human pancreatic cancer.," *Clin. Cancer Res.*, vol. 9, no. 3, pp. 991–997, Mar. 2003.

[150] T. Amano, N. Kaji, K. Ohashi, and K. Mizuno, "Mitosis-specific activation of LIM motif-containing protein kinase and roles of cofilin phosphorylation and dephosphorylation in mitosis," *J. Biol. Chem.*, vol. 277, no. 24, pp. 22093–22102, 2002.

[151] T. Sumi, A. Hashigasako, K. Matsumoto, and T. Nakamura, "Different activity regulation and subcellular localization of LIMK1 and LIMK2 during cell cycle transition.," *Experimental Cell Research*, vol. 312, no. 7, pp. 1021–1030, Apr. 2006.

[152] R. Chakrabarti, J. L. Jones, D. K. Oelschlager, T. Tapia, A. Tousson, and W. E. Grizzle, "Phosphorylated LIM kinases colocalize with gamma-tubulin in centrosomes during early stages of mitosis.," *Cell Cycle*, vol. 6, no. 23, pp. 2944–2952, Dec. 2007.

[153] K. Acevedo, R. Li, P. Soo, R. Suryadinata, B. Sarcevic, V. A. Valova, M. E. Graham, P. J. Robinson, and O. Bernard, "The phosphorylation of p25/TPPP by LIM kinase 1 inhibits its ability to assemble microtubules," *Experimental Cell Research*, vol. 313, no. 20, pp. 4091–4106, Dec. 2007.

[154] X. Yang, K. Yu, Y. Hao, D.-M. Li, R. Stewart, K. L. Insogna, and T. Xu, "LATS1 tumour suppressor affects cytokinesis by inhibiting LIMK1," *Nat. Cell Biol.*, vol. 6, no. 7, pp. 609–617, Jun. 2004.

[155] C. N. Landen, Y. G. Lin, A. Immaneni, M. T. Deavers, W. M. Merritt, W. A. Spannuth, D. C. Bodurka, D. M. Gershenson, W. R. Brinkley, and A. K.

Sood, "Overexpression of the Centrosomal Protein Aurora-A Kinase is Associated with Poor Prognosis in Epithelial Ovarian Cancer Patients," *Clinical Cancer Research*, vol. 13, no. 14, pp. 4098–4104, Jul. 2007.

[156] S. Yamamoto, M. Yamamoto-Ibusuki, Y. Yamamoto, S. Fujiwara, and H. Iwase, "A comprehensive analysis of Aurora A; transcript levels are the most reliable in association with proliferation and prognosis in breast cancer.," *BMC Cancer*, vol. 13, p. 217, 2013.

[157] J. Xu, X. Wu, W.-H. Zhou, A.-W. Liu, J.-B. Wu, J.-Y. Deng, C.-F. Yue, S.-B. Yang, J. Wang, Z.-Y. Yuan, and Q. Liu, "Aurora-A identifies early recurrence and poor prognosis and promises a potential therapeutic target in triple negative breast cancer.," *PLoS ONE*, vol. 8, no. 2, p. e56919, 2013.

[158] E. Dotan, N. J. Meropol, F. Zhu, F. Zambito, B. Bove, K. Q. Cai, A. K. Godwin, E. A. Golemis, I. Astsaturov, and S. J. Cohen, "Relationship of increased aurora kinase A gene copy number, prognosis and response to chemotherapy in patients with metastatic colorectal cancer.," *Br. J. Cancer*, vol. 106, no. 4, pp. 748–755, Feb. 2012.

[159] M. Tatsuka, S. Sato, S. Kitajima, S. Suto, H. Kawai, M. Miyauchi, I. Ogawa, M. Maeda, T. Ota, and T. Takata, "Overexpression of Aurora-A potentiates HRAS-mediated oncogenic transformation and is implicated in oral carcinogenesis.," *Oncogene*, vol. 24, no. 6, pp. 1122–1127, Feb. 2005.

[160] S. Anand, S. Penrhyn-Lowe, and A. R. Venkitaraman, "AURORA-A amplification overrides the mitotic spindle assembly checkpoint, inducing resistance to Taxol.," *Cancer Cell*, vol. 3, no. 1, pp. 51–62, Jan. 2003.

[161] T. Marumoto, T. Hirota, T. Morisaki, N. Kunitoku, D. Zhang, Y. Ichikawa, T. Sasayama, S. Kuninaka, T. Mimori, N. Tamaki, M. Kimura, Y. Okano, and H. Saya, "Roles of aurora-A kinase in mitotic entry and G2 checkpoint in mammalian cells," *Genes Cells*, vol. 7, no. 11, pp. 1173–1182, Nov. 2002.

[162] T. Sumi, K. Matsumoto, and T. Nakamura, "Mitosis-dependent phosphorylation and activation of LIM-kinase 1.," *Biochem. Biophys. Res. Commun.*, vol. 290, no. 4, pp. 1315–1320, Feb. 2002.

[163] N. Kaji, A. Muramoto, and K. Mizuno, "LIM kinase-mediated cofilin phosphorylation during mitosis is required for precise spindle positioning.," *J. Biol. Chem.*, vol. 283, no. 8, pp. 4983–4992, Feb. 2008.

149

[164] M. Gorovoy, J. Niu, O. Bernard, J. Profirovic, R. Minshall, R. Neamu, and T. Voyno-Yasenetskaya, "LIM Kinase 1 Coordinates Microtubule Stability and Actin Polymerization in Human Endothelial Cells," *Journal of Biological Chemistry*, vol. 280, no. 28, pp. 26533–26542, Jul. 2005.

[165] Y.-W. Heng, H.-H. Lim, T. Mina, P. Utomo, S. Zhong, C.-T. Lim, and C.-G. Koh, "TPPP acts downstream of RhoA-ROCK-LIMK2 to regulate astral microtubule organization and spindle orientation," *Journal of Cell Science*, vol. 125, no. 6, pp. 1579–1590, Mar. 2012.

[166] N. Kaji, K. Ohashi, M. Shuin, R. Niwa, T. Uemura, and K. Mizuno, "Cell cycle-associated changes in Slingshot phosphatase activity and roles in cytokinesis in animal cells.," *J. Biol. Chem.*, vol. 278, no. 35, pp. 33450–33455, Aug. 2003.

[167] O. Wiggan, A. E. Shaw, J. G. DeLuca, and J. R. Bamburg, "ADF/Cofilin Regulates Actomyosin Assembly through Competitive Inhibition of Myosin II Binding to F-Actin," *Dev. Cell*, vol. 22, no. 3, pp. 530–543, Mar. 2012.

[168] S. Iwase, R. Sato, P.-J. De Bock, K. Gevaert, S. Fujiki, T. Tawada, M. Kuchitsu, Y. Yamagishi, S. Ono, and H. Abe, "Activation of ADF/cofilin by phosphorylation-regulated Slingshot phosphatase is required for the meiotic spindle assembly in Xenopus laevis oocytes.," *Molecular biology of the cell*, vol. 24, no. 12, pp. 1933–1946, Jun. 2013.

[169] D. A. Moulding, E. Moeendarbary, L. Valon, J. Record, G. T. Charras, and A. J. Thrasher, "Excess F-actin mechanically impedes mitosis leading to cytokinesis failure in X-linked neutropenia by exceeding Aurora B kinase error correction capacity.," *Blood*, vol. 120, no. 18, pp. 3803–3811, Nov. 2012.

[170] I. Mendes Pinto, B. Rubinstein, A. Kucharavy, J. R. Unruh, and R. Li, "Actin depolymerization drives actomyosin ring contraction during budding yeast cytokinesis.," *Dev. Cell*, vol. 22, no. 6, pp. 1247–1260, Jun. 2012.

[171] K. C. Gunsalus, S. Bonaccorsi, E. Williams, F. Verni, M. Gatti, and M. L. Goldberg, "Mutations in twinstar, a Drosophila gene encoding a cofilin/ADF homologue, result in defects in centrosome migration and cytokinesis.," *J Cell Biol*, vol. 131, no. 5, pp. 1243–1259, Dec. 1995.

[172] M. P. Somma, B. Fasulo, G. Cenci, E. Cundari, and M. Gatti, "Molecular Dissection of Cytokinesis by RNA Interference inDrosophila Cultured Cells," *Molecular biology of …*, 2002.

[173] S. Ono, "Mechanism of Depolymerization and Severing of Actin Filaments

and Its Significance in Cytoskeletal Dynamics," *International review of cytology*, 2007.

[174] M. G. Giansanti, S. Bonaccorsi, and M. Gatti, "The role of anillin in meiotic cytokinesis of Drosophila males.," *Journal of Cell Science*, vol. 112, pp. 2323–2334, Jul. 1999.

[175] G. Vader and S. Lens, "The Aurora kinase family in cell division and cancer," *Biochimica et Biophysica Acta (BBA)-Reviews on …*, 2008.

[176] A. R. Barr and F. Gergely, "Aurora-A: the maker and breaker of spindle poles," *Journal of Cell Science*, vol. 120, no. 17, pp. 2987–2996, Aug. 2007.

[177] H. Katayama and S. Sen, "Aurora kinase inhibitors as anticancer molecules.," *Biochim. Biophys. Acta*, vol. 1799, no. 10, pp. 829–839, Oct. 2010.

[178] K. Das, P. D. N. Lorena, L. K. Ng, L. Shen, D. Lim, W. Y. Siow, K. Narasimhan, M. Teh, M. Choolani, T. C. Putti, and M. Salto-Tellez, "Aurora-A expression, hormone receptor status and clinical outcome in hormone related cancers.," *Pathology*, vol. 42, no. 6, pp. 540–546, 2010.

[179] D. Karthigeyan, S. B. B. Prasad, J. Shandilya, S. Agrawal, and T. K. Kundu, "Biology of Aurora A kinase: Implications in cancer manifestation and therapy.," *Med Res Rev*, Mar. 2010.

[180] G. Görgün, E. Calabrese, T. Hideshima, J. Ecsedy, G. Perrone, M. Mani, H. Ikeda, G. Bianchi, Y. Hu, D. Cirstea, L. Santo, Y.-T. Tai, S. Nahar, M. Zheng, M. Bandi, R. D. Carrasco, N. Raje, N. Munshi, P. Richardson, and K. C. Anderson, "A novel Aurora-A kinase inhibitor MLN8237 induces cytotoxicity and cell-cycle arrest in multiple myeloma," *Blood*, vol. 115, no. 25, pp. 5202–5213, Jun. 2010.

[181] M. Tomita and N. Mori, "Aurora A selective inhibitor MLN8237 suppresses the growth and survival of HTLV-1-infected T-cells in vitro," *Cancer Science*, vol. 101, no. 5, pp. 1204–1211, 2010.

[182] T. Macarulla, A. Cervantes, E. Elez, E. Rodríguez-Braun, J. Baselga, S. Roselló, G. Sala, I. Blasco, H. Danaee, Y. Lee, J. Ecsedy, V. Shinde, A. Chakravarty, D. Bowman, H. Liu, O. Eton, H. Fingert, and J. Tabernero, "Phase I Study of the Selective Aurora A Kinase Inhibitor MLN8054 in Patients with Advanced Solid Tumors: Safety, Pharmacokinetics, and Pharmacodynamics," *Mol. Cancer Ther.*, vol. 9, no. 10, pp. 2844–2852, Oct. 2010.

151

[183] E. C. Dees, J. R. Infante, R. B. Cohen, B. H. O'Neil, S. Jones, M. von Mehren, H. Danaee, Y. Lee, J. Ecsedy, M. Manfredi, K. Galvin, B. Stringer, H. Liu, O. Eton, H. Fingert, and H. Burris, "Phase 1 study of MLN8054, a selective inhibitor of Aurora A kinase in patients with advanced solid tumors.," *Cancer Chemother. Pharmacol.*, vol. 67, no. 4, pp. 945–954, Apr. 2011.

[184] J. Estevam, H. Danaee, R. Liu, and J. Ecsedy, "Validation of a flow cytometry based G$_2$M delay cell cycle assay for use in evaluating the pharmacodynamic response to Aurora A inhibition," *Journal of …*, 2011.

[185] A. Hoellein, A. Pickhard, F. von Keitz, S. Schoeffmann, G. Piontek, M. Rudelius, A. Baumgart, S. Wagenpfeil, C. Peschel, T. Dechow, H. Bier, and U. Keller, "Aurora Kinase Inhibition Overcomes Cetuximab Resistance in Squamous Cell Cancer of the Head and Neck," *Oncotarget*, vol. 2, no. 8, pp. 599–609, Aug. 2011.

[186] B. Rao, I. M. M. van Leeuwen, M. Higgins, J. Campbell, A. M. Thompson, D. P. Lane, and S. Lain, "Evaluation of an Actinomycin D/VX-680 aurora kinase inhibitor combination in p53-based cyclotherapy," *Oncotarget*, vol. 1, no. 7, pp. 639–650, Oct. 2010.

[187] M. De Luca, L. Brunetto, I. A. Asteriti, M. Giubettini, P. Lavia, and G. Guarguaglini, "Aurora-A and ch-TOG act in a common pathway in control of spindle pole integrity," *Oncogene*, vol. 27, no. 51, pp. 6539–6549, Oct. 2008.

[188] M. Giubettini, I. A. Asteriti, J. Scrofani, M. De Luca, C. Lindon, P. Lavia, and G. Guarguaglini, "Control of Aurora-A stability through interaction with TPX2," *Journal of Cell Science*, vol. 124, no. 1, pp. 113–122, Jan. 2011.

[189] J. Du, S. Jablonski, T. J. Yen, and G. J. Hannon, "Astrin regulates Aurora-A localization," *Biochem. Biophys. Res. Commun.*, vol. 370, no. 2, pp. 213–219, May 2008.

[190] M. De Luca, P. Lavia, and G. Guarguaglini, "Report A Functional Interplay Between Aurora-A, Plk1 and TPX2 at Spindle Poles," *Cell Cycle*, 2006.

[191] M. Carmena, S. Ruchaud, and W. C. Earnshaw, "Making the Auroras glow: regulation of Aurora A and B kinase function by interacting proteins.," *Current Opinion in Cell Biology*, vol. 21, no. 6, pp. 796–805, Dec. 2009.

[192] V. Joukov, "Aurora kinases and spindle assembly: variations on a common theme?," *Cell Cycle*, vol. 10, no. 6, pp. 895–903, Mar. 2011.

152

[193] N. Conte, B. Delaval, C. Ginestier, A. Ferrand, D. Isnardon, C. Larroque, C. Prigent, B. Séraphin, J. Jacquemier, and D. Birnbaum, "TACC1-chTOG-Aurora A protein complex in breast cancer.," *Oncogene*, vol. 22, no. 50, pp. 8102–8116, Nov. 2003.

[194] O. J. Gruss and I. Vernos, "The mechanism of spindle assembly functions of Ran and its target TPX2," *The Journal of Cell Biology*, vol. 166, no. 7, pp. 949–955, Sep. 2004.

[195] F. Eckerdt, G. Pascreau, M. Phistry, and A. L. Lewellyn, "Phosphorylation of TPX2 by Plx1 enhances activation of Aurora A," *… Cycle*, 2009.

[196] T. Sardon, R. A. Pache, A. Stein, H. Molina, I. Vernos, and P. Aloy, "Uncovering new substrates for Aurora A kinase," *EMBO Rep*, vol. 11, no. 12, pp. 977–984, 2010.

[197] "Activation of Aurora-A kinase by protein phosphatase inhibitor-2, a bifunctional signaling protein.," *Proc. Natl. Acad. Sci. U.S.A.*, vol. 101, no. 23, pp. 8625–8630, Jun. 2004.

[198] Z.-S. Zhao, J. P. Lim, Y.-W. Ng, L. Lim, and E. Manser, "The GIT-Associated Kinase PAK Targets to the Centrosome and Regulates Aurora-A," *Molecular Cell*, vol. 20, no. 2, pp. 237–249, Oct. 2005.

[199] Y. Tong, A. Ben-Shlomo, C. Zhou, K. Wawrowsky, and S. Melmed, "Pituitary tumor transforming gene 1 regulates Aurora kinase A activity," *Oncogene*, vol. 27, no. 49, pp. 6385–6395, Oct. 2008.

[200] R. W. Scott and M. F. Olson, "LIM kinases: function, regulation and association with human disease," *J Mol Med*, vol. 85, no. 6, pp. 555–568, Feb. 2007.

[201] P. Sacchetti, R. Carpentier, P. Segard, C. Olive-Cren, and P. Lefebvre, "Multiple signaling pathways regulate the transcriptional activity of the orphan nuclear receptor NURR1," *Nucleic Acids Research*, vol. 34, no. 19, pp. 5515–5527, Sep. 2006.

[202] S. T. Lee Hoeflich, C. G. Causing, M. Podkowa, X. Zhao, J. L. Wrana, and L. Attisano, "Activation of LIMK1 by binding to the BMP receptor, BMPRII, regulates BMP-dependent dendritogenesis," *EMBO J.*, vol. 23, no. 24, pp. 4792–4801, 2004.

[203] F. S. Oppermann, F. Gnad, J. V. Olsen, R. Hornberger, Z. Greff, G. Kéri, M. Mann, and H. Daub, "Large-scale proteomics analysis of the human kinome.," *Mol. Cell Proteomics*, vol. 8, no. 7, pp. 1751–1764, Jul. 2009.

[204] N. Dephoure, C. Zhou, J. Villén, S. A. Beausoleil, C. E. Bakalarski, S. J. Elledge, and S. P. Gygi, "A quantitative atlas of mitotic phosphorylation.," *Proceedings of the National Academy of Sciences*, vol. 105, no. 31, pp. 10762–10767, Aug. 2008.

[205] A. Cervantes, E. Elez, D. Roda, J. Ecsedy, T. Macarulla, K. Venkatakrishnan, S. Roselló, J. Andreu, J. Jung, J. M. Sanchis-Garcia, A. Piera, I. Blasco, L. Maños, J.-A. Pérez-Fidalgo, H. Fingert, J. Baselga, and J. Tabernero, "Phase I pharmacokinetic/pharmacodynamic study of MLN8237, an investigational, oral, selective aurora a kinase inhibitor, in patients with advanced solid tumors.," *Clin. Cancer Res.*, vol. 18, no. 17, pp. 4764–4774, Sep. 2012.

[206] N. Portier, A. Audhya, P. S. Maddox, R. A. Green, A. Dammermann, A. Desai, and K. Oegema, "A microtubule-independent role for centrosomes and aurora a in nuclear envelope breakdown.," *Dev. Cell*, vol. 12, no. 4, pp. 515–529, Apr. 2007.

[207] P. Romé, E. Montembault, N. Franck, A. Pascal, D. M. Glover, and R. Giet, "Aurora A contributes to p150(glued) phosphorylation and function during mitosis.," *The Journal of Cell Biology*, vol. 189, no. 4, pp. 651–659, May 2010.

[208] M. Venoux, J. Basbous, C. Berthenet, C. Prigent, A. Fernandez, N. J. Lamb, and S. Rouquier, "ASAP is a novel substrate of the oncogenic mitotic kinase Aurora-A: phosphorylation on Ser625 is essential to spindle formation and mitosis.," *Hum. Mol. Genet.*, vol. 17, no. 2, pp. 215–224, Jan. 2008.

[209] M. K. Tennant, J. B. Thrasher, P. A. Twomey, R. S. Birnbaum, and S. R. Plymate, "Insulin-like growth factor-binding protein-2 and -3 expression in benign human prostate epithelium, prostate intraepithelial neoplasia, and adenocarcinoma of the prostate.," *http://dx.doi.org/10.1210/jcem.81.1.8550786*, vol. 81, no. 1, pp. 411–420, Jul. 2013.

[210] S. Ohashi, G. Sakashita, R. Ban, M. Nagasawa, H. Matsuzaki, Y. Murata, H. Taniguchi, H. Shima, K. Furukawa, and T. Urano, "Phospho-regulation of human protein kinase Aurora-A: analysis using anti-phospho-Thr288 monoclonal antibodies," *Oncogene*, vol. 25, no. 59, pp. 7691–7702, Dec. 2006.

[211] L. Ritchey, R. Ottman, M. Roumanos, and R. Chakrabarti, "A functional cooperativity between Aurora A kinase and LIM kinase1: Implication in the mitotic process," *Cell Cycle*, vol. 11, no. 2, pp. 296–309, Jan. 2012.

[212] N. Hégarat, E. Smith, G. Nayak, S. Takeda, P. A. Eyers, and H. Hochegger, "Aurora A and Aurora B jointly coordinate chromosome segregation and anaphase microtubule dynamics.," *The Journal of Cell Biology*, vol. 195, no. 7, pp. 1103–1113, Dec. 2011.

[213] T. Marumoto, S. Honda, T. Hara, M. Nitta, T. Hirota, E. Kohmura, and H. Saya, "Aurora-A Kinase Maintains the Fidelity of Early and Late Mitotic Events in HeLa Cells," *Journal of Biological …*, 2003.

[214] L. H. Wang, J. Xiang, M. Yan, Y. Zhang, Y. Zhao, C. F. Yue, J. Xu, F. M. Zheng, J. N. Chen, Z. Kang, T. S. Chen, D. Xing, and Q. Liu, "The Mitotic Kinase Aurora-A Induces Mammary Cell Migration and Breast Cancer Metastasis by Activating the Cofilin-F-actin Pathway," *Cancer Res.*, vol. 70, no. 22, pp. 9118–9128, Nov. 2010.

[215] W. Moon and F. Matsuzaki, "Aurora A kinase negatively regulates Rho-kinase by phosphorylation in vivo.," *Biochem. Biophys. Res. Commun.*, vol. 435, no. 4, pp. 610–615, Jun. 2013.

[216] R. Uzbekov, I. Kireyev, and C. Prigent, "Centrosome separation: respective role of microtubules and actin filaments.," *Biol. Cell*, vol. 94, no. 4, pp. 275–288, Sep. 2002.

[217] C. M. Whitehead, R. J. Winkfein, and J. B. Rattner, "The relationship of HsEg5 and the actin cytoskeleton to centrosome separation.," *Cell Motil. Cytoskeleton*, vol. 35, no. 4, pp. 298–308, 1996.

[218] M. Théry, V. Racine, A. Pépin, M. Piel, and Y. Chen, "The extracellular matrix guides the orientation of the cell division axis : Abstract : Nature Cell Biology," *Nature cell …*, 2005.

[219] F. Toyoshima and E. Nishida, "Integrin-mediated adhesion orients the spindle parallel to the substratum in an EB1- and myosin X-dependent manner.," *EMBO J.*, vol. 26, no. 6, pp. 1487–1498, Mar. 2007.

[220] R. J. Pelham and F. Chang, "Actin dynamics in the contractile ring during cytokinesis in fission yeast.," *nature*, vol. 419, no. 6902, pp. 82–86, Sep. 2002.

[221] P. R. Grigera, L. Ma, C. A. Borgman, A. F. Pinto, N. E. Sherman, J. T. Parsons, and J. W. Fox, "Mass spectrometric analysis identifies a cortactin-RCC2/TD60 interaction in mitotic cells.," *J Proteomics*, vol. 75, no. 7, pp. 2153–2159, Apr. 2012.

[222] J. Yang, E. S. Bardes, J. D. Moore, J. Brennan, M. A. Powers, and S. Kornbluth, "Control of cyclin B1 localization through regulated binding of

the nuclear export factor CRM1.," *Genes Dev.*, vol. 12, no. 14, pp. 2131–2143, Jul. 1998.

[223] K. Mizuno, "Signaling mechanisms and functional roles of cofilin phosphorylation and dephosphorylation.," *Cellular Signalling*, vol. 25, no. 2, pp. 457–469, Feb. 2013.

[224] J. R. Wiśniewski, N. Nagaraj, A. Zougman, F. Gnad, and M. Mann, "Brain phosphoproteome obtained by a FASP-based method reveals plasma membrane protein topology.," *J. Proteome Res.*, vol. 9, no. 6, pp. 3280–3289, Jun. 2010.

[225] K. T. G. Rigbolt, T. A. Prokhorova, V. Akimov, J. Henningsen, P. T. Johansen, I. Kratchmarova, M. Kassem, M. Mann, J. V. Olsen, and B. Blagoev, "System-wide temporal characterization of the proteome and phosphoproteome of human embryonic stem cell differentiation.," *Science Signaling*, vol. 4, no. 164, pp. rs3–rs3, 2011.

[226] C. Choudhary, J. V. Olsen, C. Brandts, J. Cox, P. N. G. Reddy, F. D. Böhmer, V. Gerke, D.-E. Schmidt-Arras, W. E. Berdel, C. Müller-Tidow, M. Mann, and H. Serve, "Mislocalized activation of oncogenic RTKs switches downstream signaling outcomes.," *Molecular Cell*, vol. 36, no. 2, pp. 326–339, Oct. 2009.

[227] S. Rosso, F. Bollati, M. Bisbal, D. Peretti, T. Sumi, T. Nakamura, S. Quiroga, A. Ferreira, and A. Caceres, "LIMK1 regulates Golgi dynamics, traffic of Golgi-derived vesicles, and process extension in primary cultured neurons.," *Molecular biology of the cell*, vol. 15, no. 7, pp. 3433–3449, Jul. 2004.

[228] J. von Blume, J. M. Duran, E. Forlanelli, A.-M. Alleaume, M. Egorov, R. Polishchuk, H. Molina, and V. Malhotra, "Actin remodeling by ADF/cofilin is required for cargo sorting at the trans-Golgi network.," *The Journal of Cell Biology*, vol. 187, no. 7, pp. 1055–1069, Dec. 2009.

[229] J. V. Olsen, M. Vermeulen, A. Santamaria, C. Kumar, M. L. Miller, L. J. Jensen, F. Gnad, J. Cox, T. S. Jensen, E. A. Nigg, S. Brunak, and M. Mann, "Quantitative phosphoproteomics reveals widespread full phosphorylation site occupancy during mitosis.," *Science Signaling*, vol. 3, no. 104, pp. ra3–ra3, 2010.

[230] S. B. Salvarezza, S. Deborde, R. Schreiner, F. Campagne, M. M. Kessels, B. Qualmann, A. Caceres, G. Kreitzer, and E. Rodriguez-Boulan, "LIM kinase 1 and cofilin regulate actin filament population required for dynamin-dependent apical carrier fission from the trans-Golgi network.," *Molecular biology of the cell*, vol. 20, no. 1, pp. 438–451, Dec. 2008.

[231] G. R. X. Hickson, A. Echard, and P. H. O'Farrell, "Rho-kinase Controls Cell Shape Changes during Cytokinesis," *Curr. Biol.*, vol. 16, no. 4, pp. 359–370, Feb. 2006.

[232] K. C. Gunsalus, S. Bonaccorsi, E. Williams, F. Verni, M. Gatti, and M. L. Goldberg, "Mutations in twinstar, a Drosophila gene encoding a cofilin/ADF homologue, result in defects in centrosome migration and cytokinesis.," *The Journal of Cell Biology*, vol. 131, no. 5, pp. 1243–1259, Dec. 1995.